Hes·so VALAIS WALLIS
Haute Ecole d'Ingénierie
Hochschule für Ingenieurwissenschaften

Hes·so

Degree Programme
Life Technologies

Major Biotechnology

Bachelor's thesis
Diploma 2023

Alice Baechler

Alluvial filtration for the clarification of endotoxin-containing cell lysates

Professor
Simon Crelier

Expert
David Vinzent

Submission date of the report
18.08.2023

HES-SO Valais-Wallis • rue de l'Industrie 23 • 1950 Sion
+41 58 606 85 23 • hei@hevs.ch • www.hevs.ch/hei

Données du travail de diplôme
Aufgabenstellung der Bachelorarbeit

Filière / Studiengang **TEVI**	Année académique **/** *Studienjahr* **2022-23**	No TB / *Nr. BA* **BT/2023/02**
Mandant **/** *Auftraggeber* ☐ HES—SO Valais X Industrie ☐ Etablissement partenaire *Partnerinstitution*	Etudiant **/** *Student* **Baechler Alice** Professeur / *Dozent* **Crelier Simon**	Lieu d'exécution / *Ausführungsort* X HES—SO Valais ☐**Erreur ! Signet non défini.** Industrie ☐ Etablissement partenaire *Partnerinstitution*
Travail confidentiel / *vertrauliche Arbeit* ☐ oui / ja *X* non / nein	Expert / *Experte* *(données complètes)* **1. David Vinzent / Filtrox AG, Moosmühlestrasse 6, 9000 St. Gallen** **2. david.vinzent@filtrox.com**	

Titre / *Titel*

Alluvial filtration for the clarification of endotoxin-containing cell lysates

Description / *Beschreibung*

The company Filtrox AG based in St. Gallen produces depth filters for a variety of industrial applications since 1938. Recently developed functionalized filters have the ability to remove endotoxins from *E. coli* cell lysates. The concept has been demonstrated, but a few questions still need to be answered. During the bachelor thesis, the following objectives will be pursued:

Objectifs / *Ziele*

— Select a model host cell, establish growth conditions and analytical protocols

— Select and optimize cell lysis technique and conditions

— Identify the filter & filter aid combination; establish mass balances, realize tests at two different larger scales

— Determine product recovery after filtration, quantify endotoxin and HCP removal, and measure the achieved clarification of the broth.

— Position the project relative to the 17 UN sustainable development goals

Signature ou visa / *Unterschrift oder Visum*	Délais / *Termine*
Responsable de l'orientation / *Leiter der Vertiefungsrichtung:* 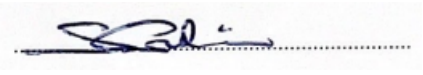 **[1]** Etudiant / Student: 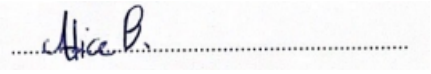	Attribution du thème / *Ausgabe des Auftrags:* **01.05.2023** Fin des travaux de diplôme dans les laboratoires de l'école / Ende der Diplomarbeiten in den Labors der Schule: **14.07.2023, 16 :15** Remise du rapport final / *Abgabe des Schlussberichts:* **18.08.2023** Expositions / *Ausstellungen der Diplomarbeiten:* **25.08.2023** – HEI **28.08.2023** – Monthey **31.08.2023** – Visp Défense orale / *Mündliche Verfechtung:* **Semaine/Woche 36 (04-07.09.2023)**

[1] *Par sa signature, l'étudiant-e s'engage à respecter strictement la directive DI.1.2.02.07 liée au travail de diplôme. Durch seine Unterschrift verpflichtet sich der/die Student/in, sich an die Richtlinie DI.1.2.02.07 der Diplomarbeit zu halten.*

Rapport reçu le / *Schlussbericht erhalten am* ……..……. Visa du secrétariat / *Visum des Sekretariats* ……..

Hes·so VALAIS WALLIS

Haute Ecole d'Ingénierie
Hochschule für Ingenieurwissenschaften

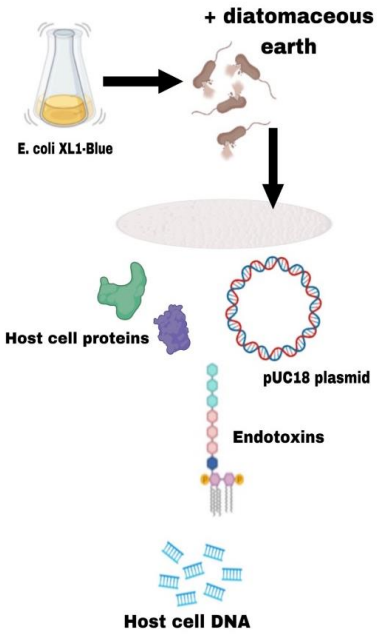

Bachelor's Thesis
| 2023 |

Degree programme
Life Technologies

Field of application
Biotechnology

Supervising professor
Simon Crelier
simon.crelier@hevs.ch

Partner
Filtrox AG

Alluvial filtration for the clarification of endotoxin-containing cell lysates

Graduate Alice Baechler

Objectives

During this project, the clarification of a E. coli XL1-Blue pUC18 lysate with alluvial filtration systems, developed by Filtrox AG, was assessed through pUC18 recovery and removal of endotoxins, turbidity, host cell proteins and DNA.

Methods | Experiences | Results

Plasmid DNA has been a growing interest for gene therapy and vaccines. While the development of upstream processing made it possible to greatly increase the cell concentrations, new technologies must be found in downstream processing to adapt. Alluvial filtration in a single-use format is the solution proposed by Filtrox AG.

The release of plasmid in E. coli by French Press lysis generates contaminants like endotoxins and host cell proteins and DNA meaning their removal must be assessed.

4 types of filters and Celpure® were tested in all 16 combinations possible in Puraspin® tubes. The 3 most adequate combinations were scaled up with the PURAFIX® BIO SD 2" capsule. Turbiditiy was reduced up to 73% with Puraspin® and 80% with Purafix®. Proteins were reduced up to 20% with Puraspin® and 14% with Purafix®. pUC18 was recovered up to 88% with Puraspin® and 81% with Purafix® while contaminant dsDNA wasn't retained overall. The removal of endotoxins was observed but recoveries were often higher than 100% meaning issues occurred using the RP-HPLC quantification with a fluorescence labelled KDO method.

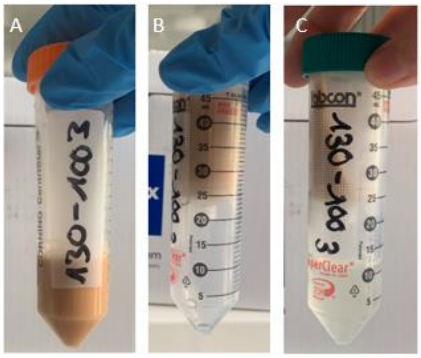

Figure 1 : (A) Filter aid added to the lysate. (B) Suspension added in Puraspin®. (C) Filtered suspension in Puraspin® after centrifugation.

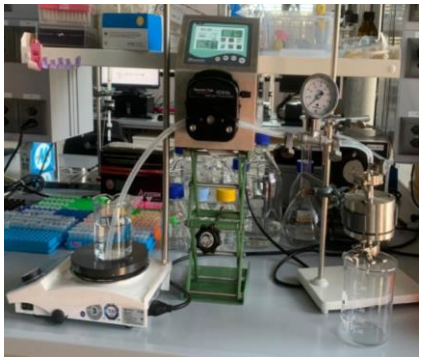

Figure 2 : Setup of the filtration at constant rate with the Purafix® 2" BIO SD capsule.

Hes·so VALAIS WALLIS

Haute Ecole d'Ingénierie
Hochschule für Ingenieurwissenschaften

FILTROX

Alluvial filtration for the clarification of endotoxin-containing cell lysates

University of Applied Sciences for Engineering HES-SO Valais/Wallis in Sion to obtain the Bachelor's degree in Life Sciences, majoring in Biotechnology

Submitted by
Alice Baechler
On the 18th of August

Oral defense on the 12th of September

Professor : Dr. Simon Crelier
Expert : David Vinzent

Acknowledgments

During the three months of practical work of my bachelor thesis, I was able to work in various laboratories at the HES-SO in Sion.

I would like to thank all the collaborators in the biotechnology pilot hall and molecular biology laboratory where I spent a good amount of time. They were there for me and my questions and kindly helped me.

The analysis of endotoxins by RP-HPLC was made possible thanks to Anika Hoffman. She took time to explain the method and always gave clear indications and explanations. I am also thankful to Pascal Jacquemettaz who was also there for me and my troubles with the HPLC.

Maria Gräfenhahn and Frédéric Maruel helped me use the turbidimeter, the viscosimeter and the bead mill. I would like to thank them for letting me and my *E. coli* cultures come in the food technology laboratory.

Rémy Dufresne was also there for me and gave many propositions and solutions that were useful for me. He kindly helped me use devices and navigate in the downstream processing laboratory.

The visit of Filtrox AG in St. Gallen was really interesting, and I particularly enjoyed seeing the process of manufacturing depth filters. I am therefore grateful to David Vinzent. He also was available for all my questions regarding filtration.

Finally, I would like to express my gratitude to my supervisor, Simon Crelier. He gave me a lot of advice and answered all my questions cordially. He helped me improve my presentations and my report.

I would also like to thank my family and my friends who gave me plenty of motivation and reassurance throughout my studies.

Table of content

1. Sustainability integration

The earth and the human society make up a strong and fragile system at the same time. The climate change crisis greatly endangers this system and requires actions to be taken. The United Nations Member States have adopted in 2015 the 2030 Agenda for Sustainable Development which contains the seventeen Sustainable Development Goals. They represent the objectives for humankind to ensure and preserve peace, prosperity for the planet and humans, in the present and the future (Un.org, 2023).

Figure 1 : The seventeen Sustainable Development Goals from the 2030 Agenda for Sustainablr Development of the United Nations (Un.org, 2023).

In that way, this bachelor thesis will be positioned regarding sustainability according to those seventeen goals. Since the main aspect of this project is alluvial filtration in a disposable format, the first part discussed will be single-use technologies and the second one the diatomaceous earth used in alluvial filtration.

Single-use technology in the biopharmaceutical industry does not seem in accordance with the twelfth goal, responsible consumption and production, at the first instance. The waste generated, notably of plastic, is way more important than for traditional facilities. However, consumption of water, chemicals and energy, like for cleaning, have been reported to be greatly reduced with the use of single-use innovations (Ottinger M *et al.*, 2022).

Considering those two aspects, single-use facilities have been reported as less impactful on the environment compared to traditional ones. However, this statement is still debated.

Diatomaceous earth is produced by mining. Those mines can destroy the land and impact animals living there. Strict mining practices are therefore important to limit the impact on the ecosystem. This corresponds to the fifteenth goal, life on land. This material is fundamentally not toxic to living beings but the danger comes from its fine dust (Progressiveplanet.com, 2023). This material is very abundant and regenerative meaning it is considered in accordance with the twelfth goal, responsible consumption and production.

Alluvial filtration can also help reduce the footprint of filtration processes with higher solids concentrations able to be filtered and more efficient clarification (Medium.com, 2023).

Figure 2 : A mine of diatomaceous earth in California, USA (Geologyforinvestors.com, 2023).

The combination of single-use technology and alluvial filtration can greatly improve the biopharmaceutical industry. It provides faster processes that can in turn lower prices of drugs and other therapies making them available to a larger group of people. This relates to the third objective of good health and well-being.

2. Introduction

2.1 Plasmid DNA : its value and the production process

Plasmids are essential for the modern biotechnology industry. They are used to produce industrial enzymes and simple recombinant proteins like insulin or more complicated ones like monoclonal antibodies (Baeshen NA *et al.*, 2014).

For a long time, plasmids were used to produce a variety of biopharmaceuticals, but their role has now shifted to also be considered biopharmaceuticals themselves (Prazeres DMF and Monteiro GA, 2014).

Indeed, therapeutic applications including nucleic acids, have recently been of an increasing interest for researchers (Ohlson J, 2020).

DNA manipulation makes it possible to express various genes of interest for gene therapy and DNA vaccines. Indeed, the development of plasmids could treat for example cardiovascular diseases or cancers (Williams PD and Kingston PA, 2011) (Martínez-Puente DH *et al.*, 2022).

According to the FDA, gene therapy is a technique with the aim of modifying a patient's genes to cure or treat diseases (FDA, 2018). It consists in expressing proteins, like cytotoxic or proapoptotic ones, enzymes and toxins capable of directly targeting problematic cells.

The exogenous genetic material has to go to the nucleus of cells in order to get target cells to produce said proteins. This is rendered possible with the use of viral and non-viral vectors, the vehicle delivering the gene of interest.

Viruses are useful as vectors thanks to the viral ability to effectively infect cells while transferring DNA to the host cell without provoking an immune response. For safety reasons, those vectors must be modified by making them incompetent for replication (Mali S, 2013).

This is where plasmids are involved in gene therapy since non-viral vectors are based on plasmids. Those vectors are easier and cheaper to produce in large amounts. They are also considered safer as there is not a possibility of recombination resulting in a competent virus causing disease.

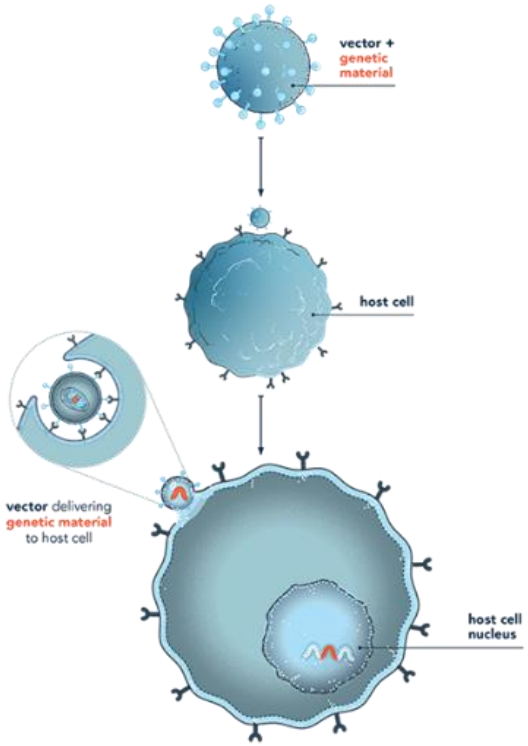

Figure 3 : The mecanism of gene therapy using plasmid vectors (Thegenehome.com, 2023).

For the manufacturing of plasmid DNA, the first step is to culture the bacteria, usually *E. coli*, bearing the plasmid of interest by maximizing the plasmid production with the most adequate growth medium, cultivation strategy and operating parameters of the bioreactor.

Since plasmid DNA is located inside the cells, the biomass is first harvested, for example by microfiltration or centrifugation. A lysis step follows to release the product of interest, usually done by alkaline lysis.

The alkaline lysis is based on four components. SDS solubilizes the phospholipids and the proteins of the cell membrane while sodium hydroxide denatures the plasmid and chromosomal DNA, and proteins. RNase A digests RNA. The lysates are then neutralized with potassium acetate, precipitating everything but the plasmid DNA. The precipitate is then eliminated either by filtration or centrifugation (Qiagen.com, 2023).

Another method developed is a pretreatment with lysozyme and a passage through a heat exchange coil at 70°C.

With the release of plasmid DNA also comes the release of all other contaminants like genomic DNA, RNA, proteins or endotoxins.

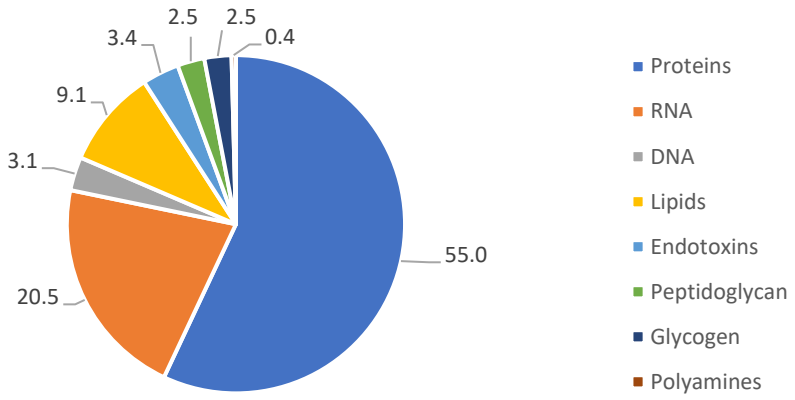

Figure 4 : Composition of E. coli (dry biomass) in the exponential phase (Zinn M, 2022).

The contaminant proteins are eliminated by salting-out with a high concentration of chaotropic salts. Plasmid DNA is also concentrated using polyethylene glycol precipitation to reduce volumes and eliminate small nucleic acids. Membranes processes follow like microfiltration, ultrafiltration and diafiltration. Chromatography like reverse-phase, hydrophobic interaction and ion is the final step of purification. Final steps of the process include ultrafiltration for buffer exchange and sterile filtration at 0.20 µm (Prazeres DMF and Monteiro GA, 2014) (Ferreira GNM *et al.*, 2000).

2.2 Filtration : different types and theorical knowledge

2.2.1 Touching the surface of filtration

Filtration is a basic but crucial and efficient step in bioprocesses. With centrifugation, these two steps make the link between the upstream and downstream processing, sometimes called midstream. This part is essential to separate cells from an extracellular product of interest or to concentrate an intracellular product of interest to proceed to purification.

Figure 5 describes the upstream and downstream steps in bioprocesses where harvesting can be considered the midstream processing.

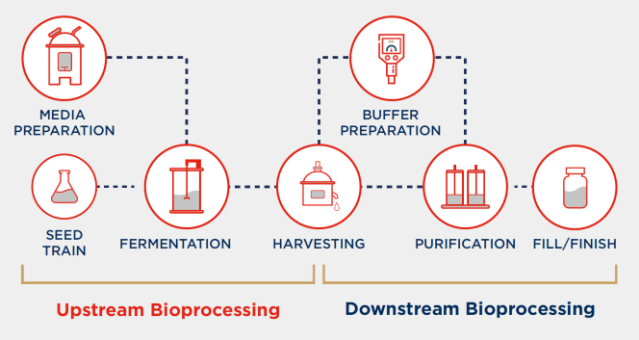

Figure 5 : Schematic description of the different steps encountered in bioprocesses (Thomaspumps.com, 2023).

Filtration is the separation of liquid from solid through a retention device driven by a pressure difference created by pressure, vacuum, gravity or centrifugation (Crelier S and Rüdt M, 2022) (Ripperger S *et al.*, 2013).

Two types of retention exist. *Figure 6* shows the visual differences between surface and depth filtration.

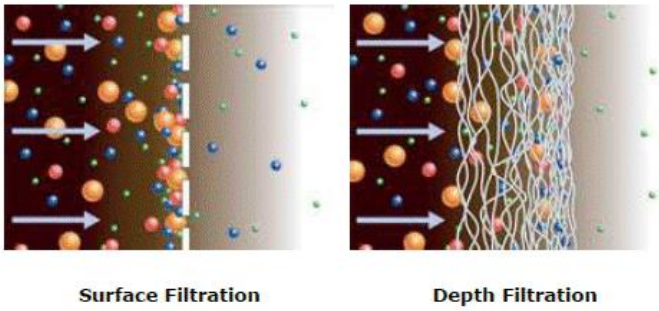

Figure 6 : Schematic description of surface and depth filtration (Icermax.com, 2023).

The first one, called surface filtration, consists of a filter, usually a membrane filter, that looks like a thin film with a precise porosity. Particles bigger than the pores are retained at the surface while smaller ones pass through or get adsorbed. The thickness of the filter is 10 to 170 µm depending on the filter type (Fisher Scientific, 2023). The usual materials for membranes are polyethersulfone, cellulose derivatives like cellulose acetate, and ceramic.

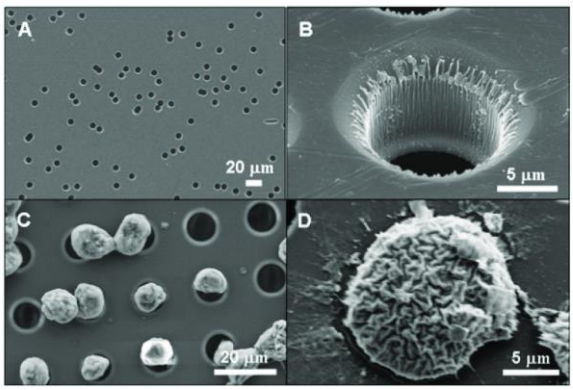

Figure 7 : Picture of a membrane filter under a microscope (Voronin D et al., 2020).

A few configurations that can be found in industry are spiral-wound modules, ceramic membranes, pleated membrane cartridges and hollow fiber modules (Crelier S and Rüdt M 1, 2022).

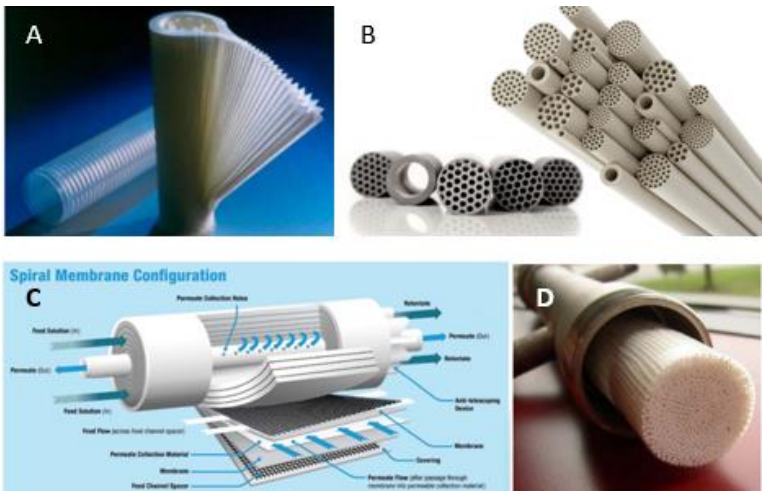

Figure 8 : Four types of membrane filtration devices. (A) Pleated membrane cartridge. (B) Ceramic membranes. (C) Spiral-wound module. (D) Hollow fiber module. (Crelier S and Rüdt M 1, 2022).

The second type is depth filtration with a three-dimensional filter and an unorganized structure. There is no well-defined size cut-off but more of a size range for retained solids. Separation is caused by mechanical retention and adsorption. Higher particles concentrations are processed than with surface filtration. The filter is also usually thicker. The filter medium may consist of a bed of coarse grains like sand with a thickness of 0.3 to 5 mm, a layer of a few centimeters of fibers like resin bonded cartridge filters, a sheet with a thickness of a few millimeters like sheet filters out of cellulose, or a layer of granular filter aid like in the form of a precoat layer.

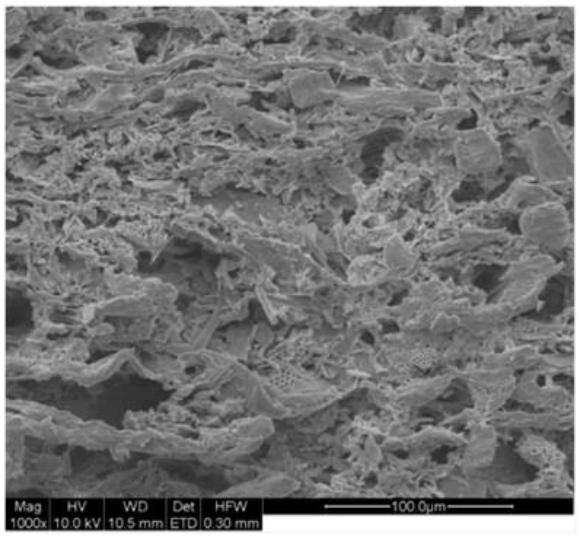

Figure 9 : A filter sheet made of cellulose under the microscope (Schreiber S et al., 2017).

Pressure filtration devices in industry include plate-and-frame, candle filters and vertical or horizontal leaf.

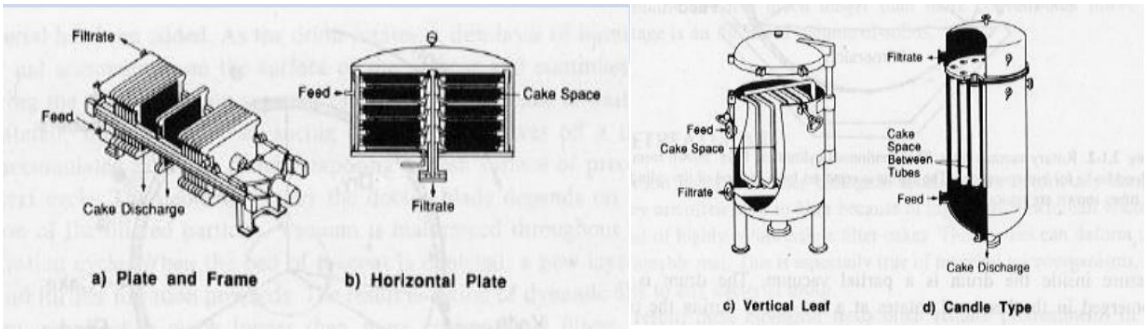

Figure 10 : Drawings of four types of pressure filtration devices (Crelier S and Rüdt M, 2022).

Vacuum filtration devices in industry include horizontal belt, rotating drum and rotating disc.

Figure 11 : Pictures of three vacuum filtration devices (A) Horizontal belt. (B) Rotating drum. (C) and (D) Rotating disc. (Crelier S and Rüdt M, 2022).

2.2.2 Depth filtration more in depth

Depth filters are usually sheets made with up to three elements.

Figure 12 : The three main elements (cellulose, diatomaceous earth and a binding resin) found in depth filters under a microscope (Nejatishahidein N and Zydney AL, 2021).

First, the randomly organized fibres of the filter sheet are made of bleached cellulose.

A binding resin can be added to act as a wet strength agent. It improves resistance of the wet fibers. Another advantage is the positive charge given to the filter. Also called zeta-potential, it gives the capability to adsorb small anionic particles depending on the lesser or greater positive charge. This translates to less work in downstream processing (Filtrox.com, 2023).

Finally filter aid is dense, particularly porous and incompressible. Two types are diatomaceous earth, also called Kieselguhr or Celite commercially, which consist of fossils of tiny aquatic organisms named diatoms, and Perlite which is the name for expanded volcanic glass.

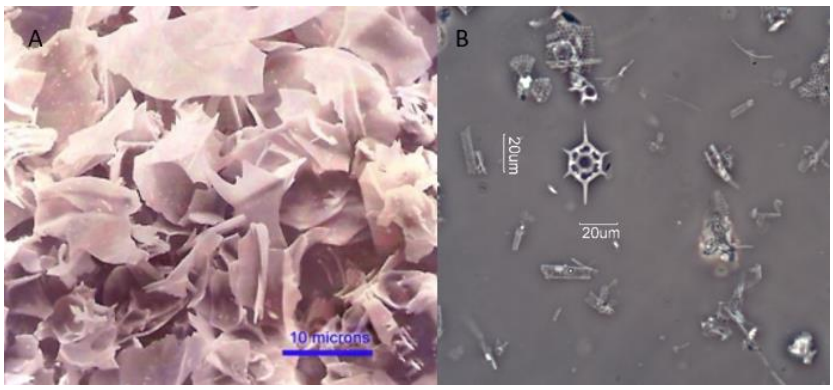

Figure 13 : (A) Perlite under a microscope (Crelier S and Rüdt M, 2022). (B) Diatomaceous earth under a microscope (Microlabgallery.com, 2023).

The process for production of the filter sheets is well-defined and stays pretty much the same across all sheets. Cellulose goes through a pulper with water of varying quality depending on the intended use of filters (pharmaceutical, food, beverages, …) to remove pulp. It is followed by a refiner to reduce fiber size. The suspension is transferred to a mixing tank, where filter aid and other chemical additives can be added according to the sheet type produced, and further transferred to a storage tank. The material is then processed through a vacuum wire to remove water and a first control of thickness and even dispersion is done. The sheets are dried by heat, laser branded and cut by a water jet cutter. Filter sheets for lenticular modules are further cut with a water jet cutter, molded and assembled with their corresponding plastic components.

Quality control consists in testing a few filter sheets per batch for wet strength, overall mass, filter integrity and, specifically for pharmaceutical grade, ions, bacterial and endotoxin concentrations. Filter integrity is tested by filtering water for one minute and measuring volume filtered.

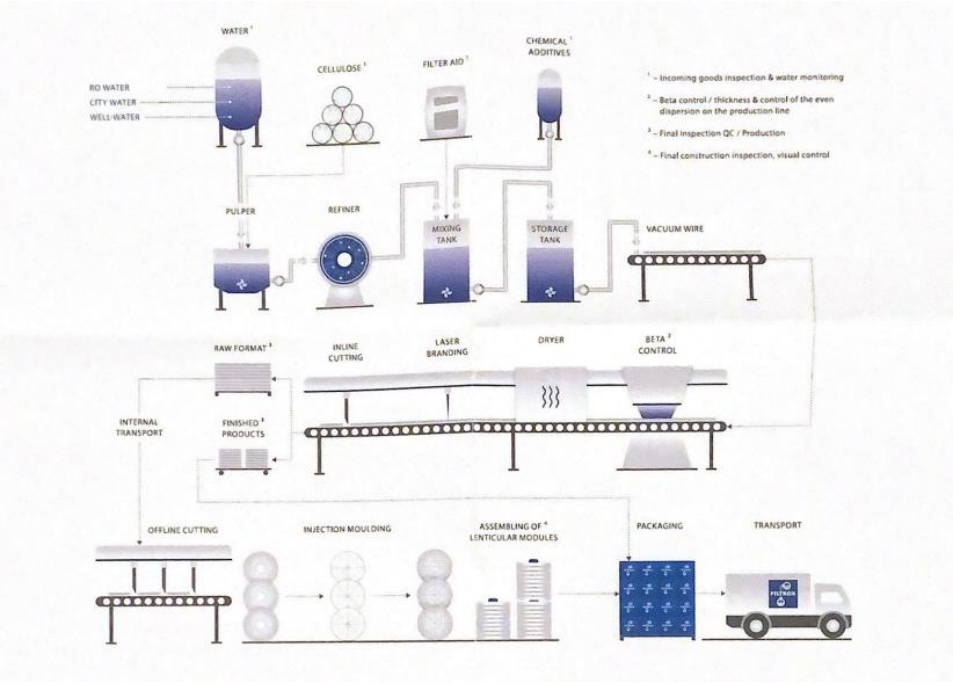

Figure 14 : Process of the production of depth filter sheets at Filtrox AG (Filtrox AG, 2023).

In bioprocesses, depth filtration is a cost-effective and efficient method for clarification of broth with the intentions of maintaining capacity of the following membrane filtration and preserving chromatography columns (Crelier S and Rüdt M, 2023). Two modes of depth filtration can be found : at constant pressure or at constant rate.

Constant pressure filtration consists in pushing the suspension, for example with air, through the filter medium. The flow rate through the filter medium is the highest at first when the cake is just starting to build up. It then decreases as the cake grows and the filter cake resistance increases. Differential pressure is fixed at a certain value through the whole filtration process (Mahdi FM and Holdich RG, 2013).

Figure 15 : Setup of a depth filtration at laboratory scale and constant pressure.

Constant rate filtration consists in pushing the suspension, for example with a peristaltic pump, through the filter medium. The differential pressure through the filter medium is the lowest at first when the cake is just starting to build up. It then increases as the cake grows and the filter and cake resistance increases. The flow rate is fixed at a certain value through the whole filtration process.

A peristaltic pump, a type of volumetric pump, is used as the delivery volume for each cycle is constant and independent from the discharge pressure. In contrary to centrifugal pumps, it results in independent flow rate and dynamic head (Falcotet F, 2022).

Figure 16 : Setup of a depth filtration at laboratory scale and constant rate.

The constant rate filtration is more widely used in industry. There are many advantages with this mode. Finer particles are less prone to penetrating the filter medium leading to filter medium blinding thanks to the initial low pressure. The more homogeneous constant growth rate of the cake gives a better packing structure independently from cake thickness. It is also considered to give more reliable data in relation with filter medium and cake resistances (Shahid M *et al.*, 2022) (Mahdi FM *et al.*, 2019).

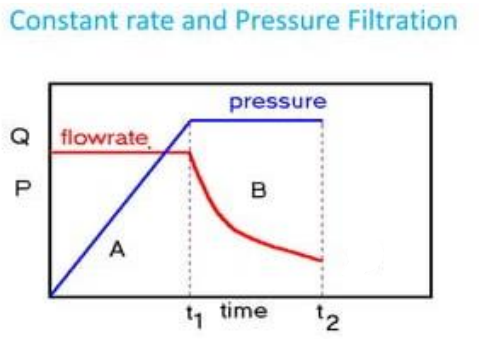

Figure 17 : Graphic of the flow rate (in red) and the differential pressure (in blue) in function of time during depth filtration. "A" is a constant rate filtration up until t_1. "B" is a constant pressure filtration from t_1 to t_2 (Slideshare.net, 2023).

For a constant pressure filtration, as seen in figure 17, the flow rate plotted against the time does not give a linear relationship between those two variables. Therefore, it is more usual to plot $\frac{area \cdot time}{filtrate\ volume}$ against $\frac{filtrate\ volume}{area}$.

The mathematical model used to describe this linear relationship is given here :

$$\frac{A \cdot t}{V} = \frac{\eta \cdot \alpha \cdot c_{ms}}{2 \cdot \Delta p} \cdot \frac{V}{A} + \frac{\eta \cdot \beta}{\Delta p}$$

Equation 1 : Mathematical model desribing filtration at constant pressure.

Δp : differential pressure [Pa]

η : dynamic viscosity [kg/m·s)]

α : cake specific resistance [m/kg]

c_{ms} : dry matter concentration in filtrate [kg/m^3]

V : volume of filtrate [m^3]

A : filter area [m^2]

t : time [s]

For a constant rate filtration, as seen in figure 17, the differential pressure plotted against the time gives a linear relationship between those two variables (Crelier S, 2017). The mathematical model used to describe this linear relationship is given here :

$$\Delta p = \eta \cdot \alpha \cdot c_{ms} \cdot \left(\frac{Q_f}{A}\right)^2 \cdot t + \eta \cdot \beta \cdot \frac{Q_f}{A}$$

Equation 2 : Mathematical model describing filtration at constant rate.

Δp : differential pressure [Pa]

η : dynamic viscosity [kg/m·s)]

α : cake specific resistance [m/kg]

c_{ms} : dry matter concentration in filtrate [kg/m^3]

Q_f : filtrate flow rate [m^3/s]

A : filter area [m^2]

t : time [s]

Filter medium, characterizing the resistance to flow of the filter medium, and cake resistance, characterizing the permeability of the cake, are useful values to calculate for the scale-up of depth filtration and to compare different filtrations trials.

When dealing with compressible particles, the cake becomes compressed, its porosity closes down, the differential pressure increases and filtration rate decreases. This is often the case when working with biological media.

The previous models don't apply in this situation for such cakes. In this case, new parameters have to be taken into account. However, the overall behaviour of a filtration does not change for compressible cakes.

$$\alpha = \alpha' \cdot \Delta p^s$$

Equation 3 : Equation for the correction of cake resistance when the cake is compressible.

α : cake specific resistance [m/kg]

α' : constant, linked to shape and size of cake particles [units=f(s)]

Δp : differential pressure [Pa]

s : cake compressibility, 0 (incompressible) < s < 1 (very compressible) [-]

Solids with a high cake compressibility require filter aid like diatomaceous earth.

2.2.3 The icing on the cake : alluvial filtration

With the tremendous development of upstream processing with higher and higher cell concentrations, the filters can no longer keep up and systems end up being clogged. More generally, traditional methods (membrane and depth filters and centrifugation) can't handle it anymore economically (Filtrox.com 1, 2023).

Cake formation is a big problem as its compressibility slows down flow rate and worsen permeability. Now, a few solutions exist to avoid this situation. The addition of flocculants or filter aids, heating and pH modification can all improve flow rate. Filter aid is probably the most frequent one since it is chemically inert and therefore usually process compatible.

The addition of filter aid to filter sheets was already talked about but in this case it is added separately. This is still called depth filtration but holds a more specific name : alluvial filtration. It can be done in two ways : precoat or body feed. The first one consists in applying an even coat on the surface before filtrating the suspension. Filter sheet is protected and filtrate clarity is improved. The second way is obtained by adding filter aid to the suspension, while stirring to keep the whole suspension homogenous, increasing flow rate. The filter sheet is only a support and the cake is the actual part where removal happens (Bächle V et *al.*, 2021). The location of filter aid in depth and alluvial filtration is shown on *figure 18*.

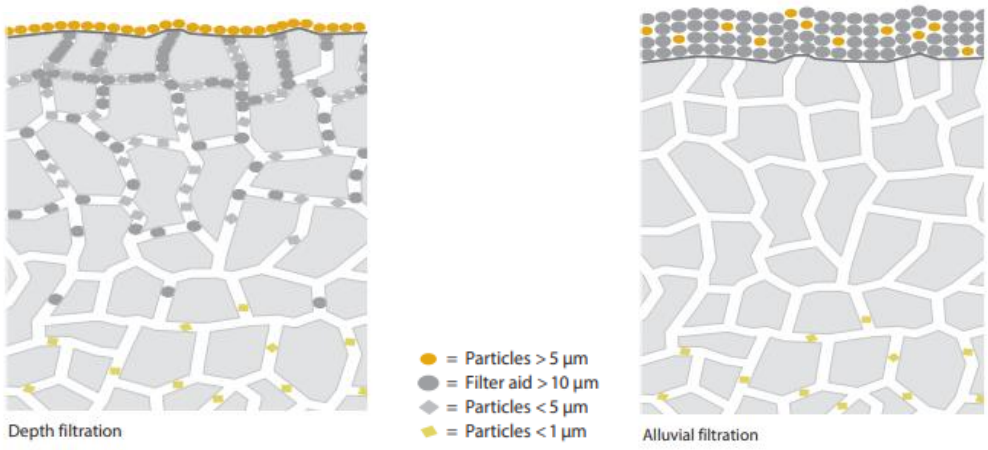

Figure 18 : Schematic description of depth and alluvial filtration (Filtrox.com 2, 2023).

Since filter aids are very porous, they modify the cake specific resistance by decreasing it thus increasing the permeability of the cake. They also help prevent clogging of the filter medium, thus

reducing resistance to flow of the filter medium (Chemicalprocessing.com, 2023) (Simplepharmanotes.com, 2023).

It is important to note that adding too little filter aid will only contribute to cake resistance and adding too much will unnecessarily contribute to the cake height.

2.2.4 Filtration technology

Compounds used to be mainly produced in bulk but with the rise of personalized treatments produced in smaller volumes, systems now require more flexibility and versatility to accommodate both large and small volumes (Susupport.com, 2023).

Depth filtration and more specifically alluvial filtration is now available in a single-use format to support the needs of the biopharmaceutical industry. This reduces cleaning and validation associated, downtime and cross-contamination. With increased capacity thanks to filter aid, the centrifugation step can even be eliminated resulting in even faster productions.

Pall Life technologies has developed the Stax™ depth filter system that does not even involve the use of a stainless-steel housing and can be operated by a single operator (Cytivalifesciences.com, 2023).

Figure 19 : The Stax™ depth filter system from Pall Life technologies (Cytivalifesciences.com, 2023).

The PURADISC® BIO SD from Filtrox AG is the first depth filter in the life science industry with the advantages of alluvial filtration technology in a disposable way. Filters are enveloped in a plastic bag making the whole discard of the module and its cake quick and safe (Filtrox.com 3, 2023).

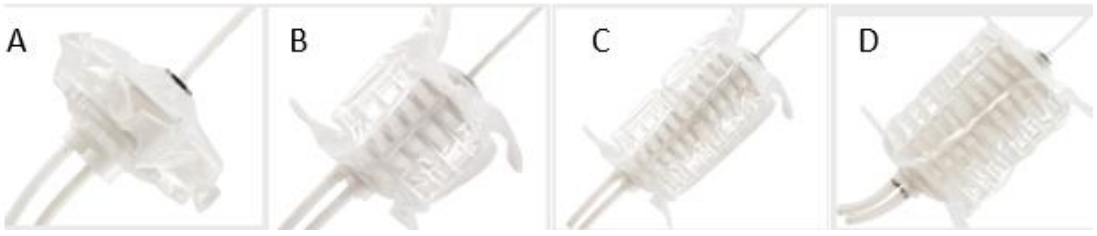

Figure 20 : Four types of PURADISC® modules from Filtrox. (A) PURADISC® 12" Short module – 12M.(B) PURADISC® 12" Single module – 12S.(C) PURADISC® 12" Double module – 12D.(D) PURADISC® 16" Double module – 16D. (Filtrox.com 3, 2023).

Dr. Müller AG has also developed a single-use alluvial filtration system that involves the use of a bag to safely dispose of the cake (Pharmaceutical-technology.com, 2023).

Figure 21 : Single-use alluvial filtration system from Dr. Müller AG (Pharmaceutical-technology.com, 2023).

Filters can also be optimized to their fullest potential by functionalizing them. A resin can be incorporated in sheets to give them a positive charge making them capable of retention of small anionic particles. Two examples are the 3M™ Zeta Plus™ Encapsulated System and the Purafix® ZP from Filtrox AG (Multimedia.3m.com) (Filtrox AG 1, 2023).

Even though depth filtration is inherently batch-wise, it is interesting to mention another technology in depth filtration that is continuous processes. This technology is less present, especially commercially. A skid has been designed to be used in continuous bioprocesses that automatically switches the feed between parallel filters at specified values (Thakur G *et al.*, 2020).

The products sold by the few filter suppliers mentioned translate the three current objectives of all filter suppliers : increase capacity due to higher cell densities in upstream processing, develop single-use technology and finally functionalize filters into removing impurities.

2.3 Objectives of the bachelor thesis

The mandator of this bachelor thesis is the company Filtrox AG from St. Gallen. Established since 1938, Filtrox is a supplier of depth filters for various industrial domains such as food, beverages, cosmetics, chemistry and biotechnology. They have now developed filters with the ability to remove endotoxins from cell lysates and the concept has been proved. Certain aspects still have to be analysed : product recovery, endotoxin, HCD and HCP removal, and clarification of the suspension.

Different objectives have been set. First, a model host cell and its growth conditions must be selected. A lysis method must be selected and optimized. After identification of the most adequate filter and filter aid combinations, two different larger scales are performed. Analytical protocols must be established in order to evaluate product recovery, endotoxin, HCD and HCP removal, and clarification of the suspension.

2.4 Products and methods approached

2.4.1 Plasmid production

The plasmid chosen, named pUC18, is a great candidate for plasmid production as it is small and of high copy number. It provides the host cell with a resistance to ampicillin making it perfect for selection (Bocascientific.com, 2023).

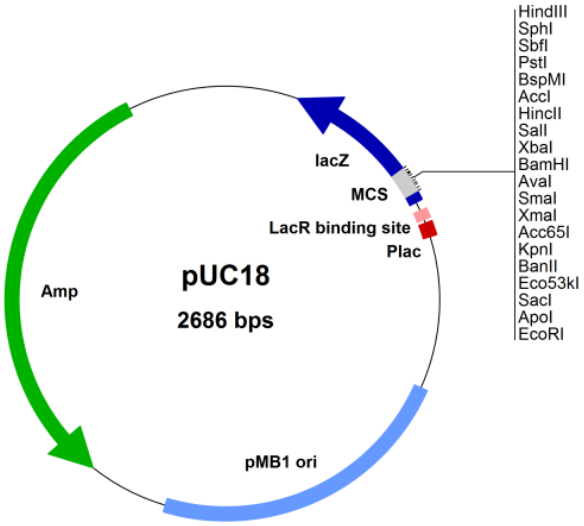

Figure 22 : Plasmid map of pUC18 that is 2686 bp in size. It contains the ampicillin resistance gene (light green arrow), the multiple cloning site (light blue) located within lacZ (dark red arrow) and the pMB1 origin of replication (yellow arrow). HindIII, SphI, SbfI, etc. show the cleavage sites for the respective restriction endonucleases (Bocascientific.com, 2023).

The plasmid is transformed in the XL1-Blue strain of *E. coli*. This strain is sold as directly competent cells by Agilent. It is endonuclease deficient, thus no endonucleases from the cells can degrade DNA, which is ideal for plasmid DNA production (Agilent.com, 2023).

The first medium tested for *E. coli* XL1-Blue is the LB medium, the most common one for the growth of *E. coli*. Different percentages of glucose are added in hope of improving the cell density. TB medium is also a great choice as it is rich medium recommended for plasmid production (Wood WN *et al.*, 2016). Another one with supplements of vitamin and salts is tested as it is also designed for plasmid production.

After medium selection at a smaller scale, the bacteria are grown in 1 L cultures in 5 L shake flasks with the most adequate medium in terms of productivity and efficiency. Shake flasks are used instead of a batch bioreactor mainly for its simpler approach.

Biomass is harvested either by centrifugation, depth filtration at constant pressure or sedimentation, and washed with PBS. Its dry mass content is measured by moisture analyzer. The biomass is resuspended in TE buffer at 4 g/L of dry biomass for lysis.

TE buffer is used in processes involving DNA or RNA. Its purpose is to solubilize DNA or RNA and protect them from degradation. It is made with Tris, a common pH buffer, and EDTA, a molecule that chelates cations. DNase, an enzyme degrading DNA and requiring Mg^{2+}, is inactivated thanks to EDTA making the said cation unavailable (Yagi N *et al.*, 1996).

2.4.2 Lysis of cells

Alkaline lysis is the method of choice in plasmid production, but endotoxin deactivation involves sodium hydroxide, especially for laboratory equipment. However, lysates obtained with alkaline lysis are usually subjected to additional steps against endotoxins like surfactants or ultrafiltration with a size cut-off of 10 kDa, suggesting that the sodium hydroxide concentration in lysis is not strong enough to significantly interfere quantification (Sartorius.com, 2023).

Nevertheless, two mechanical methods are more envisaged that would need less buffers and smaller quantities. The first one is well-established for a lot of industrial applications. The French press is made

of a hydraulic pump driving a piston. The suspension is forced through a small valve by the piston under very high pressure. The cells are exposed to shear stress and cellular disruption takes place (Beei.com, 2023).

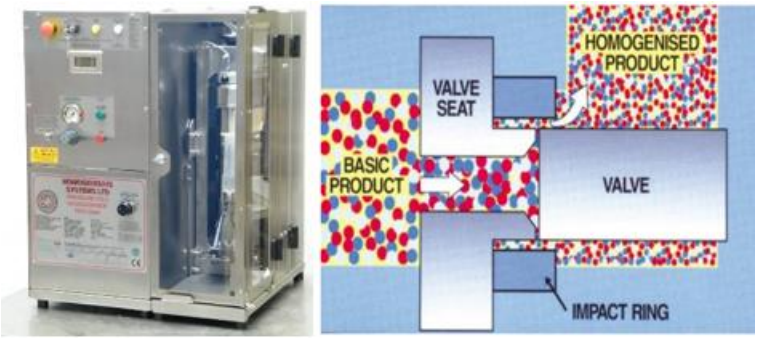

Figure 23 : The French Press from Stansted used for lysis of the suspension of dry biomass at 4 g/L (Homogenisingsystems.com, 2023) and its mechanism (Crelier S and Rüdt M 2, 2022).

Bead milling is the second method. It consists of small beads that can be made of various materials like glass, ceramic or zirconium agitated in a grinding chamber. Friction and mechanical shocks ensure disruption of cells.

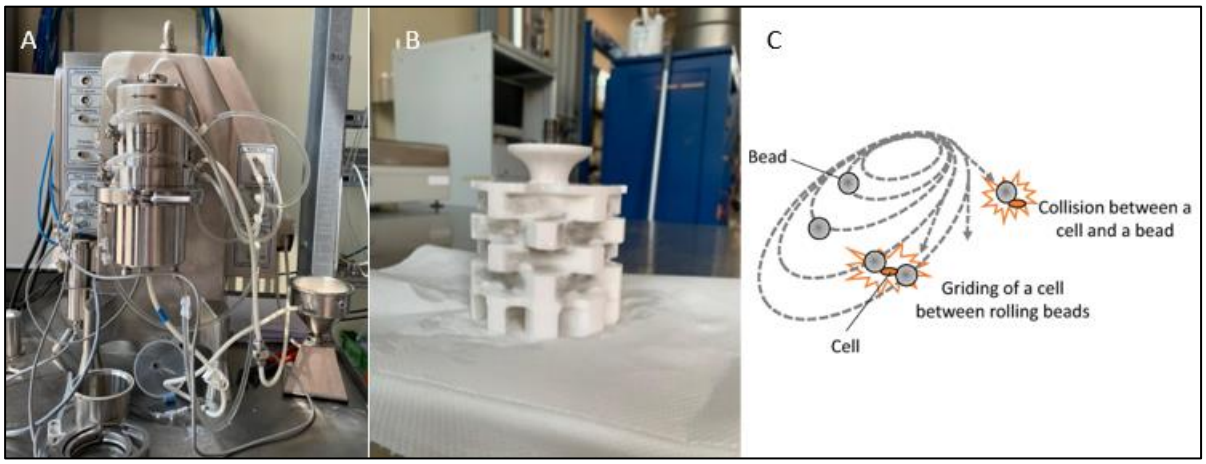

Figure 24 : (A) The FlexMill-Lab C bead mill from Frewitt. (B) The corresponding FlexMill-Lab NW-250 rotor. (C) Mechanism of a bead mill (Liu Z and Smith S, 2021).

2.4.3 Filtrations

The first step is to evaluate and find the most adequate filter and filter aid combinations in terms of clarification, product recovery and contaminants removal. Four types of filters and four grades of filter aid are tested. All sixteen combinations are done in triplicate with 15 mL of lysate in the Puraspin® devices with the help of a centrifuge.

Table 1 : Physical characteristics and components of the filter aids (Celpure®) and Puraspin® devices used (Filtrox AG 2-3-4-5-6-7-8-9, 2020).

Filter aid	Permeability [md]	Wet density [g/cm^3]	Conductivity [µS/cm^3]	Main components
Celpure® C1000	750-1250	0.10-0.26	0.1-20.0	Natural kieselguhr
Celpure® C300	150-300	0.10-0.27		
Celpure® C100	70-140	0.10-0.27		
Celpure® C65	40-80	0.10-0.28		
PURASPIN®	**Retention rate [µm]**	**Thickness [mm]**	**Filtration type**	**Main components**
PURASPIN® CH 09	10.0-30.0	3.2-3.4	Coarse	Cellulolse
PURASPIN® CH 31	5.0-12.0	4.4-4.6	Clarifying	Cellulose, perlite, natural kieselguhr
PURASPIN® CH 71	1.5-3.0	3.7-3.9	Fine	
PURASPIN® CH 130	0.4-0.6	3.7-3.10	Sterile	

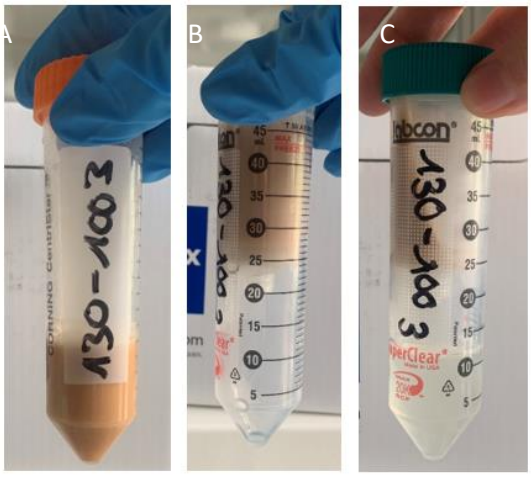

Figure 25 : (A) Filter aid added to the lysate. (B) Suspension added in Puraspin®. (C) Filtered suspension in Puraspin® after centrifugation.

After assessing the sixteen combinations, three are chosen to process on a larger scale with the 2" BIO SD capsule and corresponding Purafix® filters, at the chosen filter types. The filtrations are performed at constant rate with 200-400 mL of lysate and the help of a peristaltic pump.

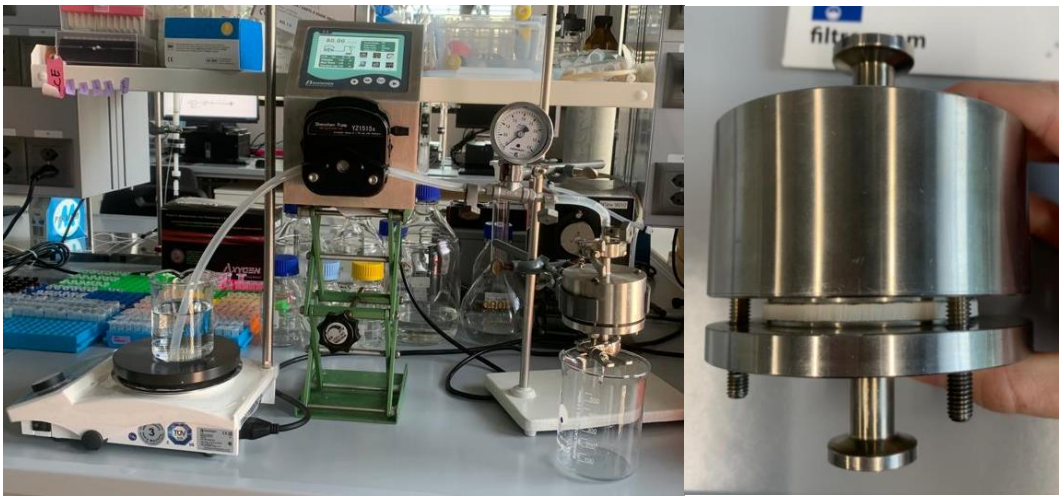

Figure 26 : Setup of the filtration with the Purafix® 2" BIO SD capsule.

After evaluation of the three combinations done each once, the most adequate one is performed once on a larger scale, still at constant rate, with the DISCSTAR® BIO SD 12" short support system and the corresponding PURADISC® 12" short module, at the chosen filter type. The volume to be filtered depends on Purafix® filtrations.

Figure 27 : Setup of the filtration with PURADISC® 12" short module (Filtrox.com 3, 2023).

2.4.4 Analytics

Turbidity

The turbidity is a basic but very important measurement for the clarification of suspension done with a turbidimeter from Hach.

Endotoxins quantification

Endotoxins, also called lipopolysaccharides (LPS) makeup the outer membrane of most of gram-negative bacteria and can induce an inflammatory reaction. Their chemical structure is heterogeneous and complex and is made up of three distinct parts. The hydrophobic lipid A consists of a glucosamine disaccharide with different acyl chains attached. The hydrophilic inner and outer core is an oligosaccharide made up of a variety of monosaccharides. Finally, the hydrophilic O-antigen is a polysaccharide (Bucsella B *et al.*, 2020).

Bacteria either express smooth LPS or rough LPS. The main differences are that rough LPS lack the O-antigen and are less common in nature (Fux AC *et al.*, 2023).

All cores of endotoxins contain one to three or four sugar acids named KDO, which are unique to endotoxins.

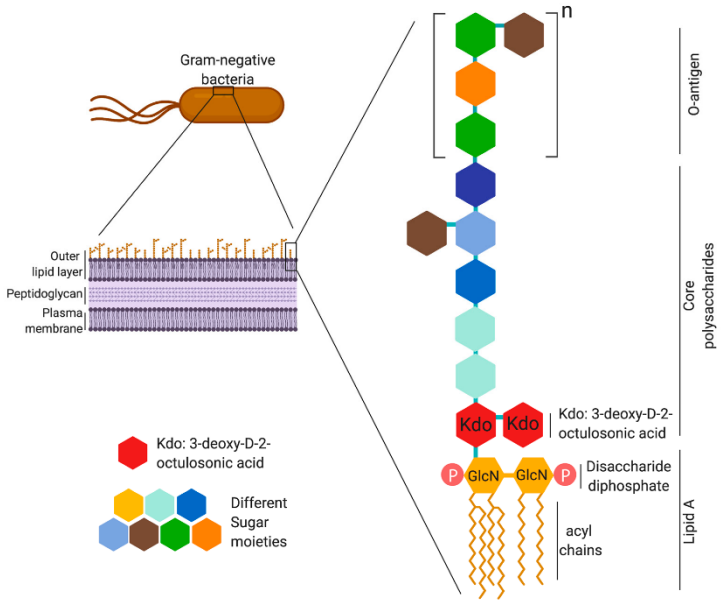

Figure 28 : Chemical structure of endotoxins (Mazgaeen L and Gurung P, 2020).

The LPS of *E. coli*, the most common strain used in industry, has an especially strong immunological activity, more than many gram-negative bacteria. The toll-like receptor 4 of dendritic cells is responsible for the inflammation due to its specificity to endotoxins (Kawahara K, 2021).

Hence the removal of endotoxins and its quantification is a critical step in purification of pharmaceutical products. The depth filters developed by Filtrox are helpful in reducing endotoxin concentrations and consequently increase operating lifetime of chromatography columns used in purification steps (Nejatishahidein N and Zydney AL, 2021).

The golden standard in industry for the quantification of endotoxins is the LAL test. It is based on the clotting of the horseshoe crab amebocyte lysate with LPS. The cartridges are expensive and have a very small dynamic measurement range, which make the analysis of a sample with an unknown endotoxin concentration much more complicated. Filters also contain β-glucans which can give false positive results that have to be further corrected to be ensured endotoxin-free (Sandle T, 2016).

Figure 29 : The horseshoe crab amebocyte which initiated the LAL test (Sandle T, 2016).

However, a less expensive and more accessible test has been recently developed by Bucsella B *et al.* as an alternative. It involves a mild acidic cleavage, the marking of KDO with the fluorescence marker DMB and finally separation with RP-HPLC coupled with FLD. β-glucans also don't react with DMB.

Total dsDNA quantification

The lysis releases undesirable DNA also called host cell DNA that must be quantified. The Qubit dsDNA BR assay is a quick, easy and sensitive way of measuring this contaminant. The fluorescent dyes used are highly specific to intact dsDNA and emit fluorescence only when bound to them. The dyes are absorbed within minutes and are read in seconds by a Qubit Fluorometer (ThermoFisher.com, 2023).

Plasmid DNA quantification

To quantify pUC18, samples have to be purified first. This is done by using the Miniprep kit from Biolabs. It is based on alkaline lysis and with the help of spin columns. Alkaline lysis has two roles : lysis and purification. The latter role was used in this case (International.neb.com, 2023).

Figure 30 : The Miniprep kit from Biolabs (International.neb.com, 2023).

After purification, the total dsDNA is quantified with the Qubit assay and the purity is measured with the TapeStation 4150 from Agilent. This device is an automatic version of gel electrophoresis (Agilent.com 1, 2023).

The gel electrophoresis is used for the separation of DNA or RNA fragments based on their size. Negatively charged nucleic acids migrate with an electrical current through the pores of an agarose gel towards the positively charged end of the gel. Smaller fragments migrate faster. The traditional version of this method is only qualitative and limited while the TapeStation 4150 takes it a step further by giving more precise sizing and allowing quantification with the help of a fluorescent marker (Technologynetworks.com, 2023).

Proteins quantification

The quantification of proteins is based on a well-established method : the Bradford assay. The Coomassie dye involved changes from brown to blue when bound to proteins under acidic conditions (Bradford MM, 1976).

The absorbance of samples is then measured at 595 nm. It is also possible to do a second measurement at 450 nm and calculate the ratio of absorbance at 595 nm to the one at 450 nm. This ratio makes the sensitivity ten times higher than just measuring at 595 nm (Zor T and Selinger Z, 1996).

The dye reacts with aromatic or basic amino acids, but the interaction is the strongest with arginine. Since the HCP population is quite diverse, standards are prepared with the BSA protein, thus giving results in BSA-equivalents.

In the pharmaceutical industry, HCPs are quantified using a much more expensive but way more reliable method known as sandwich ELISA, involving antibodies (Cytivalifesciences.com, 2023).

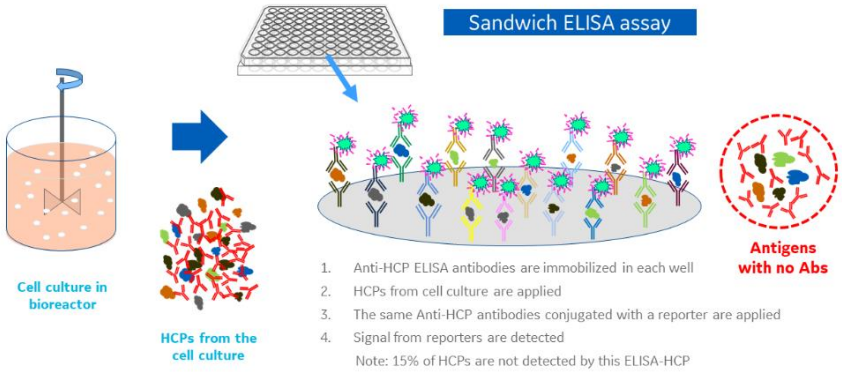

Figure 31 : Mechanism of sandwich ELISA for the quantification of HCPs (Cytivalifesciences.com, 2023).

3. Material and methods

3.1 Material

The material involved in plasmid production, harvest of biomass and cell lysis is described in *table 2*.

Table 2 : Material involved in plasmid production, harvest of biomass and cell lysis.

Product name	Supplier	Reference	Lot	Description
Escherichia coli XL1-BLUE pUC18	HES-SO	BIM, D10-E2	-	Strain
Nutrient Agar	Biolife	4018102	LG8203	Solid medium
Ampicillin sodium salt Biochemica/$C_{16}H_{18}N_3NaO_4S$	PanReac AppliChem	A0839,0025	9E011315	Antibiotic
LB Broth (Luria/Miller)	Roth	X968.2	421313267	Medium
D(+)-Glucose/$C_6H_{12}O_6$	Roth	X997.2	500303796	Medium
Copper(II) sulfate pentahydrate/$CuSO_4 \cdot 5H_2O$	Sigma-Aldrich	C3036-250G	11K3524	Medium
Iron(III) chloride hexahydrate/$FeSO_4 \cdot 6H_2O$	Sigma-Aldrich	44944-250G	BCBL0680V	Medium
Sodium molybdate dihydrate/$Na_2MoO_4 \cdot 2H_2O$	Fluka	-	-	Medium
Cobalt(II) chloride hexahydrate/$CoCl_2 \cdot 6H_2O$	Acros Organics	192092500	A0339371	Medium
Zinc chloride/$ZnCl_2$	Fluka	96469	408603/1	Medium
Hydrochloric acid 32%/HCl	Fisher Scientific	H/1100/PB15	1875656	Medium
Yeast extract	Biolife	4122204	22P019	Medium
Di-potassium hydrogen phosphate/K_2HPO_4	HES-SO	141512.0914	-	Medium
Potassium phosphate monobasic/KH_2PO_4	Acros Organics	212590025	A0425485	Medium
Glycerin 86.5%/$C_3H_8O_3$	CoChimy	930435	-	Medium
Potassium sulfate/K_2SO_4	Sigma-Aldrich	223492-500G	MKBR1323	Medium
Ammonium chloride/NH_4Cl	Reactolab	99215	-	Medium
Phosphoric acid 2M/H_3PO_4	HES-SO	-	-	Medium
Tryptone	Biolife	4122902	86P009	Medium
Sodium chloride/NaCl	Acros Organics	207790010	A0382142	Medium
Sodium posphate dibasic dihydrate/$Na_2HPO_4 \cdot 2H_2O$	HES-SO	71645-5KG	-	Medium
Magnesium sulfate heptahydrate/$MgSO_4 \cdot 7H_2O$	HES-SO	124900100	-	Medium
Thiamine hydrochloride/$C_{12}H_{22}Cl_2N_4O_3S$	Sigma-Aldrich	04573-50G-F	BCBV1156	Medium
Calcium chloride dihydrate/$CaCl_2 \cdot 2H_2O$	Sigma-Aldrich	223506-500G	BCCD0056	Medium
Potassium phosphate monobasic/KH_2PO_4	Acros Organics	424200025	A0423831	PBS
Potassium chloride/KCl	Roth	6781.1	321310219	PBS
Sodium posphate dibasic/Na_2HPO_4	Roth	P030.2	331309393	PBS
Sodium chloride/NaCl	Roth	3957.1	23332004	PBS
Sodium hydroxide 1 M/NaOH	HES-SO	-	-	PBS
Material name	**Supplier**	**Reference**	**Lot**	**Description**
Petri dish 92x16 mm with cams	Sarstedt	82.1473	2024805	NA agar plates
Sterile Syringe Filter 0.2 µm Cellulose Acetate	VWR	514-0061	FE9267	Sterilisation
Nalgene™ 150 mL Rapid-Flow™ Filter Unit 0.2 µm aPES	Thermo Fisher Scientific	565-0020	1348579	Sterilisation
Autoclave CertoClav Connect	CertoClav	8510176	C01.0036	Sterilisation
Systec VX-150 autoclave	Systec	VX-150	9641	Sterilisation
Ecotron incubator shaker	Infors HT	-	-	Plates incubation
Multitron Pro shaker	Infors HT	AJ 118	S-000124583	Shake flasks incubation
Ultrospec 2100 pro UV/Vis spectrophotometer	Biochrom	80-2112-21	13753	OD_{600} measurement
PS cuvettes	VWR	634-0676	8756	OD_{600} measurement
Air concept oven	Firlabo	AC240	-	CDW measurement
Filtration support for gravimetry	-	-	-	CDW measurement
Filtropur S 0.2 µm	Sarstedt	83.1826.001	221299103	CDW measurement
2.5 L UltraYield flask	Thomson	931136-B	-	Culture
Centrifuge	Herolab	HiCen XL	81712110202	Biomass harvest
Fibrafix AF ST 140 90 mm	Filtrox	147739	21302	Biomass harvest
Fibrafix AF ST 130 90 mm	Filtrox	147730	21467	Biomass harvest
Depth filtration support	Sartorius	16263/67	-	Biomass harvest
Centrifuge 3-30KS	Sigma	10375	177086	Biomass harvest

The products involved in plasmid production, harvest of biomass and cell lysis are described in *table 3*.

Table 3 : Products involved in plasmid production, harvest of biomass and cell lysis.

Product name	**Supplier**	**Reference**	**Lot**	**Description**
Ethylenediaminetetraacetic acid disodium salt dihydrate/$C_{10}H_{14}N_2Na_2O_8 \cdot 2H_2O$	Sigma-Aldrich	E4884-100G	BCCF1332	Resuspension solution
TRIS/$C_4H_{11}NO_3$	Roth	188.3	222324517	Resuspension solution
Sodium hydroxide/NaOH	Cochimy	-	-	Sanitization of French Press and bead mill
Material name	**Supplier**	**Reference**	**Lot**	**Description**
Pressure cell homogeniser	Stansted	SPCH-10	10260	French Press lysis
Glass beads d0.50-0.75 mm	WAB	222589	74273	Bead mill lysis
FlexMill-Lab C	Frewitt	-	200085-318	Bead mill lysis
FlexMill-Lab NW-250	Frewitt	79052	200085 308	Bead mill lysis
Folded Filters 320 mm	Schleicher & S	-	-	Bead mill lysis

The material and the products involved in the filtration of lysates are described in *table 4*.

Table 4 : Material and the products involved in the filtration of lysates.

Product name	**Supplier**	**Reference**	**Lot**	**Description**
Celpure® C1000	Filtrox	172650	512	Filter aid
Celpure® C300	Filtrox	172651	808	Filter aid
Celpure® C100	Filtrox	172652	559	Filter aid
Celpure® C65	Filtrox	172653	813	Filter aid
Material name	**Supplier**	**Reference**	**Lot**	**Description**
PURASPIN® CH 09	Filtrox	187148	1100004	Filtration tubes
PURASPIN® CH 31	Filtrox	187149	1200004	Filtration tubes
PURASPIN® CH 71	Filtrox	187150	1300004	Filtration tubes
PURASPIN® CH 130	Filtrox	187151	1500003	Filtration tubes
PURAFIX® BIO SD CH 09 Ø 6 cm	Filtrox	-	-	Filter sheet
PURAFIX® BIO SD CH 31 Ø 6 cm	Filtrox	-	-	Filter sheet
PURAFIX® BIO SD CH 71 Ø 6 cm	Filtrox	-	-	Filter sheet
PURAFIX® BIO SD CH 130 Ø 6 cm	Filtrox	-	-	Filter sheet
Centrifuge 3-30KS	Sigma	10375	177086	Filtration equipment
Pump V1	Shenchen	YZ1515x	10911140011	Filtration equipment
Manometer	Ashcroft	238A460-01	-	Filtration equipment
Steel filter holder	-	-	-	Filtration equipment
Perforated and sieve discs	-	-	-	Filtration equipment
Steel outlet nozzles	-	-	-	Filtration equipment
Silicone seals	-	-	-	Filtration equipment
Steel Tri Clamp fastener brackets	-	-	-	Filtration equipment
SCALE-UP test kit	Filtrox	-	-	Filtration equipment
Air concept oven	Firlabo	AC240	-	Endotoxin elimination

The material and products involved in the analysis of filtrates are described in *table 5*.

Table 5 : Material and products involved in the analysis of filtrates.

Product name	**Supplier**	**Reference**	**Lot**	**Description**
2-keto-3-deoxyoctonate ammonium salt ≥97%/$C_8H_{14}O{\cdot}NH_2$	Sigma-Alrdich	K2755-5MG	SLCL3220	Endotoxins quantification
1,3-benzodioxole-5,6-diamine dihydrochloride/$C_7H_8N_2O_2{\cdot}2HCl$	Apollo Scientific	OR3723	AS505418	Endotoxins quantification
2-mercaptoethanol ≥99.0%/C_2H_6OS	Sigma-Alrdich	M6250-100ML	STB117709	Endotoxins quantification
Sodium hydrosulfite/$Na_2S_2O_4$	Sigma-Alrdich	157953-100G	STBH8698	Endotoxins quantification
Acetic acid 100%/CH_3COOH	Roth	6755.1	120290803	Endotoxins quantification
Acetonitrile ChromAR® HPLC Super Gradient/CH_3CN	Macron	2856-25	2227701813	Endotoxins quantification
Methyl Alcohol, Anhydrous ChromAR® HPLC/ CH_3OH	Macron	6712-25	2222205853	Endotoxins quantification
Albumin Fraction V	Roth	0163.4	201308535	Proteins quantification
Bradford reagent	HES-SO	-	-	Proteins quantification
Invitrogen™ Qubit™ dsDNA BR Assay Kit	Thermo Fisher Scientific	Q32850	2557943	DNA quantification
Genomic DNA ScreenTape	Agilent	5067-5365	0202843-99	DNA quantification
Genomic DNA Ladder and Sample Buffer	Agilent	5067-5366	0202843-99	DNA quantification
CutSmart® Buffer	Biolabs	B7204S	1003565	DNA gel
XbaI	Biolabs	R0145S	10068590	Enzyme for DNA gel
BsaI	Biolabs	R0535	10044374	Enzyme for DNA gel
BseYI	Biolabs	R0635S	10020669	Enzyme for DNA gel
Gel Loading Dye Purple 6X	Biolabs	B7025S	10158560	DNA gel
peqGREEN DNA/RNA Dye	AxonLab	37-5010	1081201	DNA gel
TBE 1X	HES-SO	-	-	DNA gel
Quick-Load Purple 1kb plus DNA Ladder	Biolabs	N0550S	10158560	DNA gel
Agarose Standard Rotigarose DNA/RNA	Roth	3810.4	-	DNA gel
Monarch® Plasmid Miniprep Kit	Biolabs	T1010L	10053934	Plasmid purification
Material name	**Supplier**	**Reference**	**Lot**	**Description**
Column Triart C18 ExRS 150 x 2.1 mml.D. S-3 µm, 8 nm	YMC	TAR08S03-15Q1PTH	125HB20169/19915	Endotoxins quantification
1260 DAD WR	Agilent	G7115A	DEAC611701	Endotoxins quantification
1260 FLD Spectra	Agilent	G7121B	DEAEE00232	Endotoxins quantification
1260 Vialsampler	Agilent	G7129C	DEAGQ02407	Endotoxins quantification
1260 MCT	Agilent	G7116A	DEAEM07052	Endotoxins quantification
CHROMAFIL® Xtra PA-45/13	Macherey-Nagel	729249	210201	Endotoxins quantification
300µl Conical Glass Insert	BGB	110502	9031171	Endotoxins quantification
1.5ml Crimp Neck Vial, amber glass	BGB	LP-11093148	21106087	Endotoxins quantification
Micro tube 1.5ml, PP	Sarstedt	72.692.005	2084821	Endotoxins quantification
Ultrasonic bath	Bandelin	RK 100 H	312245 117	Endotoxins quantification
Single use syringes 2 mL	Codan	62.2611	J80759-1	Endotoxins quantification
Needles for syringes	Terumo	NN-2425R	1405017	Endotoxins quantification
Thermoshaker pro	CellMedia	112000	20T1200539	DNA and endotoxins quantification
ChemiDoc™ Imaging System	Bio-Rad	12003153	733BR0306	DNA gel
Optical Cap, 8x Strip	Agilent	6553439	1336727	DNA quantification
Optical Tube, 8x Strip	Agilent	401428	1348639	DNA quantification
Combi-Spin	Biolabo	FVL-2400N	560603023	DNA quantification
TapeStation 4150	Agilent	G2992A	DEDAB02720	DNA quantification
MS 3 B Vortexer	IKA	0003617000	220000891	DNA quantification
Loading Tip	Agilent	5067-5598	393302208A	DNA quantification
PCR® Tubes	Axygen	PCR-05-C	5722017	DNA quantification
Qubit 2.0	Life Technologies	Q32866	1012002321	DNA quantification
Microplate Reader spectrophotometer	LabGene Scientific	AMR-100	-	Proteins quantification
Microplate PS 96 F	Paul Boettger GmbH&Co. KG	05-031-0100	-	Proteins quantification
Weighing pans 100 x 7 mm	VWR	176154710	210845/16	Dry mass content measurement
Quartz sand 0.3 - 0.9 mm	HES-SO	-	-	Dry mass content measurement
Moisture analyzer	Mettler Toledo	HR83-P	1124010926	Dry mass content measurement
Microscope slides	Süsse	7626	-	Microscopy
Cover Slips	DWK	235503104	-	Microscopy
Microscope	Olympus	CX43RF	9J47571 201909	Microscopy
Turbidimeter	Hach	9680300	2020080C0149	Turbidity measurement
Glass cuvettes 11 mm	Hach	LYY621	23060255	Turbidity measurement
Modular Compact Rheometer	Anton Paar	MCR 302	81059065	Viscosity measurement
CC27	Anton Paar	78234	29037	Viscosity measurement

3.2 Methods

3.2.1 NA agar plates

2.3 g of nutrient agar were added to 100 mL of distilled water and autoclaved for 15 minutes at 121°C. 100 µl of ampicillin 100 mg/mL filtered at 0.2 µm were added after cooling down to approximately 50°C. Once poured in plates, the medium was let to solidify and dried under laminar flow for 15 minutes. Plates were streaked with *Escherichia coli* XL1-BLUE pUC18 glycerol stocks and incubated overnight at 37°C or at room temperature for 72 hours. Plates were stored at 4°C.

3.2.2 Medium selection

Escherichia coli XL1-BLUE pUC18 was cultured in several mediums to find the most adequate one.

LB medium and TB medium

The LB medium was made by adding 25 g of LB-medium powder per liter of demineralized water and preparing a stock solution of glucose at 40% and autoclaving them at 121°C for 15 minutes. Ampicillin at 100 mg/mL filtered at 0.2 µm and 40% glucose were added after to obtain a final concentration of 100 µg/mL of ampicillin and 0.4%, 1% or 2% glucose.

1 L of TB medium is made by preparing two solutions in demineralized water and combining them after autoclaving at 121°C for 15 minutes.

Table 6 : Recipe for the preparation of 1 L TB medium (Cshprotocols.cshlp.org, 2023).

Product	Quantity	Solubilized in
Glycerin 86.5%	4 mL	900 mL
Yeast extract	24 g	
Tryptone	12 g	
KH_2PO_4	2.3 g	100 mL
K_2HPO_4	16.4 g	

Ampicillin at 100 mg/mL was added after combination of mediums to obtain a final concentration of 100 µg/mL of ampicillin.

The precultures were done in 250 mL shake flasks and contained 50 mL of TB medium or LB medium with 0% glucose. A colony from a NA agar plate was picked and transferred to the precultures to incubate overnight at 37°C and 140 rpm.

The cultures were done in 500 mL shake flasks and contained 100 mL of TB medium or LB medium supplemented with glucose, with an initial OD_{600} of 0.1. The incubation was set to 37°C and 140 rpm.

Medium with a supplement of salts and vitamin

The solutions to add after autoclaving were made according to *table 7* and filtered at 0.2 µm.

Table 7 : Recipe of solutions for the medium with a supplement of salts and vitamin.

Solution	Component	Concentration
ECPM TES	$ZnCl_2$	17 g/L
	$CoCl_2 \cdot 6H_2O$	2.0 g/L
	$Na_2MoO_4 \cdot 2H_2O$	2.35 g/L
	$CuSO_4 \cdot 5H_2O$	1.86 g/L
	$FeSO_4 \cdot 6H_2O$	27 g/L
	HCl 32%	9.1 mL/L
Thiamin	$C_{12}H_{22}Cl_2N_4O_3S$	10.0 g/L
$MgSO_4$ solution	$MgSO_4 \cdot 7H_2O$	247 g/L
CaCl2 solution	$CaCl_2 \cdot 2H_2O$	13.2 g/L
Ampicillin solution	$C_{16}H_{18}N_3NaO_4S$	100 mg/mL

The preculture was made according to *table 8.* The glycerin, yeast extract, KH_2PO_4, K_2HPO_4, NH_4Cl and K_2SO_4 were solubilized together in demineralized water and the pH was corrected to 7.0 with 1 M NaOH before autoclaving at 121°C for 15 minutes.

Table 8 : Recipe for the preculture with the medium with a supplement of salts and vitamin.

Product	Concentration
Glycerin	10 g/L
Yeast extract	24 g/L
KH_2PO_4	1.0 g/L
K_2HPO_4	4.0 g/L
NH_4Cl	1.0 g/L
K_2SO_4	2.4 g/L
$CaCl_2$ solution	10 mL/L
$MgSO_4$ solution	3.0 mL/L
Thiamin solution	0.8 mL/L
Ampicillin solution	1.0 mL/L
ECPM TES	2.0 mL/L

The precultures were done in 500 mL shake flasks and contained 150 mL of medium. A colony from a NA agar plate was picked and transferred to the precultures to incubate at 30°C and 150 rpm until an OD_{600} of 3 to 8 is obtained.

The culture was made according to *table 9*.

Table 9 : Recipe for the culture with the medium with a supplement of salts and vitamin.

Product	Concentration
Glycerin	10 g/L
Yeast extract	24 g/L
KH_2PO_4	1.0 g/L
K_2HPO_4	4.0 g/L
NH_4Cl	1.0 g/L
K_2SO_4	2.4 g/L
$CaCl_2$ solution	10 mL/L
$MgSO_4$ solution	0.8 mL/L
Thiamin solution	1.0 mL/L
Ampicillin solution	1.0 mL/L
ECPM TES	3.0 mL/L

The glycerin, yeast extract, KH_2PO_4, K_2HPO_4, NH_4Cl and K_2SO_4 were solubilized together in demineralized water and the pH was corrected to 7.0 with 1 M NaOH before autoclaving at 121°C for 15 minutes.

The cultures were done in 2.5 L Ultra Yield flasks and contained 1 L of medium with 50 mL of preculture. The incubation was set to 37°C and 140 rpm.

All the information regarding the preparation of this medium were given orally by Prof. S. Crelier.

OD_{600} measurements

The growth of cultures was followed by measuring periodically the OD_{600} with a spectrophotometer until the late log-phase or early stationary phase was reached.

Cell dry weight concentration quantification

Final cell dry weight concentrations of the cultures were determined before harvest by pipetting 5 mL of culture in triplicate on a tared filter which is then dried at 100°C and weighted.

Calculations related to method 3.2.2 "Medium selection"

- $Volume\ of\ preculture\ to\ add\ [mL] = \frac{0.1 \cdot V}{(OD_{600,p} - OD_{600,m})}$

Equation 4 : Volume of preculture to add to culture to have a starting OD_{600} of 0.1.

V : volume of culture [mL]

$OD_{600,\ p}$: OD_{600} of preculture [-]

$OD_{600,\ m}$: OD_{600} of medium [-]

- To obtain the maximal specific growth rate, the natural logarithm of OD_{600} was plotted against time and a regression line was then performed on the exponential phase giving the following equation :

$$y = a * x + b$$

Equation 5 : Regression line equation on the exponential phase where OD_{600} was plotted against time.

y [-] : natural logarithm of OD_{600}

b [-] : intercept of regression line

a [h^{-1}] : slope of regression line, corresponding to the maximal specific growth rate μ_{max}

x [h] : time

- $Cell\ dry\ weight\ concentration\ \left[\frac{g}{L}\right] = \frac{(m_2 - m_1)}{V}$

Equation 6 : Determination of cell dry weight concentration of cultures.

m_2 : filter mass after filtration of culture [mg]

m_1 : filter mass tare [mg]

V : volume of culture filtered [mL]

3.2.3 *E. coli* XL1-BLUE pUC18 culture and harvest

Culture

Medium preparation was the same as described in *method 3.2.2 "LB medium and TB medium".*

The precultures were done in 250 mL shake flasks and contained 50 mL of TB medium. A colony from a NA agar plate was picked and transferred to the precultures to incubate overnight at 37°C and 140 rpm.

The cultures were done in 5 L shake flasks and contained 1 L of TB medium with an initial OD_{600} of 0.1. The incubation was set to 37°C and 140 rpm.

The growth of the cultures and cell dry weight concentration were determined as described in *method 3.2.2 "OD_{600} measurements" and "Cell dry weight concentration quantification".*

Harvest

Harvest was done with 3 possible methods. The first one consisted of centrifugating cultures in 500 mL fractions at 6000 x g for 15 minutes at 4°C.

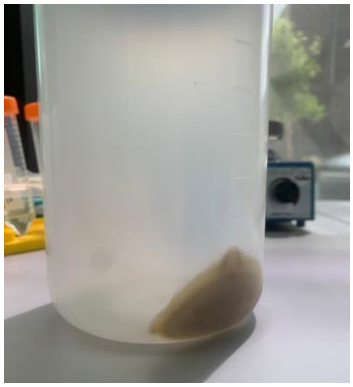

Figure 32 : Harvest of biomass by centrifugation.

The second harvest method is transferring cultures to separatory funnels which were left to sediment overnight at 4°C. The biomass concentrated at the bottom was collected in 50 mL Falcon tubes and centrifuged at 10000 x g for 15 minutes at 4°C.

Figure 33 : Harvest of biomass by sedimentation with separatory funnels.

The last method is constant pressure depth filtration at 0.4-0.6 or 0.2-0.4 µm and 1.5-2.0 bar. The filters used were the Fibrafix AF ST 140 and 130 with a diameter of 90 mm from Filtrox AG.

Figure 34 : Harvest of biomass by depth filtration.

Wet biomass obtained from any of the separation methods mentioned was washed with PBS at a pH of 7.4.

Table 10 : Recipe for the preparation of the PBS buffer (Stjohnslabs.com, 2023).

Product	Concentration
KH_2PO_4	0.24 g/L
KCl	0.2 g/L
Na_2HPO_4	1.42 g/L
NaCl	8.0 g/L

The pH was adjusted with NaOH 1 M to 7.4 and the solution was autoclaved at 121°c for 15 minutes. Biomass from cultures made on the same day were pooled together and stored at -20°C.

Calculations related to method 3.2.3 "E. coli XL1-BLUE pUC18 culture and harvest"

The calculations are the same as in *method 3.2.2 "Calculations related to method 3.2.2 "Medium selection"".*

3.2.4 Cell lysis

Biomass suspension preparation

The biomass dry matter content was determined with the moisture analyzer from a mixture of 1 g of biomass and 5 g of water. The biomass suspension was then prepared at 4 g/L of dry biomass in TE buffer before lysis.

Table 11 : Recipe for the preparation of 1 L of TE buffer (Aatbio.com, 2023).

Product	Quantity	Final concentration
Tris-base 1 M stock solution	10 mL	0.01 M
EDTA 0.5 M stock solution	2 mL	0.001 M
Demineralized water	988 mL	-

The Tris and EDTA stock solutions were adjusted to pH 8.0 with 6 M HCl and solid NaOH, respectively, before combination. Once combined, the solution was autoclaved for 15 minutes at 121°C. All prepared lysates were filtered on the same day to ensure the preservation of pUC18.

French press lysis

The Pressure Cell Homogenizer from Stansted was first sanitized with 0.5 M NaOH for 15 minutes and rinsed with TE buffer until a pH of 8 was reached to ensure correct NaOH rinsing. The suspension at 4 g/L of dry biomass was then lysed at 720-790 bar in two cycles while lysates were kept on ice between cycles to minimize temperature increase.

The lysates for filtration were prepared with this method but an experience was also performed at 750 bar and 1000 bar for 4-5 cycles to find the most adequate conditions.

Bead mill lysis

180 mL of glass beads with a diameter of 0.50-0.75 mm were added in the reservoir of the FlexMill-Lab C from Frewitt which was then filled with 0.5 M NaOH. Sanitization was done for 20 minutes at 300 mL/min. The rotor was set to 310 rpm. The whole system was then rinsed with TE buffer until a pH of 8 was obtained to ensure correct NaOH rinsing, still at 300 mL/min and 310 rpm.

The water-cooling system was set to 15.2°C and 0.98 L/min while the circulation of the mechanical seal circulation was set to 1.52 bar and 1.19 L/min.

295 mL of suspension at 4 g/L of dry biomass was added at 500 mL/min while the rotor was set to 1500 rpm. The time and the temperature before and after the grinding head were monitored during the whole process. A 2 mL sample was taken every 2 minutes for 35 minutes in total.

This method wasn't used to obtain the lysates for filtration and only a preliminary experience to find adequate conditions was done.

Calculations related to method 3.2.4 "Cell lysis"

- $Biomass\ dry\ matter\ [\%] = \frac{b_d}{\frac{b_w \cdot s_2}{s_1}} \cdot 100$

Equation 7 : Determination of the dry mass percentage in harvested biomass.

s_1 : suspension mass [g]

b_w : wet biomass mass in suspension [g]

s_2 : initial suspension mass loaded on moisture analyzer [g]

b_d : dry mass [g]

3.2.5 Filtration of the lysates

PURASPIN®

The types of Puraspin® and filter aids used are described in the following table :

Table 12 : Physical characteristics and components of the filter aids (Celpure®) and Puraspin® devices used (Filtrox AG 2-3-4-5-6-7-8-9, 2020).

Filter aid	**Permeability [md]**
Celpure® C1000	750-1250
Celpure® C300	150-300
Celpure® C100	70-140
Celpure® C65	40-80
PURASPIN®	**Retention rate [µm]**
PURASPIN® CH 09	10.0-30.0
PURASPIN® CH 31	5.0-12.0
PURASPIN® CH 71	1.5-3.0
PURASPIN® CH 130	0.4-0.6

All the sixteen combinations possible were tested in triplicate.

8 mL of ultrapure water were added to Puraspin® tubes and centrifuged at 4000 x g for 4 minutes (6 minutes for the CH 130 filter). The filtrate was discarded.(Filtrox AG 2, 2023).

15 mL of lysate was mixed with 57 g/L of filter aid and added to the tubes. The tubes were centrifuged at 4000 x g for 4 minutes (6 minutes for the CH 130 filter). The filtrates were kept at -20°C.

PURAFIX® BIO SD 2" capsule

All metallic and glass parts in contact with the lysate were treated overnight at 200°C to remove endotoxin contaminants. Before each filtration trial, the system was rinsed with 800 mL of ultrapure water at 120 mL/min, 200 mL of NaOH 1 M at 40 mL/min and finally 800 mL of ultrapure water at 120 mL/min. The pH of the filtrate was checked to evaluate if NaOH was correctly rinsed. The filter was placed and rinsed with 100 mL of ultrapure water.

350 mL of lysate was mixed with 57 g/L of filter aid in a beaker and placed on a magnetic stirrer on a low agitation speed. Mixing must be ensured for five minutes before starting the filtration process. The peristaltic pump must be the highest point in the installation. The pressure, filtrate volume, flux and time were monitored every two minutes until maximal differential pressure or a maximal value of 2.5 bar was reached. The maximal cake height should be 3 cm and the minimal flux should be 300-350 L/(m^2·h) (Filtrox AG 2, 2023).

The Purafix® filters and filter aids combinations performed are described in the following table with the flow rate set on the pump during filtration.

Table 13 : Combinations of filter aid grade and Purafix® types and feed rates for the PURAFIX® BIO SD 2" capsule trials.

Filter aid	PURAFIX® BIO SD filter	Pump set flow rate [mL/min]	Filtrate theorical flux [L/(m²·h)]
Celpure® C1000	PURAFIX® BIO SD CH 130	20.00	571
Celpure® C300	PURAFIX® BIO SD CH 71	20.00	571
Celpure® C100	PURAFIX® BIO SD CH 71	15.00	429

Those combinations were chosen based on turbidity reduction, pUC18 recovery and endotoxin removal results obtained with the Puraspin® filtrations.

Calculations related to method 3.2.5 "Filtration of the lysates"

- $\Delta p = \eta \cdot \alpha \cdot c_{ms} \cdot \left(\frac{Q_f}{A}\right)^2 \cdot t + \eta \cdot \beta \cdot \frac{Q_f}{A}$

Equation 8 : Mathematical model of depth filtration at constant rate.

Δp : differential pressure [Pa]

η : dynamic viscosity [kg/m·s)]

α : cake specific resistance [m/kg]

c_{ms} : dry matter concentration in filtrate [kg/m³]

Q_f : suspension flow rate [m³/s]

A : filter area [m²]

t : time [s]

β : filter resistance [m⁻¹]

3.2.6 Endotoxin quantification

This method is based on the article of Bucsella B *et al.*

Samples were treated in an ultrasonic bath for 45 minutes. 1 mL of each sample was filtered through a syringe filter with a 0.45 µm porosity. 100 µl of filtered samples (diluted with ultrapure water 50 times for filtrates or 100 times for lysates), a blank consisting of ultrapure water and a 2-keto-3-deoxyoctonate ammonium salt (KDO) standard at 250 ng/mL were placed in screw cap tubes with 2 µl of 100% acetic acid. The tubes were vortexed, spinned down and incubated at 80°C for 1.5 hours. Tubes were then immediately put on ice and centrifuged for 5 minutes at 10000 rpm (11800 x g) and 4°C.

100 µl of a solution containing 1,3-benzodioxole-5,6-diamine dihydrochloride (DMB) was added in a room with low light exposure to avoid light degradation. The solution contained 14 mM DMB, 16.11% (v/v) acetic acid, 3.5% (v/v) 2-mercaptoethanol, 36 mM sodium thiosulfate. The volume was completed with ultrapure water. Tubes were incubated at 60°C for 1.5 hours, put immediately on ice and centrifuged for 5 minutes at 10000 rpm (11800 x g) and 4°C.

The content of the tubes was transferred to brown vials containing a 300 µL insert and analyzed by RP-HPLC with a YMC-Triart C18 ExRS column.

The HPLC system was rinsed as described in *table 14*.

Table 14 : Conditions for the rinsing of the HPLC system and column for endotoxin quantification. The "" means the valve is open and nothing passes in the column.*

Duration [min]	Flowrate [mL/min]	Ultrapure water [%]	Methanol 64%, Acetonitrile 34% [%]
5	5.000*	40.00	60.00
30	0.150	20.00	80.00
5	0.250	100.00	0.00
45	0.310	100.00	0.00

The mobile phase is described in *table 15*.

Table 15 : Composition of the mobile phase for endotoxin quantification.

Time [min]	Ultrapure water [%]	Methanol 64% Acetonitrile 34% [%]
0.00	100.00	0.00
0.10	89.00	11.00
9.60	89.00	11.00
9.70	5.00	95.00
13.70	5.00	95.00
14.00	100.00	0.00

The main parameters for the RP-HPLC and FLD detector are resumed in *table 16*.

Table 16 : Main parameters for the RP-HPLC and FLD detector for endotoxin quantification.

Injection volume	10.00 µL
Column temperature	40.0 °C
Sample temperature	4.0 °C
Fluorescence detection	Excitation : 373 nm Emission : 448 nm

Calculations related to method 3.2.6 "Endotoxin quantification"

- $KDO\ concentration\ \left[\frac{ng}{mL}\right] = \frac{x \cdot d \cdot std_{conc.}}{std}$

Equation 9 : Determination of the KDO concentration for endotoxin quantification.

x : sample peak area [LU·s] or height [LU]

d : dilution factor [-]

$std_{conc.}$: KDO standard concentration [ng/mL]

std : KDO standard peak area [LU·s] or height [LU]

- $Endotoxin\ concentration\ [\frac{ng}{mL}] = \frac{KDO_{conc.}}{f}$

Equation 10 : Determination of endotoxin concentration.

$KDO_{conc.}$: KDO concentration [ng/mL]

f : fraction of KDO in endotoxin [-] (w/w)

- $Endotoxin\ concentration\ \left[\frac{EU}{mL}\right] = ET_{conc.} \cdot\ ET_{activity}$

Equation 11 : Determination of endotoxin concentration.

$ET_{conc.}$: endotoxin concentration [ng/mL]

$ET_{activity}$: endotoxin biological pyrogenic activity [EU/ng]

3.2.7 dsDNA quantification and purification

dsDNA quantification by Qubit

A working solution was first prepared by diluting the dsDNA BR reagent 1:200 in dsDNA BR buffer. The two standards (0 and 100 ng/µL) were prepared by adding 10 µl to 190 µl of working solution in 0.5 mL tubes (Tools.thermofisher.com, 2023).

The samples were prepared by adding 5 µl to 195 µl of working solution in 0.5 mL tubes. Filtrate samples were first centrifuged for 5 minutes at 10000 x g before 5 µl of supernatant are added.

Tubes were vortexed for 2-3 seconds, incubated at room temperature for 2 minutes and measured with the Qubit fluorometer.

dsDNA quantification by TapeStation 4150

1 µl of sample or Genomic DNA Ladder was added to 10 µl of Genomic DNA Sample Buffer in the specific tubes of the TapeStation 4150. Samples were diluted with sterile water if the concentration in dsDNA was superior to 100 ng/µl (Agilent.com 1, 2023).

Once capped, the tubes were vortexed using the IKA MS3 vortexer at 2000 rpm for 1 minute and spinned down for another minute. Caps were removed and placed in the instrument. The genomic DNA ScreenTape device was flicked to eliminate any bubbles and inserted in the TapeStation instrument for analysis.

Plasmid purification by Miniprep

Plasmid purification follows a modified Monarch® Plasmid Miniprep Kit (International.neb.com, 2023).

Samples were first centrifuged for 5 minutes at 10000 x g. 200 µL of the supernatant and 200 µL of Plasmid Lysis Buffer were added to 1.5 mL sterile tubes which were then inverted gently 5-6 times and incubated 1 minute at ambient temperature. Neutralization was done by adding 400 µL of Plasmid Neutralization Buffer, inverting the tubes and incubating 2 minutes at ambient temperature.

Tubes were centrifuged 5 minutes at 16000 x g and the supernatant was transferred to the spin columns. The spin columns were centrifuged for 1 minute and the flow-through was discarded. 200 µL of Plasmid Wash Buffer 1 were added and spin columns were centrifuged for 1 minute at 16000 x g. 400 µL of Plasmid Wash Buffer 2 were added and spin columns were centrifuged for 1 minute at 16000 x g.

The columns were placed on new sterile 1.5 mL tubes and 30 µL of DNA Elution Buffer were added. After an incubation of 1 minute at ambient temperature, the tubes were centrifuged 1 minute at 16000 x g to elute DNA.

Yield determination of plasmid purification

The yield of this method was determined by lysing in triplicate 1.5 mL of a suspension at 4 g/L of dry biomass in TB medium following the Monarch® Plasmid Miniprep Kit.

The suspension was centrifuged for 30 seconds at 16000 x g in sterile 1.5 mL tubes and the supernatant was discarded. The pellet was resuspended in 200 µL Plasmid Resuspension Buffer and mixed by vortexing. The addition of Plasmid Lysis Buffer and remaining steps are the same as described in *method 3.2.7 "dsDNA quantification and purification - Plasmid purification by Miniprep"*.

Out of the 30 µL resulting from the Miniprep, 10 µL were used for total dsDNA quantification using the *method 3.2.7 "dsDNA quantification and purification - dsDNA quantification by Qubit"* while the remaining 20 µL were diluted with 180 µL of TE buffer. This 200 µL solution was then purified again according to *method 3.2.7 "dsDNA quantification and purification - Plasmid purification by Miniprep"*.

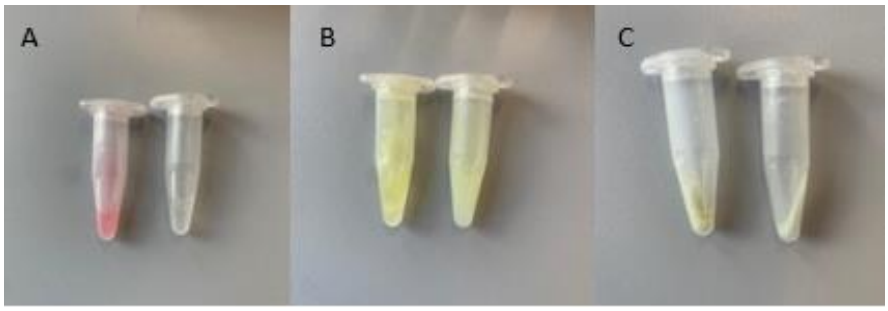

Figure 35 : Visual differences between a Miniprep on a biomass suspension (left tube) or a supernatant (right tube) after addition of (A) Plasmid Lysis Buffer and (B) Plasmid Neutralization Buffer and (C) pellet after neutralization.

Agarose gel

A sample purified by Miniprep was analyzed on agarose gel (HES-SO Valais Wallis, 2023). The first enzymatic reaction is done to linearize the plasmid according to *table 17*.

Table 17 : Preparation of the first enzymatic reaction with a Miniprep sample containing pUC18 and the XbaI enzyme for an agarose gel.

	Initial concentration	**Quantity needed**	**Volume [µL]**
Miniprep sample pUC 18 DNA	43.1 ng/µL	500 ng	11.6
CutSmart Buffer	10x	1x	2.0
XbaI	20.0 U/µL	10.0 U	0.5
Sterile water	-	-	5.9
Total volume	20.0 µL		
Incubation time	1 h		
Incubation temperature	37°C		

The second enzymatic reaction consists in cutting the plasmid in two specific parts according to *table 18*.

Table 18 : Preparation of the second enzymatic reaction with a Miniprep sample containing pUC18 and the BsaI and BseYI enzymes for an agarose gel.

	Initial concentration	Quantity needed	Volume [µL]
Miniprep sample pUC 18 DNA	43.1 ng/µL	500 ng	11.6
CutSmart Buffer	10x	1x	2.0
BsaI	20.0 U/µL	10.0 U	0.5
BseYI	20.0 U/µL	10.0 U	0.5
Sterile water	-	-	5.4
Total volume	20.0 µL		
Incubation time	1 h		
Incubation temperature	37°C		

A negative control was also done by simply diluting the sample without any enzyme according to *table 19*.

Table 19 : Preparation of the negative control with a Miniprep sample containing pUC18 for an agarose gel.

	Initial concentration	Quantity needed	Volume [µL]
Miniprep sample pUC 18 DNA	43.1 ng/µL	200 ng	4.6
Sterile water	-	-	5.4
Total volume	10.0 µL		

The gel was prepared by adding 1% agarose in TBE 1X with the addition of 5 µL of PeqGREEN. The samples were loaded on the gel as described in *table 20*.

Table 20 : Volume of Gel Loading Dye Purple to add in function of the total volume of sample.

Sample volume	20.0 µL	10.0 µL
Gel Loading Dye Purple volume to add	5.0 µL	2.0 µL

Migration was then started at 140 V for 40 minutes.

The NEBcutter® tool software (v3.0.17) from Biolabs was used to determine the expected bands after enzymatic reactions. The sequence of pUC18 was also directly given by the NEBcutter® tool.

Calculations related to method 3.2.7 "dsDNA quantification and purification"

- $Miniprep\ purification\ yield\ [\%] = \frac{M_2 \cdot V_2}{M_1 \cdot V_1} \cdot 100$

Equation 12 : Determination of the yield of a Miniprep purification.

M_1 : total dsDNA concentration of sample after first Miniprep purification [ng/µL]

V_1 : volume of sample after first Miniprep purification for second purification [µL]

M_2 : total dsDNA concentration of sample after second Miniprep purification [ng/µL]

V_2 : volume of sample after second Miniprep purification [µL]

- $pUC18\ concentration\ \left[\frac{ng}{\mu L}\right] = \frac{\frac{c_2}{c_3} \cdot c_1 \cdot V_2}{V_1} \cdot \frac{100}{Y}$

Equation 13 : Determination of the pUC18 plasmid concentration.

c_1 : total dsDNA concentration of sample after Miniprep purification by Qubit [ng/µL]

c_2 : pUC18 concentration of sample after Miniprep purification by TapeStation 4150 [ng/µL]

c_3 : total dsDNA concentration of sample after Miniprep purification by TapeStation 4150[ng/µL]

V_1 : volume of sample before Miniprep purification [µL]

V_2 : volume of sample after Miniprep purification [µL]

Y : yield of purification by Miniprep [%]

3.2.8 Proteins quantification

The calibration curve was done by diluting with demineralized water a stock solution of BSA at 2.0 g/L to obtain the following BSA concentrations : 0, 0.05, 0.1, 0.2, 0.4, 0.6, 0.8 and 1.0 g/L (HES-SO Valais Wallis 1, 2023).

Samples were first centrifuged for 5 minutes at 10000 x g and diluted with demineralized water either 4 times for filtrates or 20 times for lysates.

200 µL of Bradford reagent were added to a 96 wells plate with 10 µL of supernatant or standard. The plate was incubated 10 minutes at ambient temperature and the absorbance was measured at 595 and 450 nm. All measurements were done in triplicate.

Calculations related to method 3.2.8 "Proteins quantification"

A calibration curve was made by plotting the ratio of absorbances at 595 nm to 450 nm against the corresponding BSA standards. A regression line was then performed.

- $Protein\ concentration\ \left[\frac{g}{L}\right] = \frac{\left(\frac{A_{595\ nm}}{A_{450\ nm}}\right) - b}{a} \cdot d$

Equation 14 : Determination of the proteins quantification.

$A_{595\ nm}$: absorbance at 595 nm [-]

$A_{450\ nm}$: absorbance at 450 nm [-]

d : dilution factor [-]

a : slope of regression line [L/g]

b : intercept of regression line [-]

The protein concentration is given in BSA equivalent.

3.2.9 Turbidity

5 mL of filtrate or lysate were added to glass tubes and placed in the turbidimeter for measurement. No dilutions were needed.

3.2.10 Viscosity

20 mL of lysate was added in the metallic tube which was then placed in the rheometer for measurement. No dilution is needed.

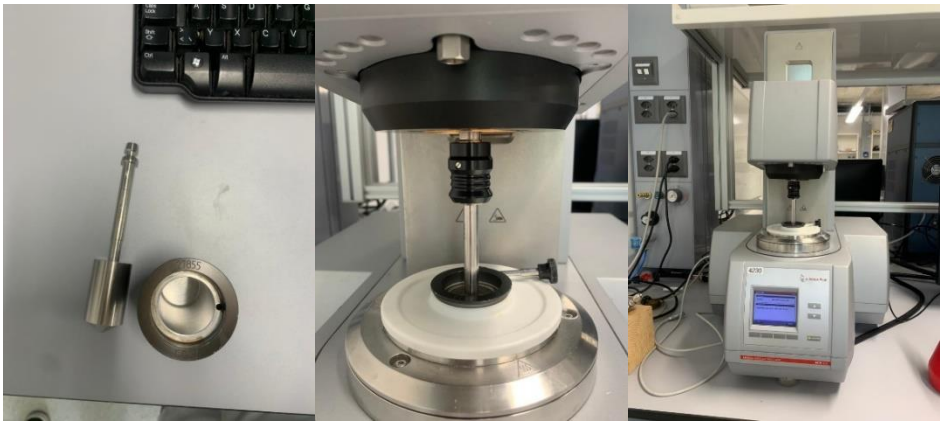

Figure 36 : The Modular Compact Rheometer from Anton Paar for the measurement of viscosity.

4. Results and discussion

4.1 Medium selection

Five different mediums were tried according to *method 3.2.2 "Medium selection"* to find the most appropriate one for *E. coli* XL1-Blue pUC18. The OD_{600} over time for the four cultures with a volume of 100 mL are shown in *figure 37*.

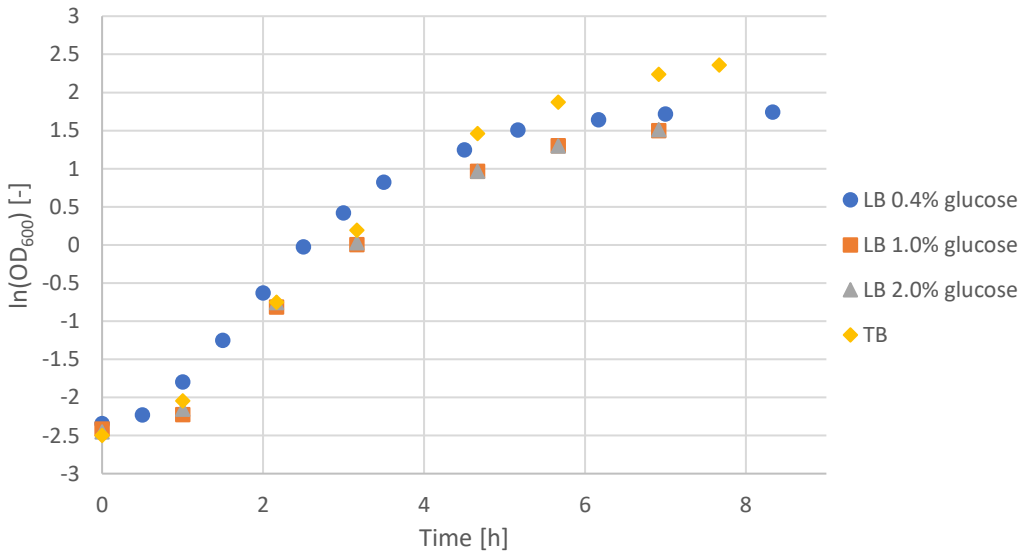

Figure 37 : Natural logarithm of OD_{600} in function of time for four cultures of E. coli XL1-Blue, each with a different medium.

The OD_{600} of the culture with medium supplemented with salts and vitamin was not measured in its entirety as the stationary phase was still not reached after 25.5 hours so the incubation had to be continued overnight with no possibility of measurement. It is unknown how many hours were needed for *E. coli* XL1-BLUE to reach stationary phase.

Table 21 : Duration and corresponding OD_{600} of the culture and preculture with the medium supplemented with salts and vitamin.

	Duration [h]	OD_{600} [-]
Preculture	19.3	6.463
Culture	0.0	0.444
	25.5	6.654
	41.5	10.274

The final OD_{600}, incubation time, cell dry weight concentration and maximal specific growth rates of the five mediums are resumed in *table 22*.

Table 22 : OD_{600}, incubation time, cell dry weight concentration and μ_{max} at the end of cultures with five different media.

	Duration [h]	OD_{600} [-]	CDW [g/L]	μ_{max} [h^{-1}]
LB 0.4% glucose	8.3	5.701	1.96 ± 0.13 (±0.05;95%;3)	0.68
LB 1.0% glucose	6.9	4.469	-	0.63
LB 2.0% glucose	6.9	4.539	-	0.63
TB	7.7	10.564	3.97 ± 0.35 (±0.14; 95%;3)	0.68
Medium with supplement of salts and vitamin	41.5	10.274	-	-

The best medium for the growth of *E. coli* XL1-BLUE was the TB medium as the OD_{600} was among the highest and having the highest biomass concentration possible is the main criteria.

The culture with the medium supplemented with salts and vitamin reached a similar OD_{600}. However, the duration was much longer and more components were needed. This medium was tested as reported final OD_{600} were in the vicinity of 40 after 25 h for the strain *E. coli* DH5α with an agitation of 180 rpm (oral communication by Prof. S. Crelier). Flasks were covered with aluminum foil as opposed to traditional seals resulting in less aeration. Differences in yeast extract composition, strain and agitation can also have an influence.

In literature, a maximal specific growth rate of 0.58 h^{-1} in TB medium and 0.63 h^{-1} in LB medium was found for the *E. coli* strain DH5α with a 6.0 kbp plasmid. The growth conditions were similar with a temperature of 37°C and an agitation speed of 150 rpm using 250 mL shake flasks with an 80% headspace. The exact stationary phase period and the effect of the plasmid are however unknown (Galindo J *et al.*, 2016).

TB producing a higher titer of biomass is in accordance with the literature confirming this medium is ideal for plasmid production (Wood WN *et al.*, 2016).

Cultures with the selected TB medium were scaled-up to 1 L in 5 L shake flasks according to *method 3.2.3 "E. coli XL1-BLUE pUC18 culture and harvest"*. Three trials consisting of three separate shake flasks each were done, and their growth are shown in *figure 38*.

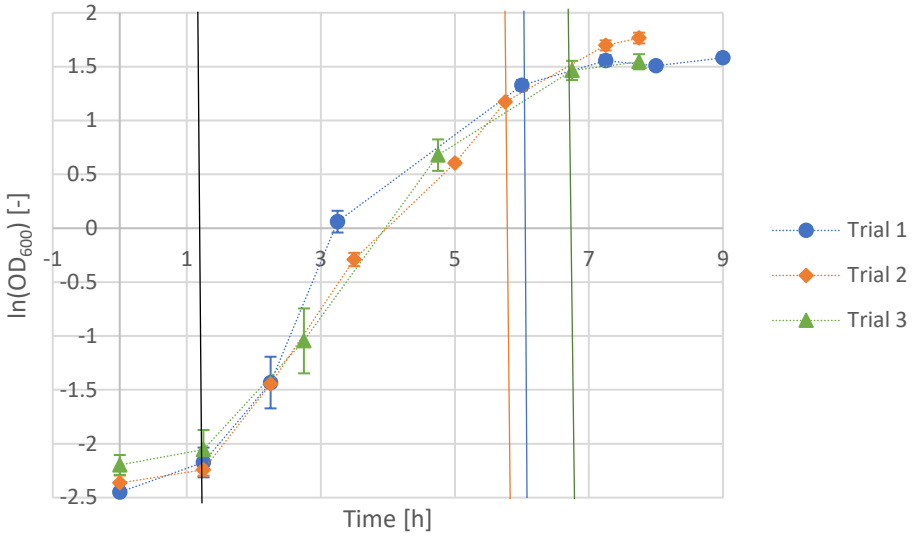

Figure 38 : Natural logarithm of OD_{600} in function of time for three trials in TB medium, each consisting of three cultures of E. coli XL1-Blue. The black line shows the start of the exponential phase while the colored lines show the end for each trial.

Table 23 : Final cell dry weight of three trials in TB medium each consisting of three cultures of E. coli XL1-Blue.

	Culture	CDW [g/L]
Trial 1	1	1.73 ± 0.08 (±0.03;95%;3)
	2	1.48 ± 0.08 (±0.03;95%;3)
	3	1.57 ± 0.17 (±0.07;95%;3)
Trial 2	1	1.95 ± 0.06 (±0.02;95%;3)
	2	1.95 ± 0.14 (±0.06;95%;3)
	3	1.98 ± 0.10 (±0.04;95%;3)

The cell dry weight concentration was determined for the first two trials. The concentration dropped to more than half of the concentration of the scaled-down culture.

Parameters like vessel geometry, hydrodynamic conditions, power density and gas transfer all have to be kept similar in order to ensure a proper scaled-up culture with similar growth and biomass production (Crelier S and Rüdt M 3, 2022).

For the development of a similar liquid distribution in shake flasks of different sizes, the ratio of the eccentricity of the shaker to the radius of the shake flask would have to be kept constant. Eccentricity in mathematics describes the flattening of an ellipse in comparison to a cercle (Thomas GB and Finney RL, 1979).

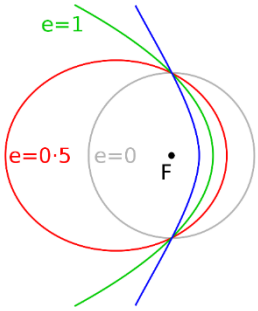

Figure 39 : Schematic description of eccentricity in mathematics (wikimedia.org, 2023).

Since usually only shakers with a fixed eccentricity are available, similar flow conditions can't occur in shake flasks of different sizes. A geometric scale-up from small to large shake flasks is therefore not possible despite a similar vessel geometry (Storhas W, 2003).

Based on figure 40, the power density does not change a lot between shake flasks sizes at the rotation speed used of 140 rpm.

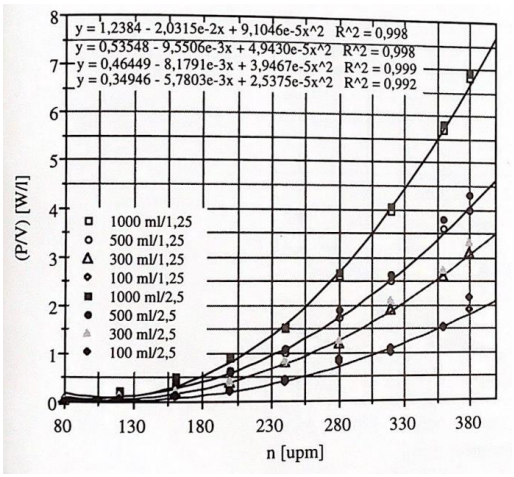

Figure 40 : Power density in function of shaking frequency at two shaking radius (1.25 or 2.5 cm) for different shake flasks without baffles (Storhas W, 2003).

It is important to note that the shake flasks used for the experiment on the figure 40 didn't have baffles like the ones used for the cultivation of *E. coli* XL1-Blue. The variation in the shape of the baffles can also have an influence on the agitation.

The percentage of air available was kept at 80% for both the 500 mL and 5 L shake flasks to try to keep the gas transfer constant. But since hydrodynamics aren't similar as stated before, the area available for transfer was therefore not the same.

The maximal specific growth rate is similar for the three trials with a coefficient of variation of 2% which means *E. coli* XL1-Blue growth is repeatable in TB medium. The scaled-down model shows however a μ_{max} of 0.68 h^{-1} which is still similar as the coefficient of variation is 6%.

Table 24 : Maximal specific growth of three trials in TB medium, each consisting of three cultures of E. coli XL1-Blue.

	μ_{max} [h^{-1}]
Trial 1	0.74
Trial 2	0.75
Trial 3	0.73
Average	0.74 ± 0.03(±0.01;95%;3)

4.2 Harvest

The classic and most effective way of harvesting the biomass and separating it from the culture is the centrifuge. However, as the centrifuge used broke down during laboratory work, alternatives had to be found.

Depth filtration at 0.4-0.6 and 0.2-0.4 µm wasn't optimal as the concentration in solids was too high and clogged the filter resulting in a very slow filtrate flux. The dry biomass recovered was 2 g from two 1 L TB medium cultures.

Using separatory funnels to sediment biomass was more effective and less time consuming. The dry biomass recovered was 5.2 g from four 1 L TB medium cultures. This method is therefore the best alternative to the centrifuge as it allows a better biomass recovery.

Those three methods are described in *method 3.2.3 "E. coli XL1-BLUE pUC18 culture and harvest"*.

4.3 Lysis

The lysis step is very important and determines the product quality. The ideal lysis should be strong enough to liberate the plasmid from the cytosol but gentle enough to not damage it. Two mechanical methods of lysis were experienced according to *method 3.2.4 "Cell lysis"*.

The first one is the bead mill. The diameter of the glass beads was 0.50 to 0.75 mm. The circulation flow rate of the suspension was 500 mL/min with a grinding head at 1500 rpm. A sanitization step with NaOH was done before proceeding to cell lysis.

The OD_{600} and total dsDNA concentration, according to *method 3.2.7 "dsDNA quantification and purification – dsDNA quantification by Qubit",* were measured for 35 minutes every 2 minutes.

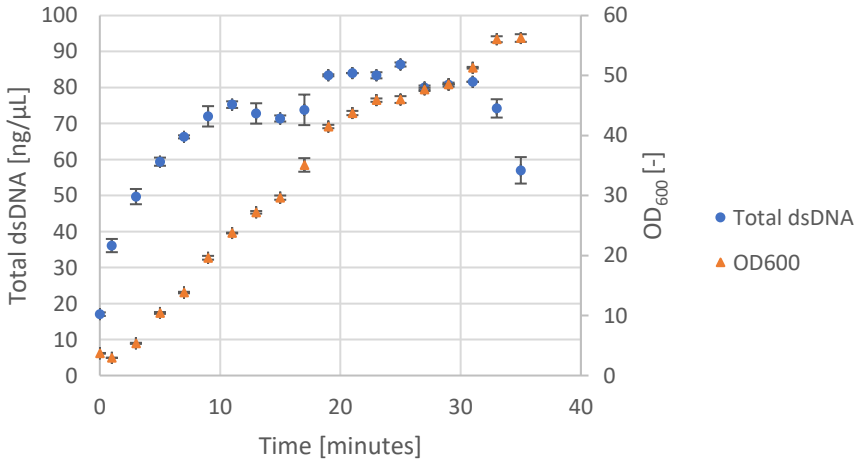

Figure 41 : Total dsDNA concentration and OD_{600} in function of time during lysis of a 4 g/L dry biomass suspension with the bead mill.

The total dsDNA concentration was maximal at 86.4 ng/µL and 25 minutes but decreased past this point. DNA damage by shearing is the most likely cause as the Qubit only measures intact dsDNA.

DNA can make up 1 to 5% of dry biomass in *E. coli*. For a 4 g/L suspension, this represents a concentration of 40 to 200 ng/µL. The maximal concentration obtained is well within that range (Zinn M, 2022).

The OD_{600} kept increasing over time. During cell lysis, the OD_{600} should decrease gradually which is not the case here (Rajnovic D *et al.*, 2019).

The lysate appeared bright white after 35 minutes but the suspension before lysis was pale yellow. 1 mL of lysate was centrifuged 10 minutes at 10000 x g. The resulting pellet consisted of three colors : a pale yellow, like a biomass pellet, mixed with black and a bright opaque white part. The pellet was then further observed under microscope.

Figure 42 : Pellet of samples taken during lysis of a 4 g/L dry biomass suspension with the bead mill.

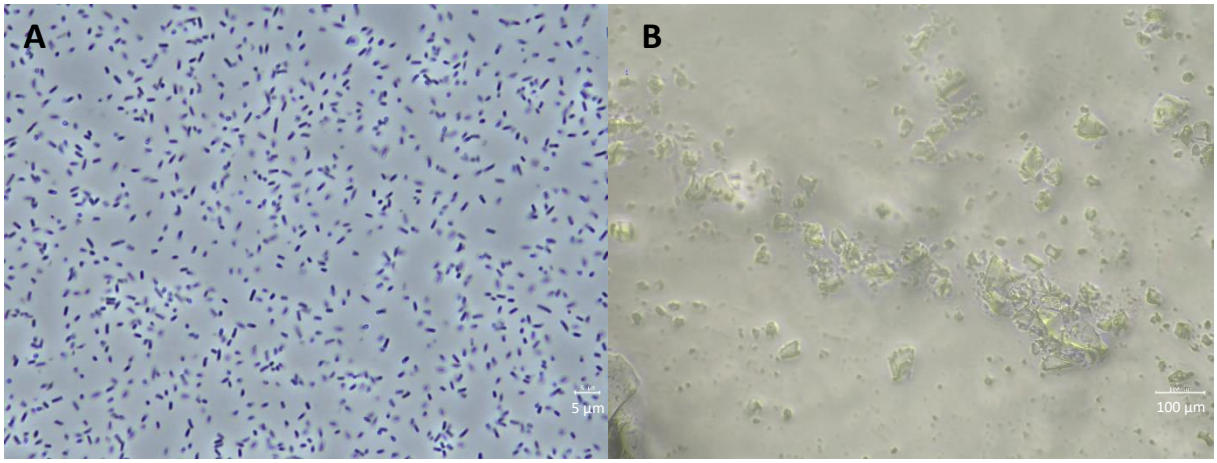

Figure 43 : (A) Pellet from a 4 g/L dry biomass suspension before lysis under a microscope. (B) Pellet from a 4 g/L dry biomass suspension after lysis with the bead mill under a microscope.

Sharp particles resembling crushed glass could be observed. The hardness of glass is 4.5 to 6.5 on the Mohs scale while the hardness of the rotor in ceramic is 7 (Surfanet.org, 2023). The rotor is most likely harder than the glass beads which results in broken beads small enough to exit the grinding head with the suspension. Using ceramic beads could have easily solve this problem.

The second method is the French Press. The pressure varied between 720 and 790 bar and five cycles were done. A sanitization step with NaOH was done before lysing a suspension of dry biomass at 4 g/L.

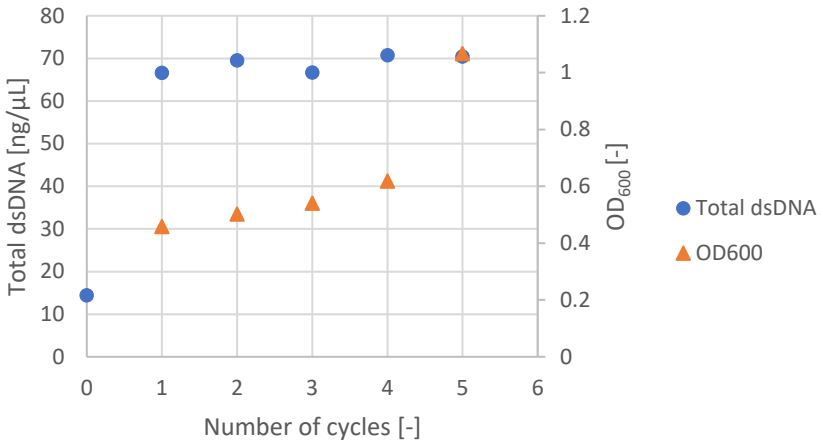

Figure 44 : Total dsDNA concentration and OD_{600} in function of time during lysis of a 4 g/L dry biomass suspension with the French Press. Initial OD_{600} at zero cycle is 4.09.

OD_{600} increased over the five cycles. The total dsDNA concentration increased for the first two cycles and was stable for the following cycles. The maximal concentration obtained is also within the range stated before of 40 to 200 ng/µL.

The optical density should decrease over the cycles as lysis increases which was not the case here. The cause of this reverse trend couldn't be explained.

A lysis performed again showed the expected trend of the optical density. The concentration of dry biomass was 10 g/L and the pressure was 1000 bar.

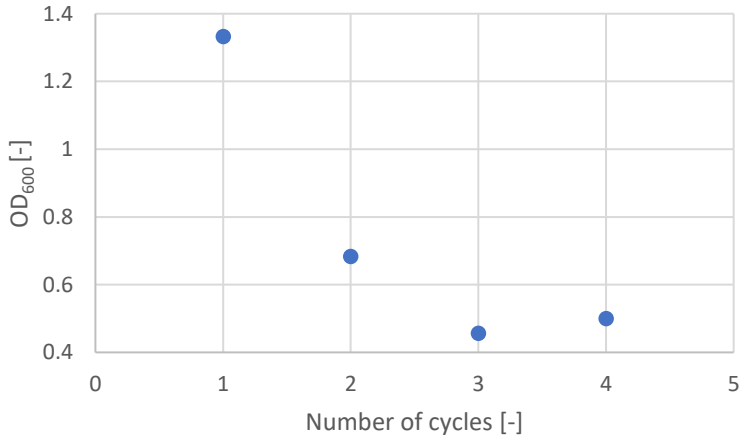

Figure 45 : OD_{600} in function of time during lysis of a 4 g/L dry biomass suspension with the French Press. Initial OD_{600} at zero cycle is 21.8.

1 mL of lysate obtained after two cycles at 720-790 bar was centrifuged 10 minutes at 10000 x g and observed under a microscope.

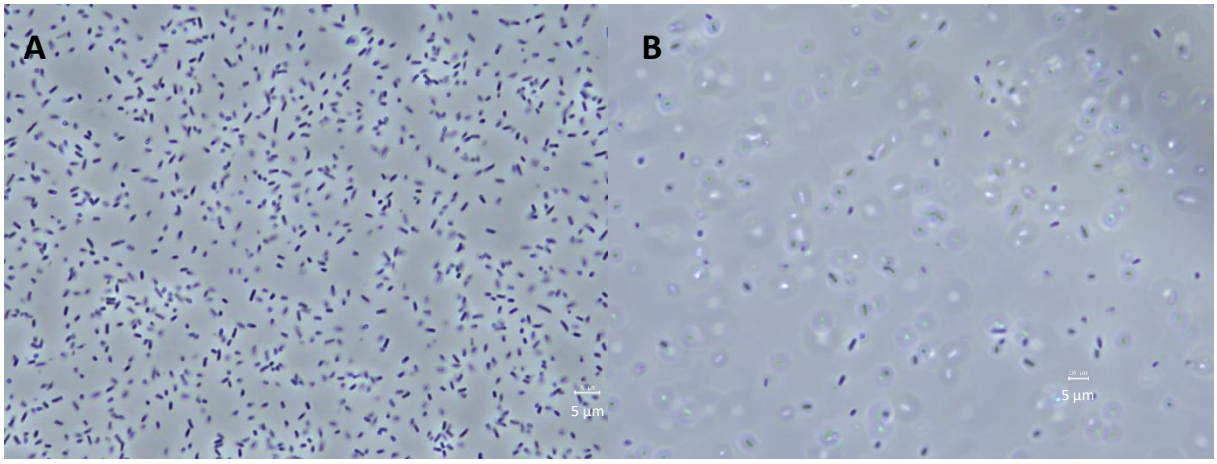

Figure 46 : (A) Pellet from a 4 g/L dry biomass suspension before lysis under a microscope. (B) Pellet from a 4 g/L dry biomass suspension after lysis with the French Press under a microscope.

Bacteria that weren't lysed were noticed since two cycles aren't enough to entirely lyse the suspension.

Proteins concentration, according to *3.2.8 "Proteins quantification"*, and temperature were also measured for the two methods of lysis.

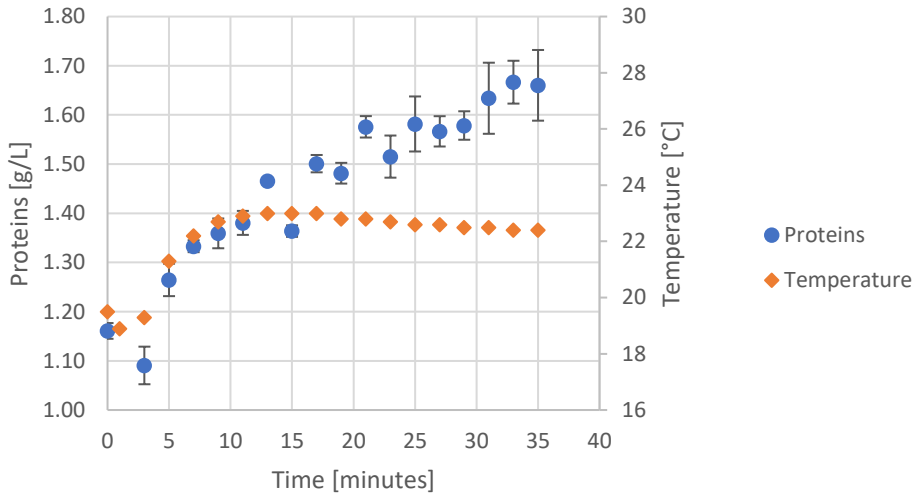

Figure 47 : Proteins concentration and temperature in function of time during lysis of a 4 g/L dry biomass suspension with the bead mill.

The bead mill cooling system was able to keep the temperature of the lysate to a maximum of 23°C. This is quite advantageous as high temperatures could potentially damage the pUC18 plasmid. The suspension was most likely not entirely lysed as the proteins concentration kept increasing over time.

Proteins can make up 15 to 75% of dry biomass in *E. coli*. For a 4 g/L suspension, this represents a concentration of 0.6 to 3 g/L. The maximal concentration obtained is well within that range (Zinn M, 2022).

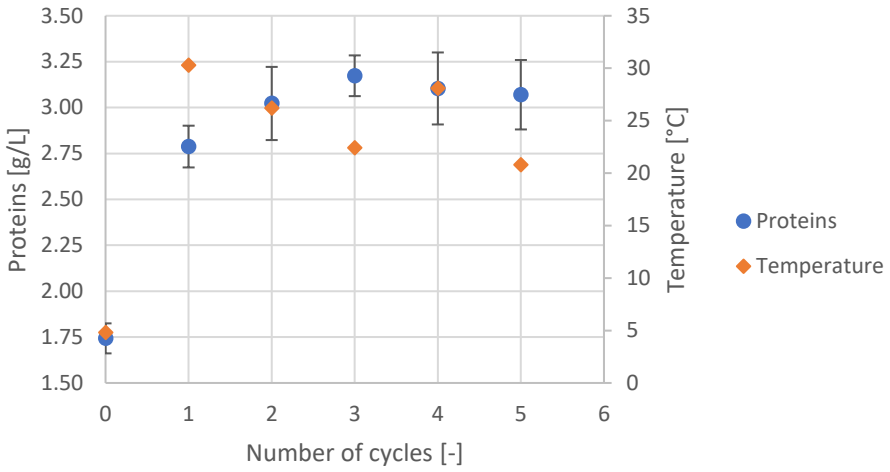

Figure 48 : Proteins concentration and temperature in function of time during lysis of a 4 g/L dry biomass suspension with the French Press.

For the French Press, the biomass suspension was kept on ice between cycles since there is not any cooling system. The temperature increase in the French Press is more important and less controllable. The proteins concentration reached a maximal value of 3.17 g/L after three cycles. The concentration in proteins seems very high. An incorrectly prepared suspension and dilution or pipetting errors are plausible.

A Miniprep lysis was performed on a non-lysed suspension of dry biomass at 4 g/L to better recognize potential peaks corresponding to pUC18 on the TapeStation device according to *method 3.2.7 "dsDNA quantification and purification – dsDNA quantification by TapeStation 4150" and* the Monarch® Plasmid Miniprep Kit (International.neb.com, 2023).

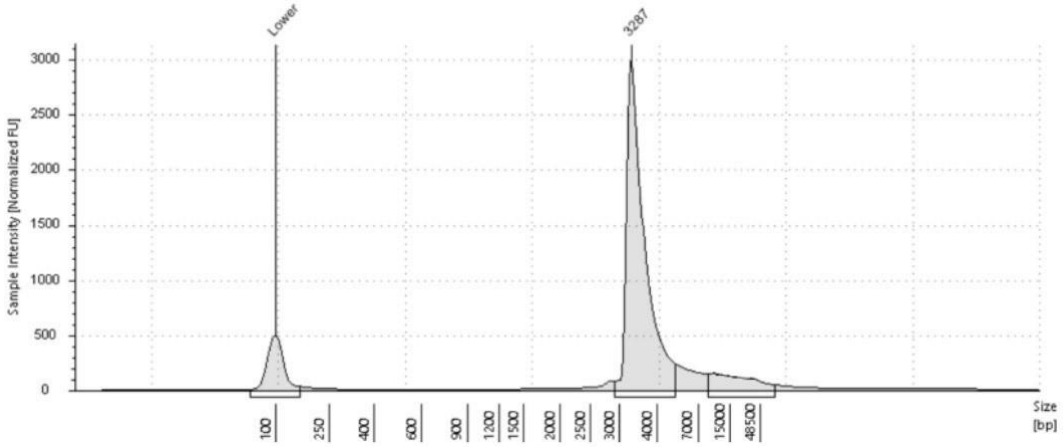

Figure 49 : Electropherogram of a 4 g/L dry biomass suspension lysed by Miniprep on the TapeStation 4150.

The electropherogram clearly shows the expected size of pUC18 in a non-linearized form. Contaminant HCD is effectively eliminated with this method and only the plasmid remains. The Miniprep kit is based on alkaline lysis which is very efficient in obtaining a relatively pure plasmid.

The two experimented lysis were then measured on the TapeStation 4150 to know whether pUC18 was found or not.

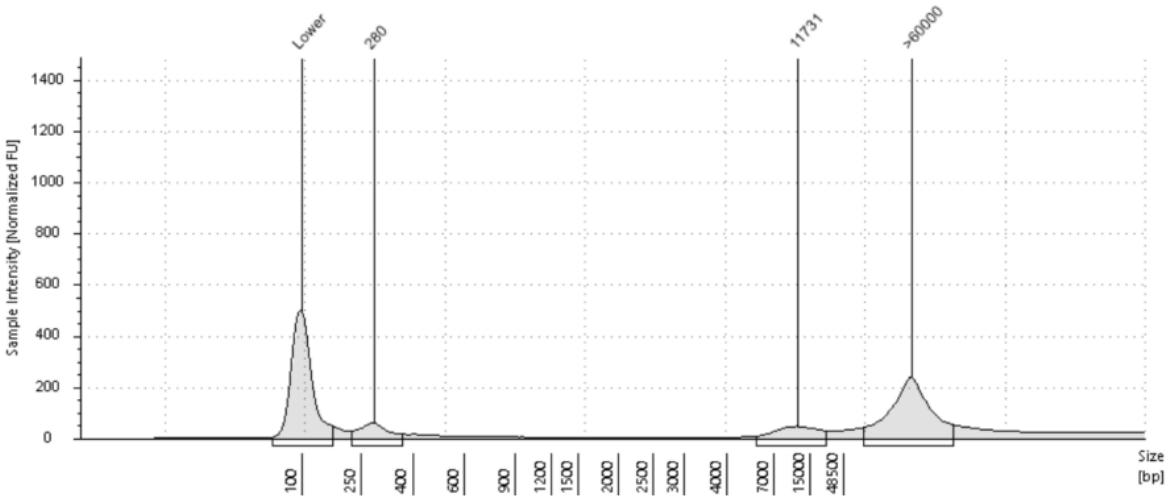

Figure 50 : Electropherogram of a 4 g/L dry biomass suspension on the TapeStation 4150.

The suspension before lysis already contained some released dsDNA. This was already observed in the *figures 41* and *44* at zero cycle and zero minute.

For the French Press method, only the lysates after one, three and five cycles were analyzed on the TapeStation 4150.

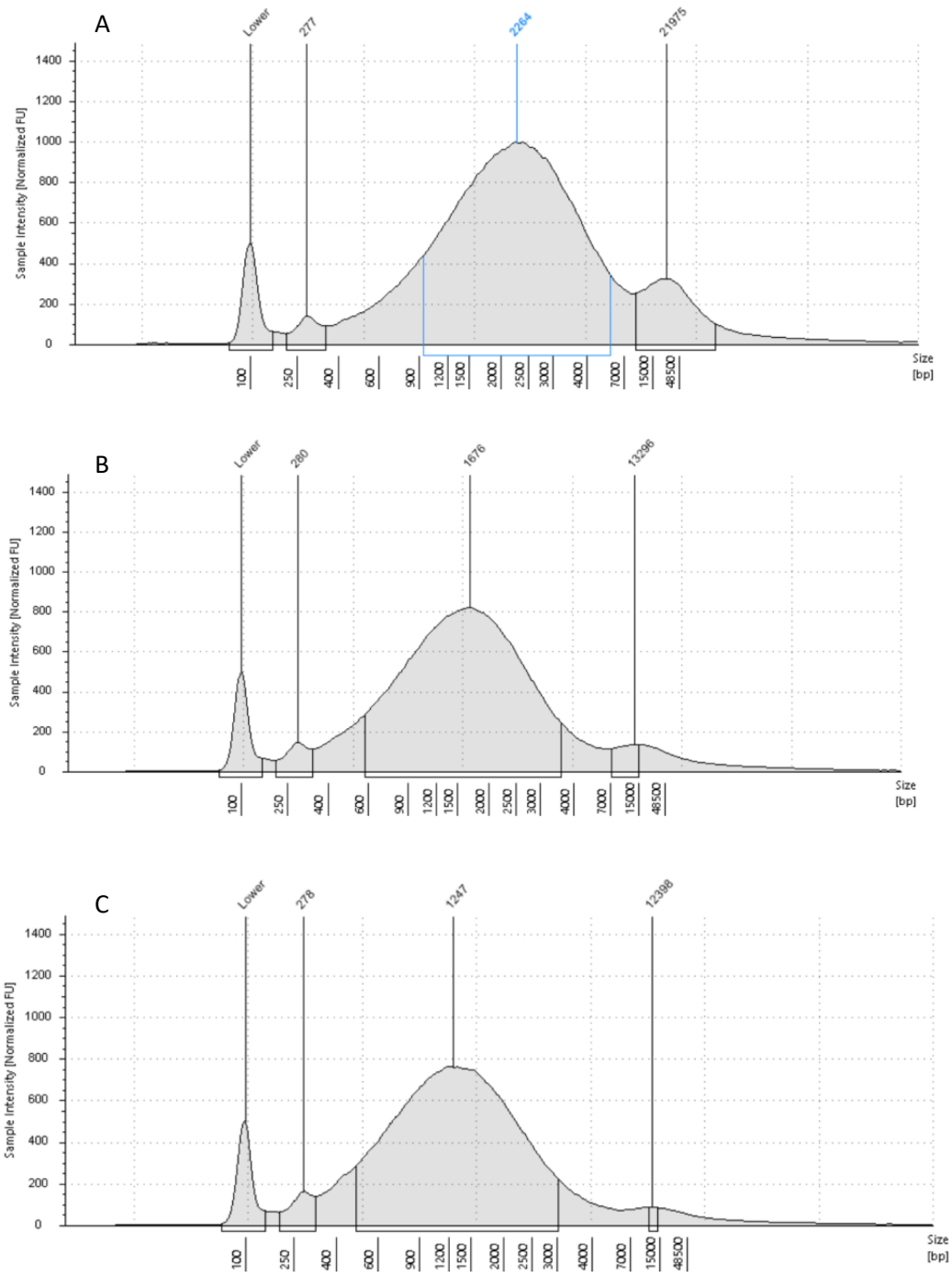

Figure 51 : Electropherogram of a 4 g/L dry biomass suspension lysed by French Press after (A) 1, (B) 3 and (C) 5 cycles, on the TapeStation 4150.

The peaks aren't very sharp and no peaks similar to the size of pUC18 could be found for the French Press method.

For the bead mill method, only the lysates obtained after 15 and 30 minutes were analyzed on the TapeStation 4150.

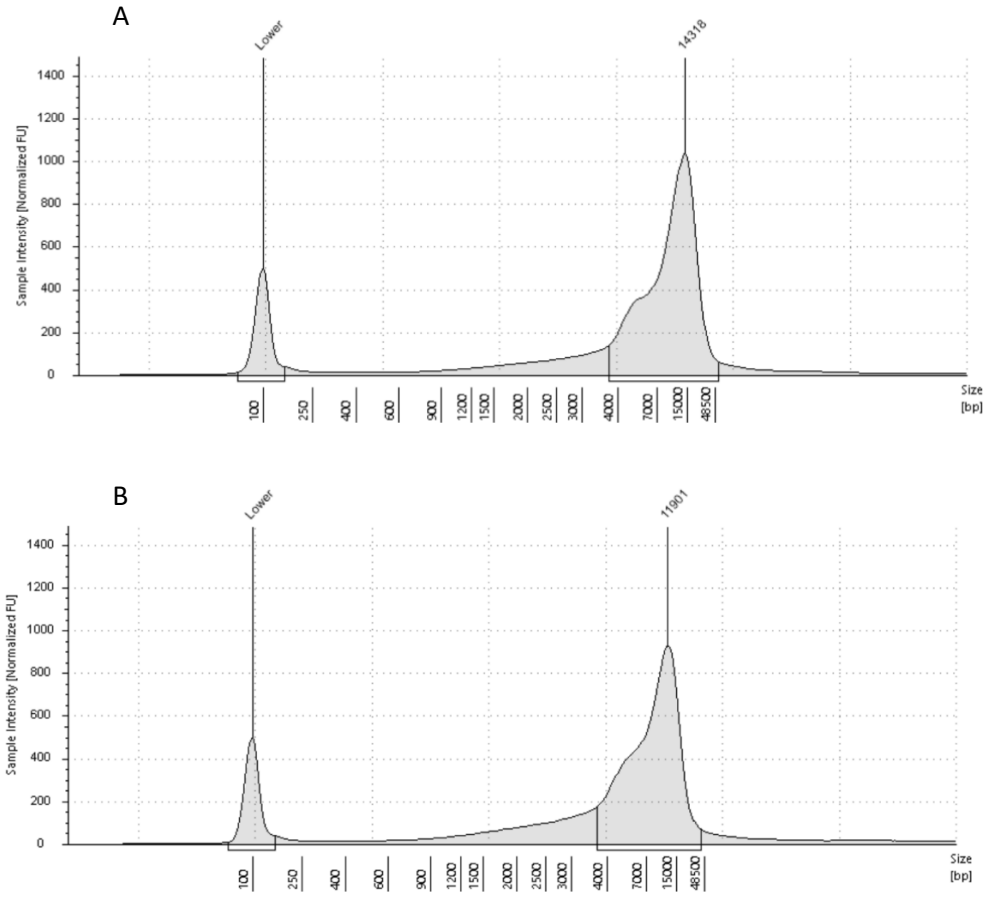

Figure 52 : Electropherogram of a 4 g/L dry biomass suspension lysed by bead mill after (A) 15 and (B) 30 minutes, on the TapeStation 4150.

The peaks aren't very sharp and no peaks similar to the size of pUC18 could be found.

Since no peaks were found in the vicinity of 3000 bp for both methods, the samples measured on the TapeStation 4150 were first purified by Miniprep according to *method 3.2.7 "dsDNA quantification and purification - Plasmid purification by Miniprep"* and analyzed again.

The Miniprep kit was chosen as a purification method as it not only lyses the cells but also efficiently purifies plasmid DNA at the same time.

For the French Press method, only the purified lysates after one, two and three cycles were analyzed on the TapeStation 4150.

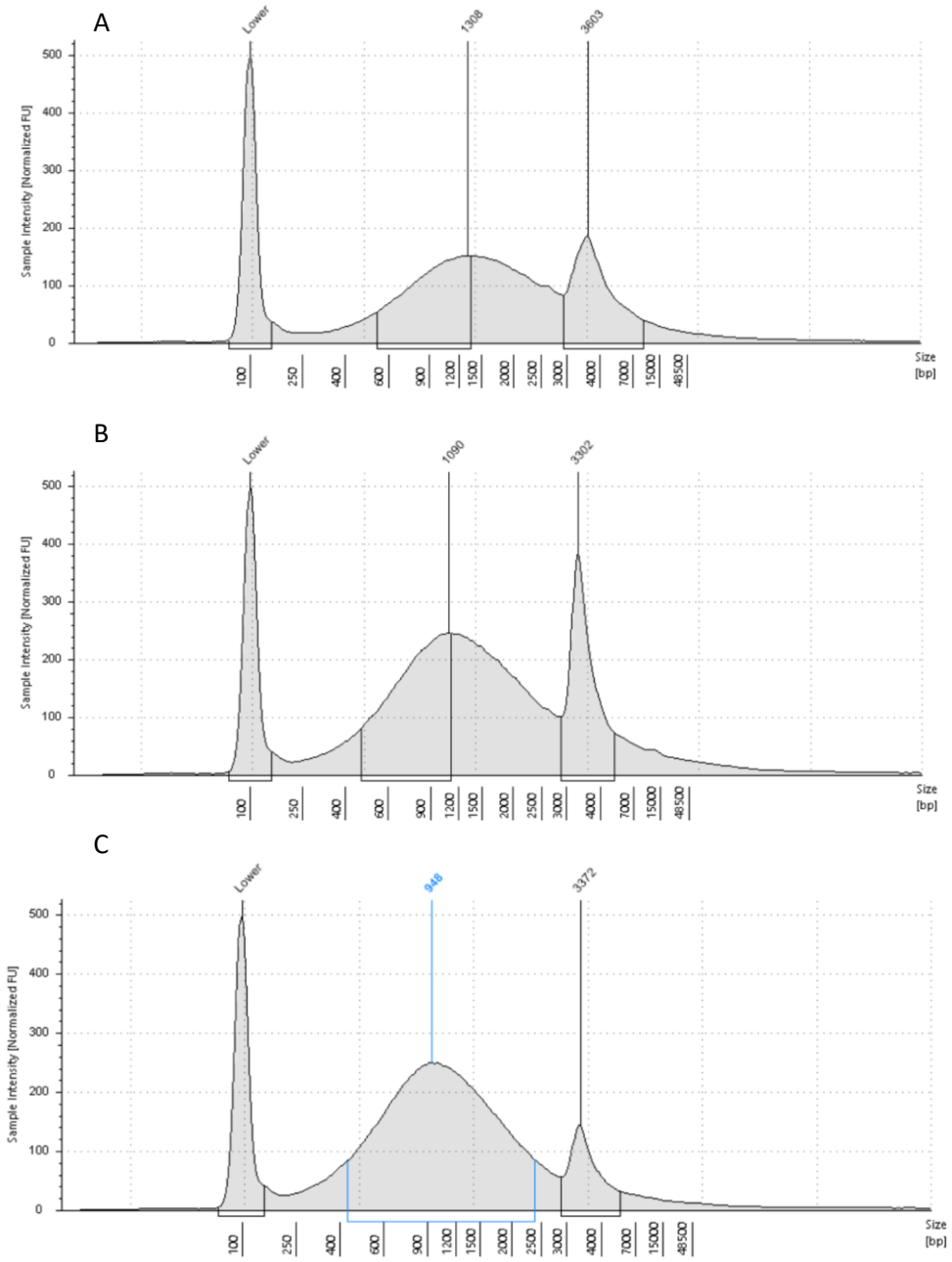

Figure 53 : Electropherogram of a 4 g/L dry biomass suspension lysed by French Press after (A) 1, (B) 3 and (C) 5 cycles and purified by Miniprep, on the TapeStation 4150.

The electropherograms of the lysates previously done didn't show the plasmid as it was hidden from all the HCD. Purifying the lysates by Miniprep made it possible to obtain a peak corresponding to pUC18 and eliminate most HCD. Contaminant DNA of a small size can't be eliminated with a Miniprep treatment. Indeed, vortexing too vigorously is not recommended according to a Miniprep protocol (Qiagen.com, 2023) as it causes shearing of chromosomal DNA that will copurify with the plasmid DNA. However, shearing of DNA can't be avoided when lysing with the French Press method.

The peak that could correspond to the pUC18 decreases on the third cycle, indicating damage to the plasmid. The most frequent size also decreases with the cycles showing the effect of shearing on DNA.

Based on plasmid integrity, two cycles were therefore the adequate conditions before the quantity of pUC18 decreases.

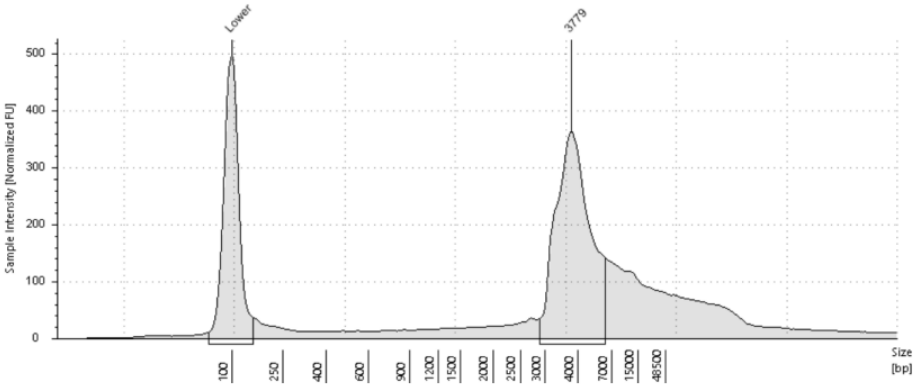

Figure 54 : Electropherogram of a 4 g/L dry biomass suspension lysed by bead mill after 15 minutes and purified by Miniprep, on the TapeStation 4150.

The electropherogram shows less contaminant DNA of a smaller size. The bead mill is a gentler method keeping DNA overall more intact (Frewitt.com, 2023).

The lysate obtained after two cycles in the French Press was analyzed on agarose gel to further confirm the peak at 3302 bp was the plasmid according to *method 3.2.7 "dsDNA quantification and purification – Agarose gel"*.

The pUC18 plasmid was enzymatically cut in two different ways. The first way results in a linearized plasmid which can migrate normally contrary to the supercoiled form. The expected band size is 2686 bp. The second way results in a plasmid cut in two places with the expected band sizes being 2036 and 650 bp.

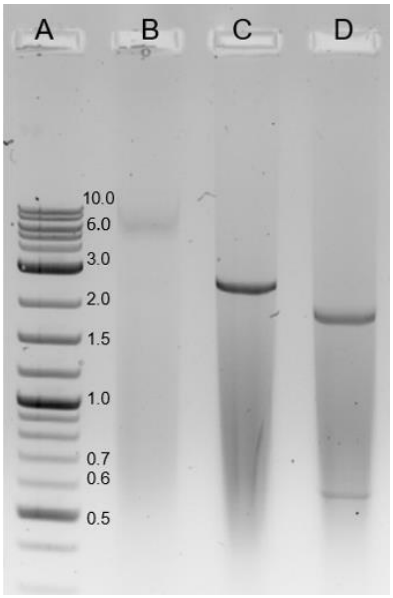

Figure 55 : Agarose gel with a lysate obtained after two cycles of French Press and purified by Miniprep. (A) Quick-Load Purple 1kb plus DNA Ladder. (B) Negative control, lysate without enzymes. (C) Lysate reacted with XbaI. (D) Lysate reacted with BsaI and BseYI. The current was at 140 V for 40 minutes.

The bands of *lanes C* and *D* showing up on *figure 55* match the expected sizes and number of bands thus confirming the presence of pUC18.

The uncut plasmid in *lane A* has an approximate size of 6.0 kb while the TapeStation 4150 determined a peak at 3302 bp. The exact reason for this difference in size for the same sample is unknown. The electrophoresis gel composition or the general electrophoresis conditions may have an influence and the plasmid was probably not in a dimeric form in the agarose gel since the same sample was used. All Minipreps performed showed a peak in the vicinity of 3.0 kb for TapeStation 4150. Analyzing a linearized pUC18 on TapeStation 4150 would have been useful to assess its sizing accuracy and the variation in size from the uncut plasmid.

The fact that those sizes are both higher than the real size of 2686 bp for pUC18 however is not surprising as non-linearized plasmids are known to migrate differently due to their form (De Mattos JCP *et al.*, 2004).

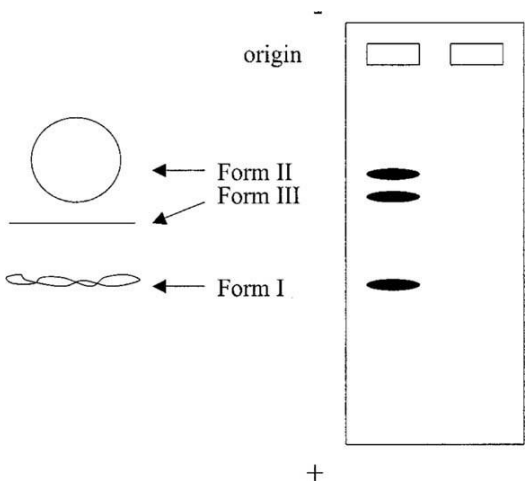

Figure 56 : Changes in migration depending on plasmid form : (Form I) open-circular, (Form I) linear and (Form III) supercoiled (De Mattos JCP et al., 2004).

The obtained plasmid was therefore most probably in a circular form, so it migrates slower. Supercoiled plasmids are the general forms found *in vivo* but shearing can cause the form of plasmids to change to circular (Chih-Hui L *et al.*, 2011).

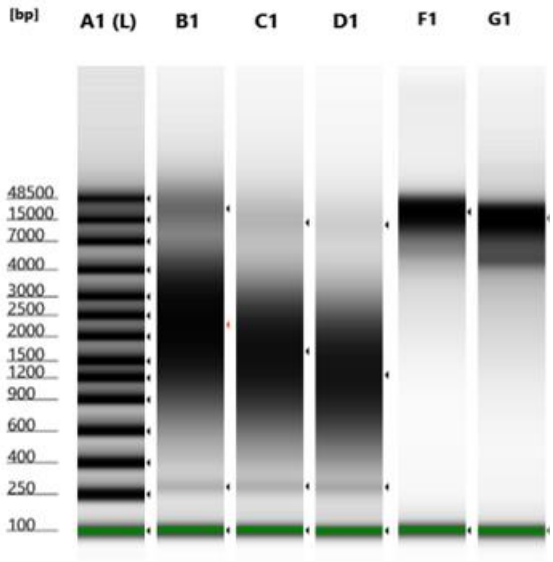

Figure 57 : Tapestation 4150 gel of (A1) Genomic DNA Ladder and a 4 g/L dry biomass suspension lysed by French Press after (B1) 1, (C1) 3, (D1) 5 cycles and lysed by bead mill after (F1) 15 and (G1) 30 minutes. (E1) is not represented.

The TapeStation 4150 features a unique value named DIN for DNA Integrity Number. This number can be used to assess DNA integrity with 1, the minimal value, being a very degraded sample and 10, the maximal value, a highly intact sample (Gassmann M and McHoull B, 2015).

Purified samples obtained after French Press all had a DIN value around 3.0 while those obtained after bead mill were around 6.0.

DIN values are higher for lysates obtained by bead mill further attesting the gentleness of the whole process towards DNA. Those values also attest a partially degraded DNA which could explain the circular form of the plasmids.

The bead mill has many advantages like having a better temperature control and being a gentler method resulting in less contaminant DNA after a Miniprep purification. It is also able to process a greater volume at once.

However, the French Press was the method chosen as its system is more compact, simpler and still fast enough. It also didn't need any utilities like water or pressurized air. The sanitization step required less 0.5 M NaOH and TE buffer thus being shorter in time. The temperature increase didn't seem to be high enough to cause serious DNA degradation and pUC18 was still easily quantified.

4.4 Filtrations

4.4.1 PURASPIN®

The goal of the Puraspin® filtrations is to find the three best combinations of filter type and filter aid grade among all possibilities available for the scaled-up trials with the Purafix® BIO SD 2" capsule.

The sixteen combinations of Puraspin® and filter aid were first performed in triplicate according to *method 3.2.5 "Filtration of the lysates - Puraspin®"*.

After the filtration combinations were done, filter aid could be found in almost all Puraspin® tubes at varying degrees.

Figure 58 : A Puraspin® tube with a contaminated filtrate.

The solid found in the bottom of filtrates was observed under a microscope to confirm its origin.

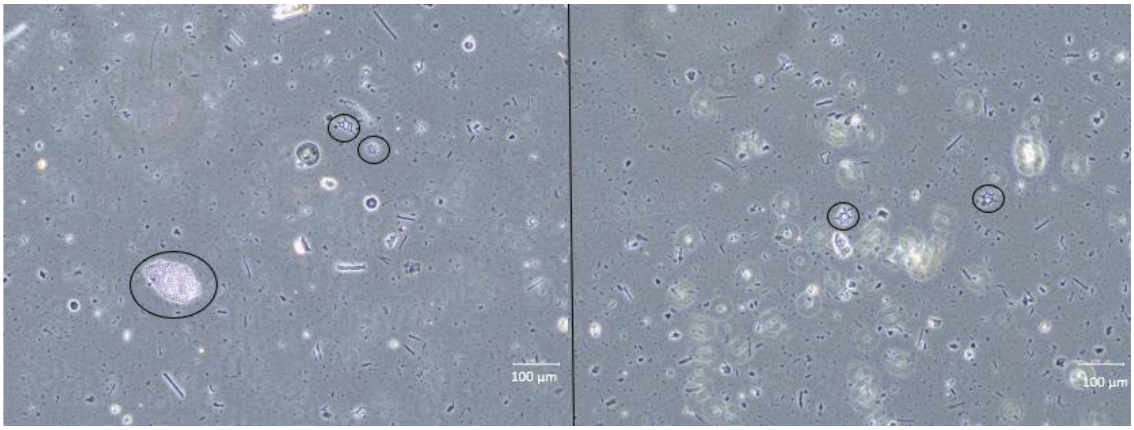

Figure 59 : A contaminated filtrate from Puraspin® under microscope. The black circles show diatomaceous earth.

Several particles looking like diatomaceous earth could be found. This confirms the filtrates were contaminated with filter aid. The problem was found to be the hole that ensures ventilation. The centrifugal force pushed filter aid through this hole thus skipping the filter. The varying degree of contamination was caused by the random position of the hole in the centrifuge for all Puraspin® tubes.

Figure 60 : Hole on the Puraspin® tube where filter aid escaped.

To solve this problem, the hole was marked with a black line to know its location before putting the tubes in the centrifuge with the marks towards the center of the rotor as shown in *figure 61*.

Figure 61 : Process established to prevent contamination of filter aid in filtrates of Puraspin®.

A filtrate was observed under a microscope to confirm the absence of filter aid. All filtrates were visually clear.

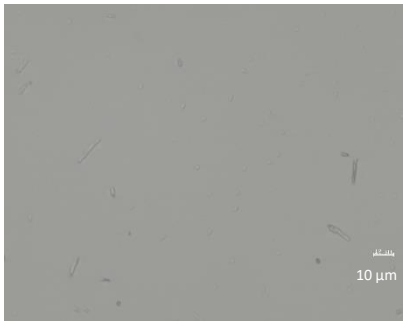

Figure 62 : A filtrate from Puraspin® under microscope.

The cakes weren't regular due to the fixed-angle rotor of the centrifuge. A swing-bucket rotor would have resulted in more uniform cakes and would at the same occasion probably solve the problem encountered with contaminated filtrates. Some cakes also looked slightly too wet while the majority didn't.

Figure 63 : Cakes of varying Celpure® grades on varying Puraspins®.

A uniform cake is more desirable since filter aid is supposed to act as the filtering agent. In that way, filtrations may be less effective and quantification of HCD, endotoxins and such, more fluctuating.

4.4.2 PURAFIX® BIO SD 2" capsule

After analysis of the Puraspin® filtrates, three combinations were chosen for a scale-up based on turbidity reduction, pUC18 recovery and endotoxin removal. The three combinations are shown in *table 25*.

Table 25 : The three chosen combinations of Celpure® grades and Purafix® BIO SD filter.

Filter aid	PURAFIX® BIO SD filter
Celpure® C1000	PURAFIX® BIO SD CH 130
Celpure® C300	PURAFIX® BIO SD CH 71
Celpure® C100	PURAFIX® BIO SD CH 71

CH71P-C300 was mainly chosen since its Puraspin® equivalent had the highest pUC18 recovery. CH130-C1000 and CH71-C100 were mainly chosen since their Puraspin® equivalents had the highest removal of endotoxins.

After a sanitization step with 1 M NaOH to eliminate contaminant endotoxins in the filtration system, 350 mL of lysate was mixed with 57 g/L of filter aid in a heat-treated beaker under constant low agitation according to *method 3.2.5 "Filtration of the lysates - PURAFIX® BIO SD 2" capsule"*. The peristaltic pump was set to the flow rates shown in *table 26*.

Table 26 : The three chosen combinations of Celpure® grades and Purafix® BIO SD filter and set peristaltic pump flow rate.

Filter aid	PURAFIX® BIO SD filter	Pump set flow rate [mL/min]	Filtrate theorical flux [L/(m²·h)]
Celpure® C1000	PURAFIX® BIO SD CH 130	20.00	571
Celpure® C300	PURAFIX® BIO SD CH 71	20.00	571
Celpure® C100	PURAFIX® BIO SD CH 71	15.00	429

The volume of filtrate and the differential pressure were noted every 2 minutes, the values are shown on *figures 64*, *65* and *66*.

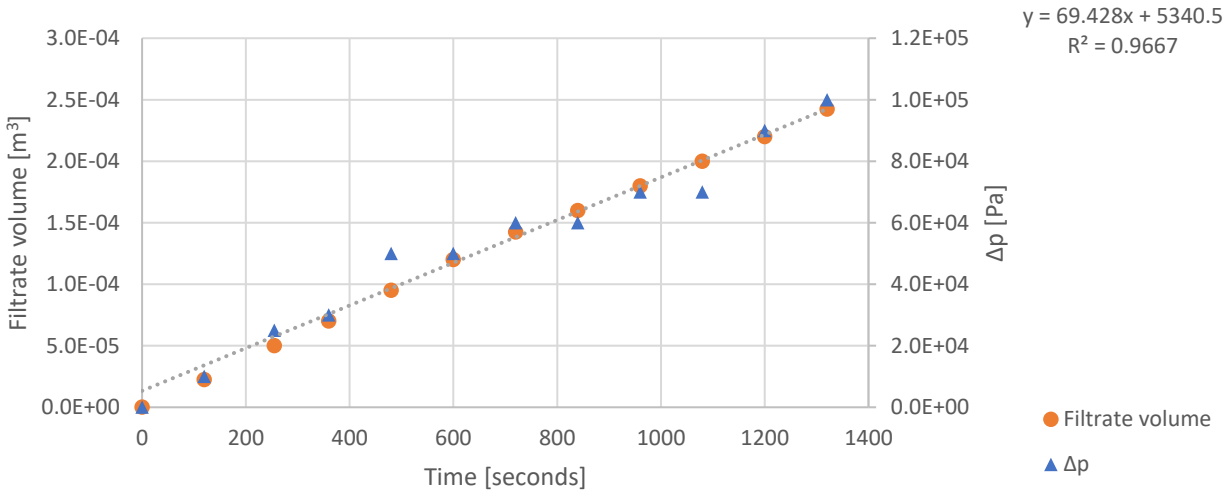

Figure 64 : Filtrate volume and differential pressure in function of time for the filtration of a 4 g/L dry biomass lysate with the CH71P Purafix® filter and C100 Celpure®.

The coefficient of variation of the filtrate flux calculated every 2 minutes is equal to 3% which means the filtration was approximately at constant flux.

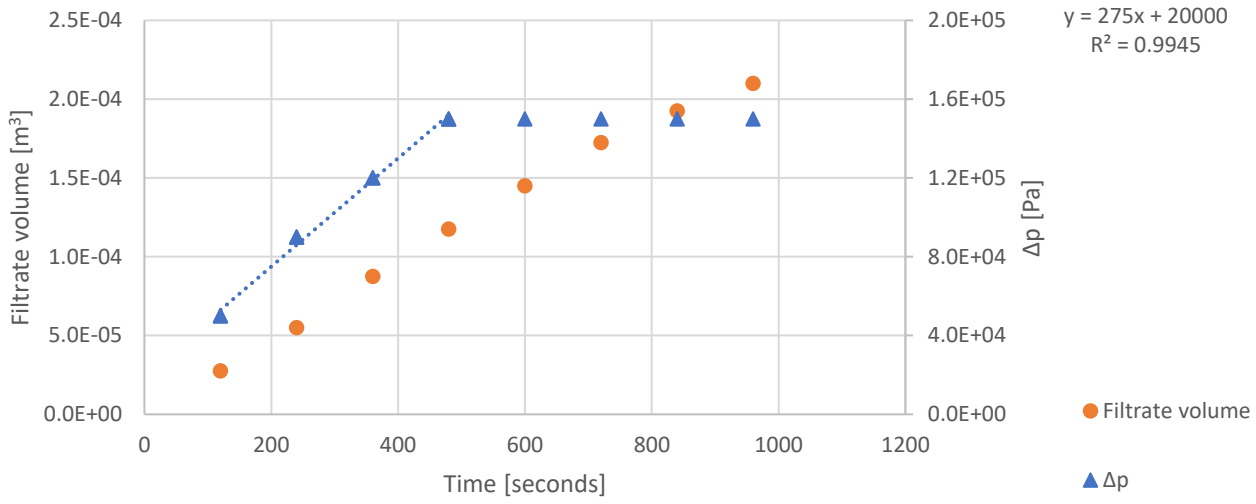

Figure 65 : Filtrate volume and differential pressure in function of time for the filtration of a 4 g/L dry biomass lysate with the CH130P Purafix® filter and C1000 Celpure®.

The coefficient of variation of the filtrate flux calculated every 2 minutes is equal to 4% which means the filtration was approximately at constant flux.

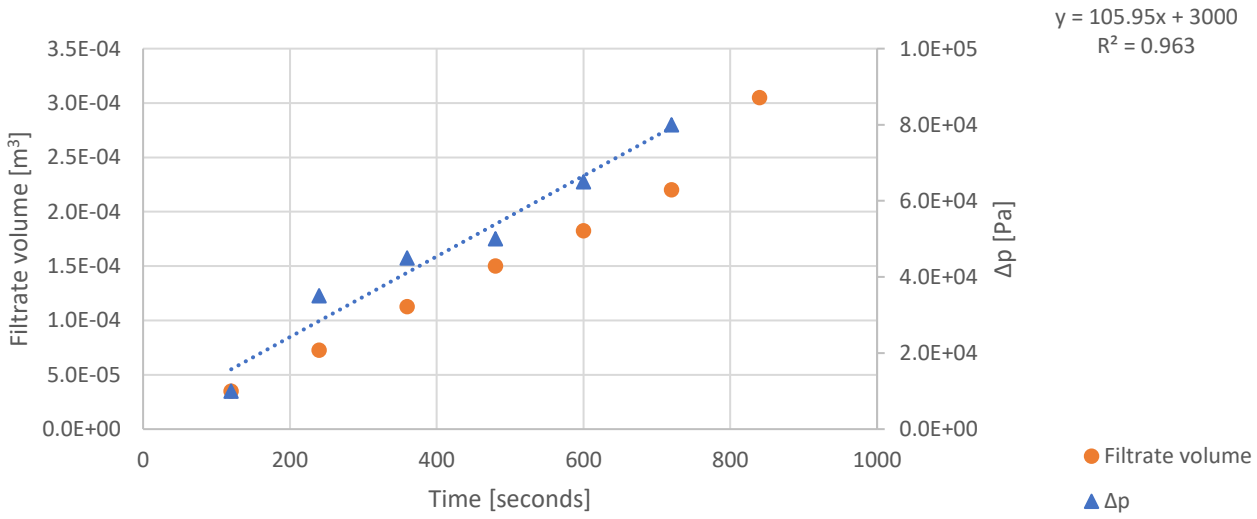

Figure 66 : Filtrate volume and differential pressure in function of time for the filtration of a 4 g/L dry biomass lysate with the CH71P Purafix® filter and C300 Celpure®.

The coefficient of variation of the filtrate flux calculated every 2 minutes is 7% which means the filtration was approximately at constant flux.

The parameters necessary for the calculation of the cake resistance and the filter resistance are shown in *table 27*.

Table 27 : Parameters and calculated cake and filter resistances of the three of Purafix® BIO SD 2" capsule filtrations at constant rate of the combinations CH71P-C100, CH130P-C1000 and CH71-C300.

	CH71P-C100	CH130P-C1000	CH71P-C300
Final Δp reached [Pa]	1.0E+05	1.5E+05	8.0E+04
Filtrate flux [L/(m^2·h)]	328	402	522
Filtrate flow rate [m^3/s]	1.91E-07	2.34E-07	3.05E-07
Filter area [m^2]	2.1E-03		
Solids concentration [kg/m^3]	6.07E-05		
Viscosity of the liquid [Pa·s]	1.18E-03		
Slope of regression line [N/(m^2·s)]	69.428	275	105.95
Intercept of regression line [N/m]	5340.5	20000	3000
Cake average specific resistance α [m/kg]	1.2E+17	3.1E+17	7.0E+16
Filter resistance β [m^{-1}]	5.0E+10	1.5E+11	1.8E+10

The peristaltic pump flux was set to 429 L/(m^2·h) for the trial with the CH71P filter and C100 filter aid. However, the observed flux was 328 L/(m^2·h) and too close to the minimal flux recommended of 300-350 L/(m^2·h). The flux on the peristaltic pump was increased to 571 L/(m^2·h) for the succeeding trials.

A few theorical statements can be made for constant rate filtration.

The decrease of filter aid permeability is linked to an increase of the cake average specific resistance, while a decrease of porosity of the filter is linked to an increase of the filter resistance, given the filtration conditions are the same.

Increasing the filtrate flux causes the capsule to be filled quicker meaning Δp_{max} would be lower. Having a lower Δp_{max} translates to less force applied to the cake and filter medium thus decreasing resistances overall (Saleem M *et al.*, 2012).

Due to all variations most likely due to filtrate flux changes, comparisons between the three trials were quite difficult and not entirely in accordance with the theory stated before.

However, some observations between the three filtrations were still able to be linked to some theorical statements. The most influential parameter seemed to be the Δp_{max} reached. Increasing the Δp_{max} increased cake and filter resistance. Also, the filter resistances were lower with the CH71P than the CH130. Lower porosities translate to a more restricted flow, synonym of an increase in resistance.

Comparisons with theorical values are complex as many variables influence cake and filter resistances like the viscosity, the type of solids and its concentration, or even the whole filtration system setup.

The generated cakes were photographed as shown in *figure 67*.

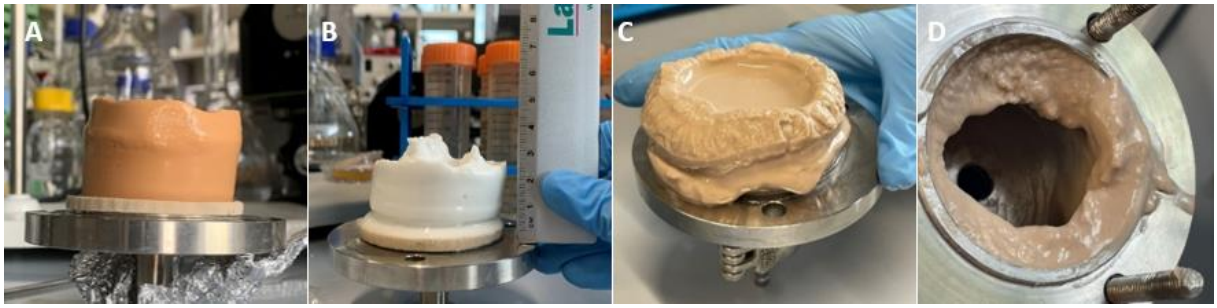

Figure 67 : Cakes of Purafix® BIO SD 2" capsule filtrations. (A) Cake of the CH71P-C100 filtration combination. (B) Cake of the CH130P-C1000 filtration combination. (C) Cake of the CH71P-C300 filtration combination.

The cakes were still very wet and soft which isn't the ideal aspect of a cake as it should be drier and more compact. A lower feed rate seems to provide better packing since cakes looked firmer with decreasing feed rate.

A phenomenon was observed during all three filtrations experienced. After about 15 minutes, the differential pressure quickly dropped to 0 bar and a lot of foam exited the capsule.

Normally, it should increase until it reaches a maximal value or if the capsule is filled with cake.

This drop in differential pressure could have three potential causes : leaks, air going in the entering tube or a clogged pressure gauge. None of the first two causes were detected by the operator but they're still a valid explanation. The pressure gauge would have to stay blocked at 0 bar after the first filtration to be really clogged but differential pressure worked normally at the start of the following filtrations. Additionally, the use of a diaphragm seal prevents clogging (Orzikowski H, 2023).

Figure 68 : Foam coming out of the capsule towards the moment the differential pressure drops quickly of Purafix® BIO SD 2" capsule filtrations.

Another unusual observation was made. After defrosting the fractions of all three filtrations, a sediment was seen in all tubes that wasn't observed before any storage at -18°C.

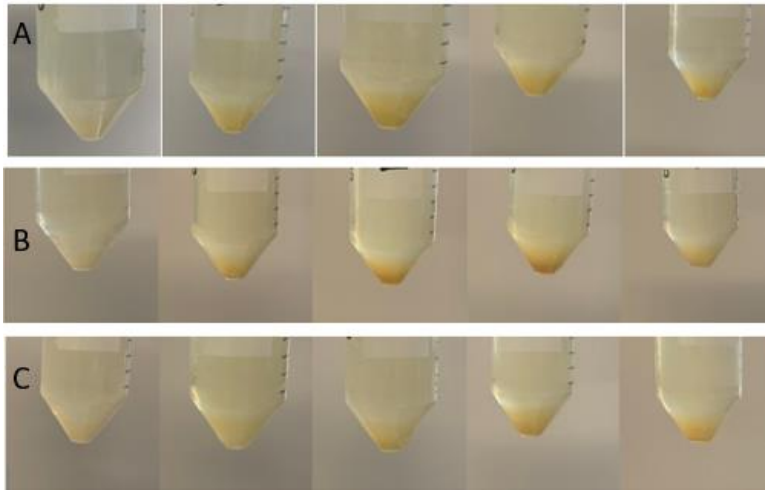

Figure 69 : Sediments found in every 50 mL filtrate fraction (50 to 250 mL, left to right) of Purafix® BIO SD 2" capsule. (A) CH71P-C100 filtration combination. (B) CH130P-C1000 filtration combination. (C) CH71P-C300 filtration combination.

One of these sediments was checked under a microscope and something resembling diatomaceous earth could be seen. However, apart from this, nothing else was found. This means that the origin of this sediment is maybe not entirely filter aid as more should have been seen under the microscope.

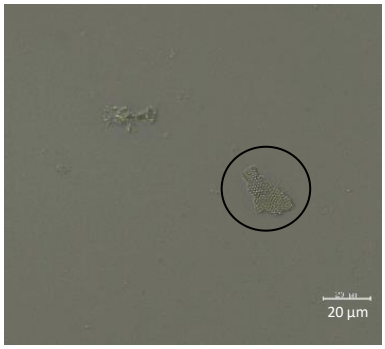

Figure 70 : A sediment found in all filtrates of Purafix® BIO SD 2" capsule under microscope. The circle shows a piece of diatomaceous earth.

4.4.3 PURADISC® BIO SD 12" 12M module

To scale up filtrations with Puradisc® BIO SD 2" capsule to 12" module, calculations must be performed according to the Scale-up Test Kit of Filtrox AG. Due to time constraints, filtrations with 12" module weren't performed. However, the calculations mentioned were still done with the CH71P-C100 combination since it had the most intact cake.

- $c_1 = A_1 \cdot h_1$

Equation 15 : Calculation to determine the volume occupied by cake.

- $c_2 = \frac{V_2 \cdot c_1}{V_1}$

Equation 16 : Calculation to determine the volume able to be filtered for alluvial filtration.

c_1 : Cake volume obtained with Purafix® BIO SD 2" capsule [m^3]

A_1 : Filter area with Purafix® BIO SD 2" capsule [m^2]

h_1 : Cake height with Purafix® BIO SD 2" capsule [m]

V_1 : Volume to filter with Purafix® BIO SD 2" capsule [m^3]

V_2 : Volume to filter with Puradisc® BIO SD 12" 12M module [m^3]

C_2 : Cake volume obtained with Puradisc® BIO SD 12" 12M module [m^3]

The space needed for the cake for the next scale is directly proportional to the feedstock volume (for a given cake height). In this case, the maximum space is known since the type of module to use is fixed. Therefore, the maximal volume that can be filtered until complete filling of the cake is 0.0149 m^3.

Table 28 : Maximal cake volume capacity of Puradisc® BIO SD 12" 12M module and calculated maximal volume able to be filtered based on the CH71P-C100 combination Purafix® BIO SD 2" capsule filtration.

Maximal cake volume with Puradisc® BIO SD 12" 12M module [m^3]	0.0035
Maximal volume to be filtered with Puradisc® BIO SD 12" 12M module [m^3]	0.0149

This trial would have needed a large amount of lysate, but the methods used at a smaller scale wouldn't be compatible. Biomass production could have been increased by cultivating in a stirred tank reactor in batch mode. To save time and process smaller volumes, the concentration of dry biomass before lysis could be increased and the suspension would have been diluted to 4 g/L after lysis.

Additionally, those two alternatives could have been applied for the preparation of lysates for Puraspin® and Purafix® filtrations to save time.

4.5 Analytics

4.5.1 Turbidity

The turbidity of the Puraspin® and Purafix® filtrates were measured to assess removal of solids according to *method 3.2.9 "Turbidity"*. The values are shown in *figures 71* and *72*.

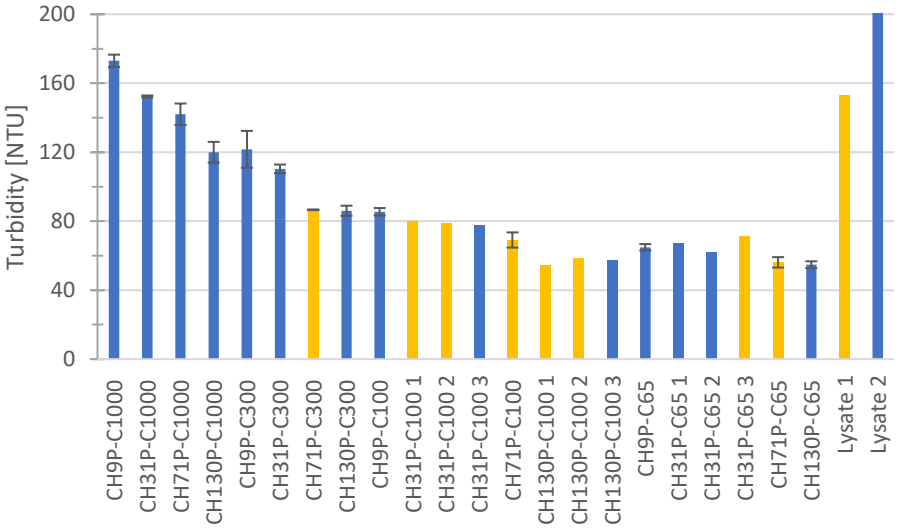

Figure 71 : Turbidity measurement of Puraspin® filtrates and lysates before filtration. The two colors represent the two different starting materials. When the averages of triplicates couldn't be done due to the different starting materials, the concerned combination is followed either by a 1, 2 or 3.

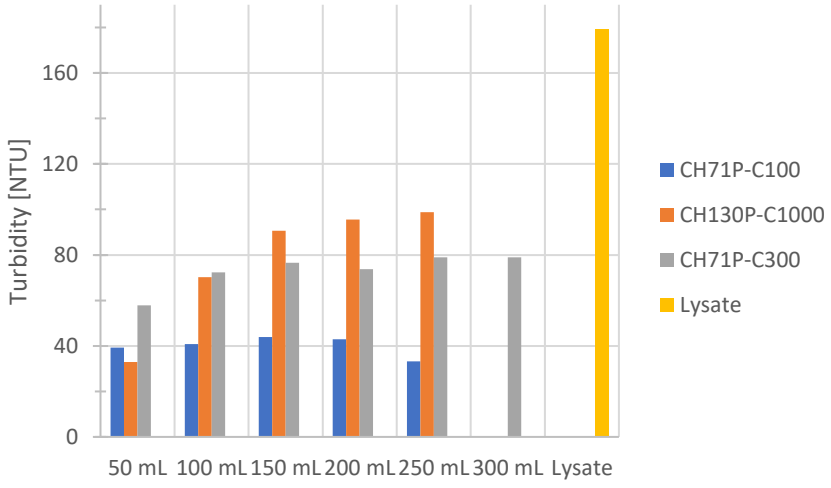

Figure 72 : Turbidity measurement of Purafix® 50 mL filtrate fractions and the lysate before filtration.

The percentage of removed turbid matter was then calculated to better compare the different trials since different lysates were processed.

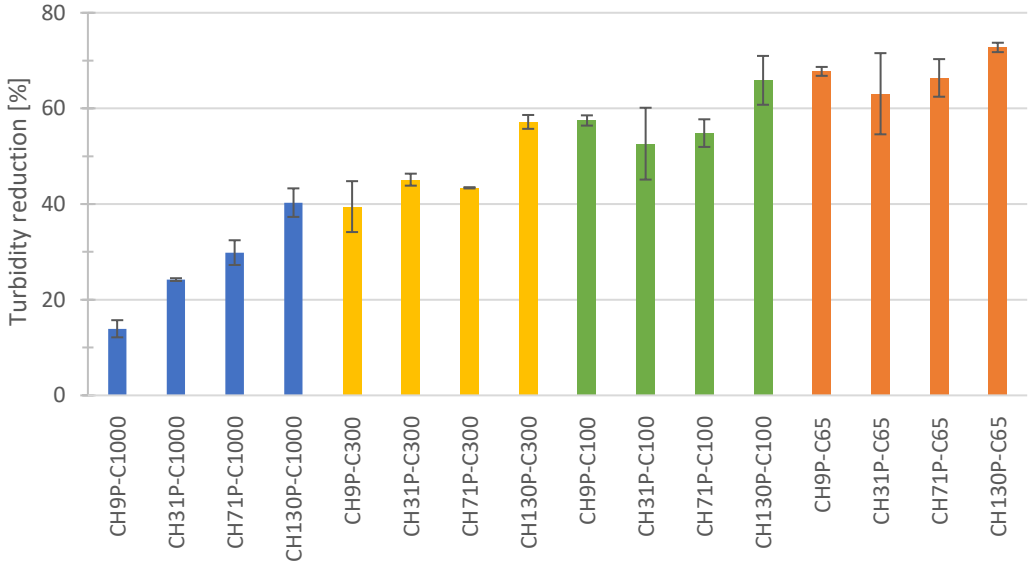

Figure 73 : Percentage of removed turbid matter of Puraspin® filtrates compared to lysates before filtration.

The trend observed here seems to be that decreasing filter porosity and filter aid granulometry reduces the turbidity of the lysate.

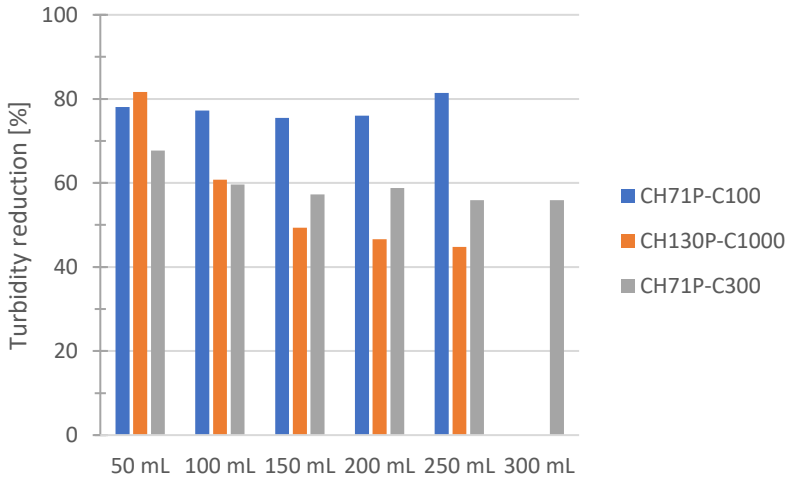

Figure 74 : Percentage of removed turbid matter of Purafix® 50 mL filtrate fractions compared to the lysate before filtration.

The same trend is observed for the scaled-up filtrations : decreasing filter porosity and filter aid granulometry decreases turbidity. CH130P-C1000 and CH71P-C300 trials have also what looks like a breakthrough curve while the CH71P-C100 trial does not. The cause may be the slower flux.

The CH71P-C100 combination achieved a 55% reduction with the Puraspin® and an 82% reduction with the Purafix® filter. This improvement in turbid matter removal may be thanks to the slower flux of the filtrate.

The CH130P-C1000 combination achieved a similar reduction in turbidity for the Puraspin® and Purafix® filtrations, 40% and 45%, respectively.

The CH71P-C300 combination achieved a slightly better reduction in turbidity for the Purafix® filtration with 56%. The Puraspin® one achieved a reduction of 43%.

Two Puraspin® filtrations per filter type were also done but without any filter aid to further assess the influence of filter aid and its necessity. The turbidity and the turbidity reductions are shown in *figures 75* and *76*.

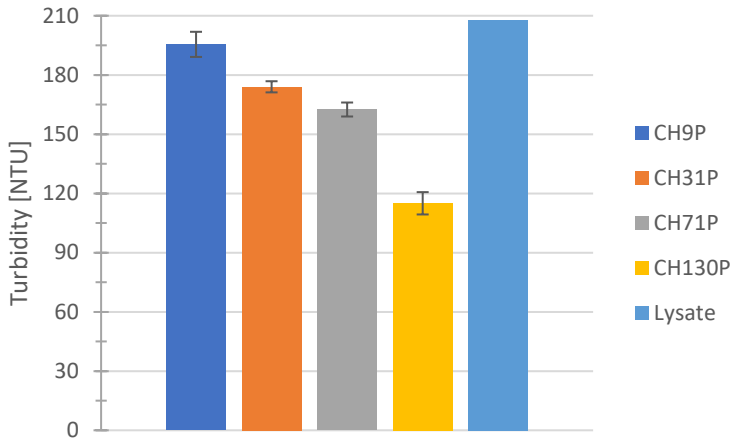

Figure 75 : Turbidity measurement of Puraspin® filtrates and lysate before filtration. The filtrations were performed without filter aids.

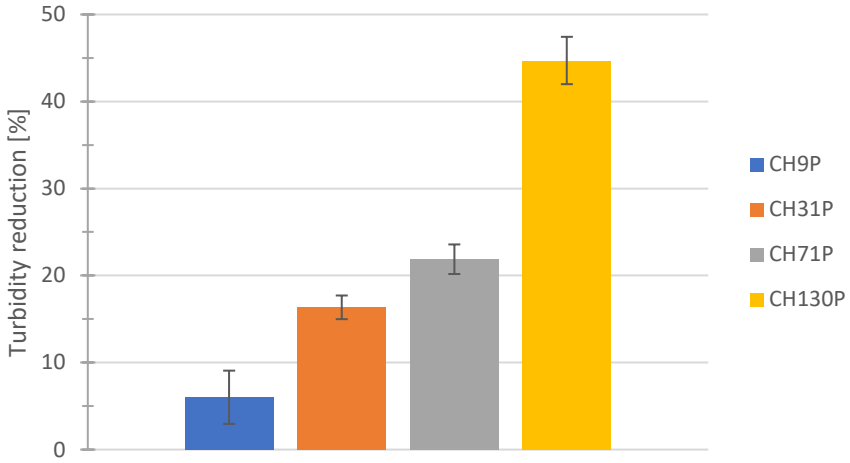

Figure 76 : Percentage of removed turbid matter of Puraspin® filtrates compared to the lysate before filtration. The filtrations were performed without filter aids.

The CH9P filter was able to only reduce turbidity by 5% but when the finest grade of diatomaceous earth was added, C65, the turbidity was reduced by 68%. The CH31P, CH71P and CH130P filters were able to reduce turbidity by 16, 22 and 48%, respectively while the addition of the finest grade of diatomaceous earth helped turbidity to be reduced by 63, 66 and 72%, still in the same order.

Using filter aid clearly has an advantage on clarifying the lysates.

4.5.2 Endotoxins

The endotoxin content of the filtrates was analyzed by RP-HPLC according to *method 3.2.6 "Endotoxin quantification"*. After hydrolysis with acetic acid and labelling with DMB, samples were separated on

a column, YMC-Triart C18 ExRS with a mobile phase consisting of an aqueous part, ultrapure water and an organic part, methanol 64% and acetonitrile 34%.

The retention time of the marker peak was in the vicinity of 1.5 to 2 minutes while the peak of the labelled KDO was found at 10 to 11 minutes.

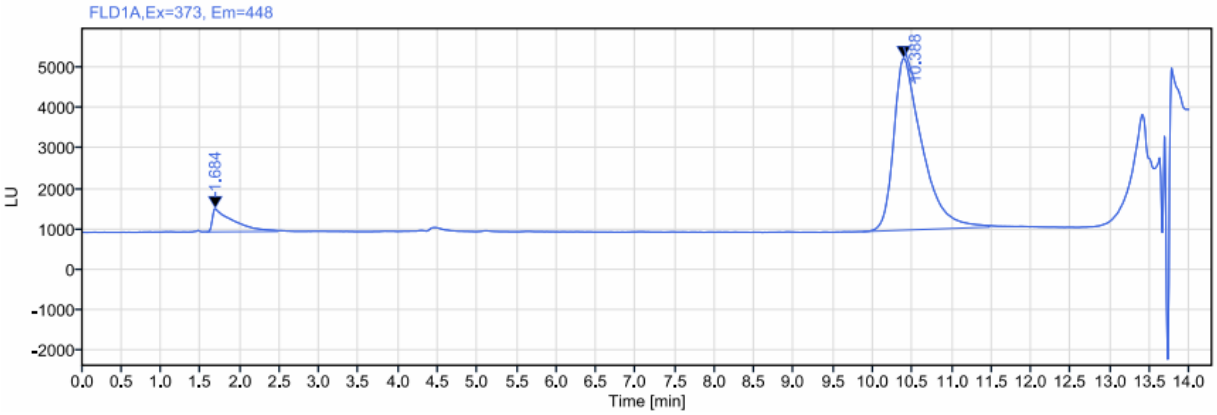

Figure 77 : Chromatogram obtained after injecting the KDO standard at 250 ng/mL that has been marked with a fluorescence marker, DMB, on RP-HPLC with FLD. Excitation is at 373 nm and emission at 448 nm. The peak of the labelled KDO is found at 10.388 minutes while the marker is found at 1.684 minutes.

The peaks corresponding to KDO were then quantified with the 250 ng/mL KDO standard. The peak area of chromatograms was used for the calculations.

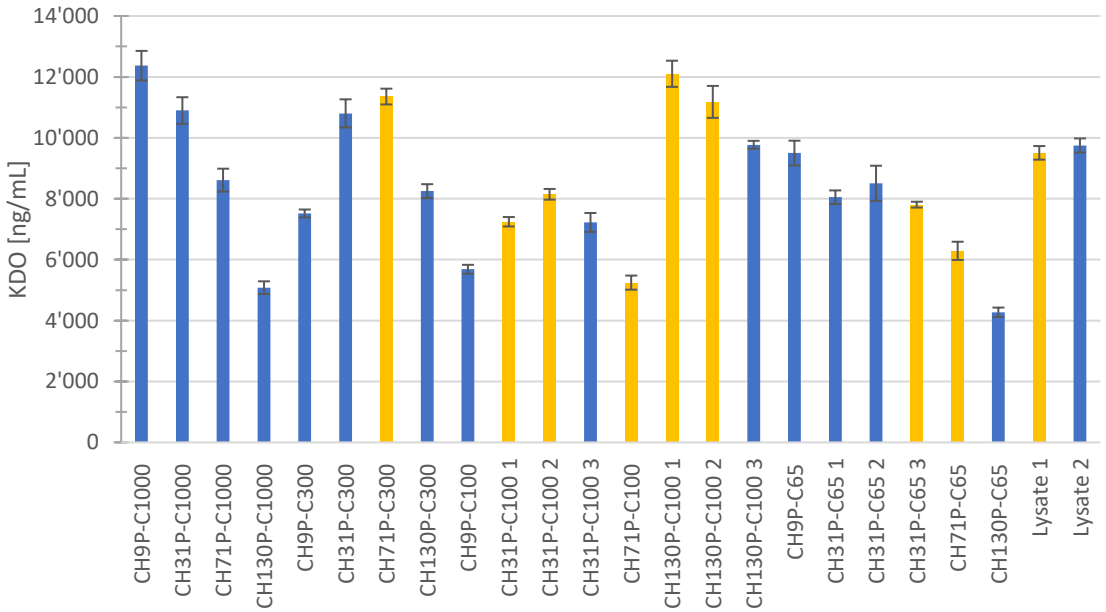

Figure 78 : KDO concentration of Puraspin® filtrates and lysates before filtration. The two colors represent the two different starting materials. When the averages of triplicates couldn't be done due to the different starting materials, the concerned combination is followed either by a 1, 2 or 3. Calculations were performed using the peak areas on chromatograms.

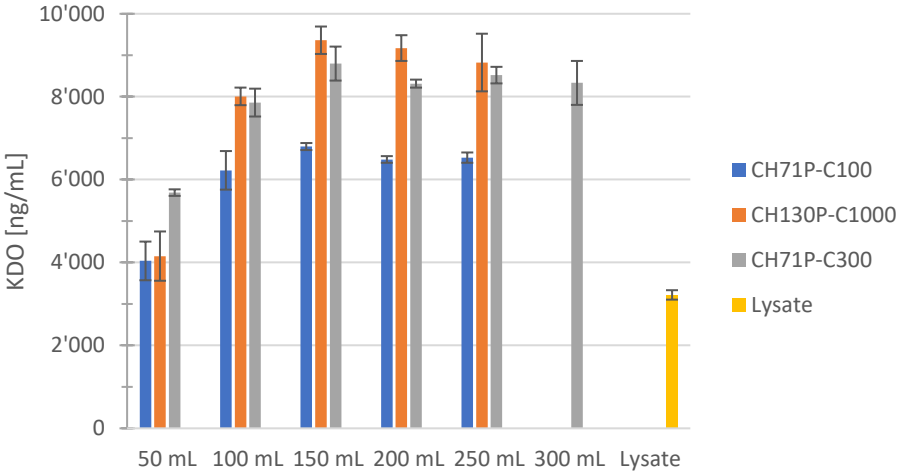

Figure 79 : KDO concentration of Purafix® 50 mL filtrate fractions and the lysate before filtration. Calculations were performed using the peak areas on chromatograms.

KDO was also quantified using the height of the peak in chromatograms.

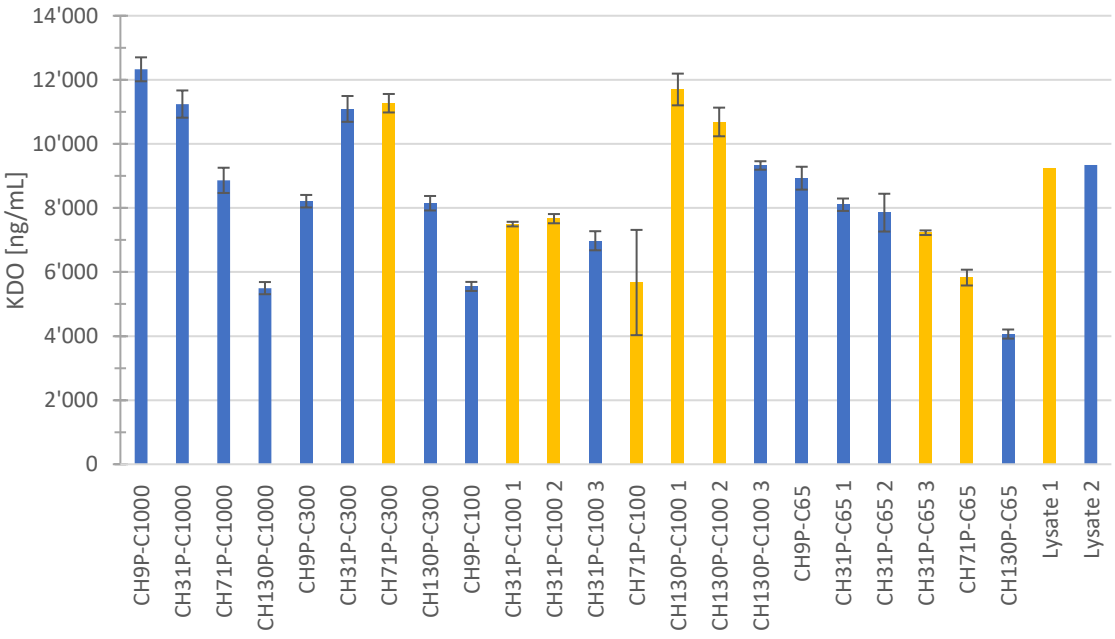

Figure 80 : KDO concentration of Puraspin® filtrates and lysates before filtration. The two colors represent the two different starting materials. When the averages of triplicates couldn't be done due to the different starting materials, the concerned combination is followed either by a 1, 2 or 3. Calculations were performed using the peak heights on chromatograms.

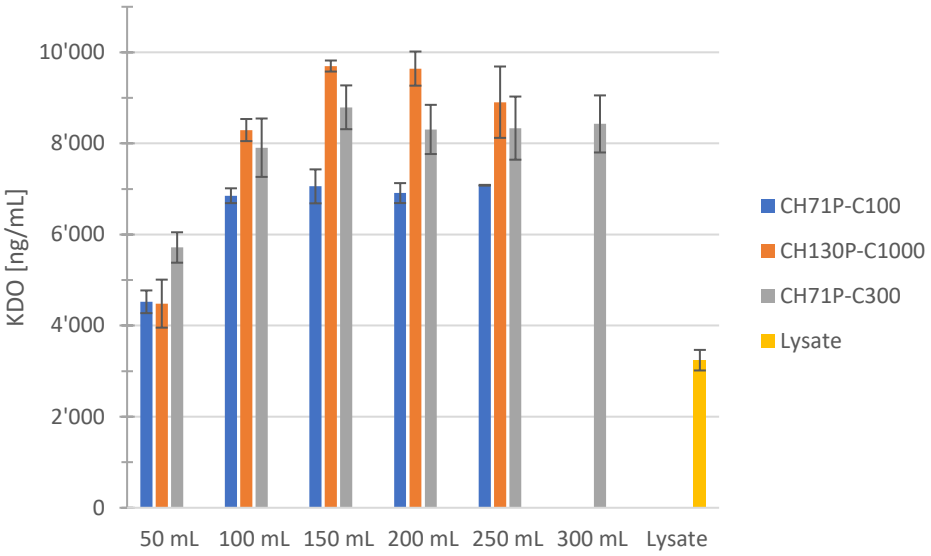

Figure 81 : KDO concentration of Purafix® 50 mL filtrate fractions and the lysate before filtration. Calculations were performed using the peak heights on chromatograms.

Since quantifications by height or area gave similar values, all the next calculations were carried out based on peak area.

For the calculation of endotoxins concentrations, a best-case and worst-case scenario were assumed since the *E. coli* strain has an unknown endotoxin content.

In the worst-case scenario, one ET contains one KDO and has a maximal monomeric molecular weight of 40 kDa (for a smooth type LPS). The ratio of KDO to endotoxin is 0.6 (w/w)%.

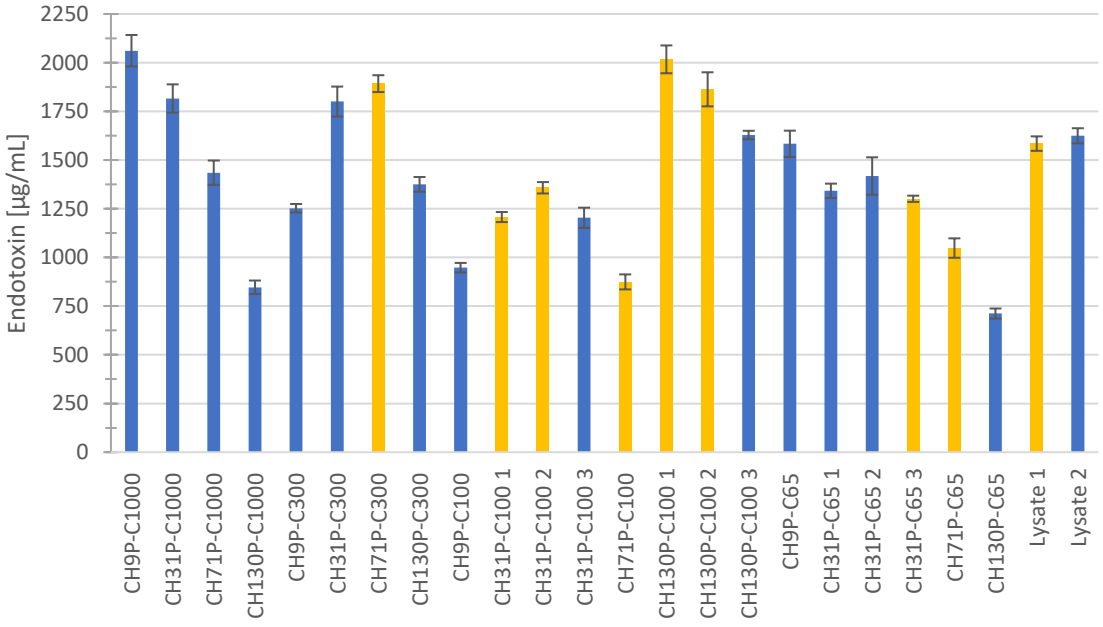

Figure 82 : Endotoxin concentration of Puraspin® filtrates and lysates before filtration. The two colors represent the two different starting materials. When the averages of triplicates couldn't be done due to the different starting materials, the concerned combination is followed either by a 1, 2 or 3. This follows the worst-case scenario where the ratio of KDO to endotoxin is 0.6 (w/w)%.

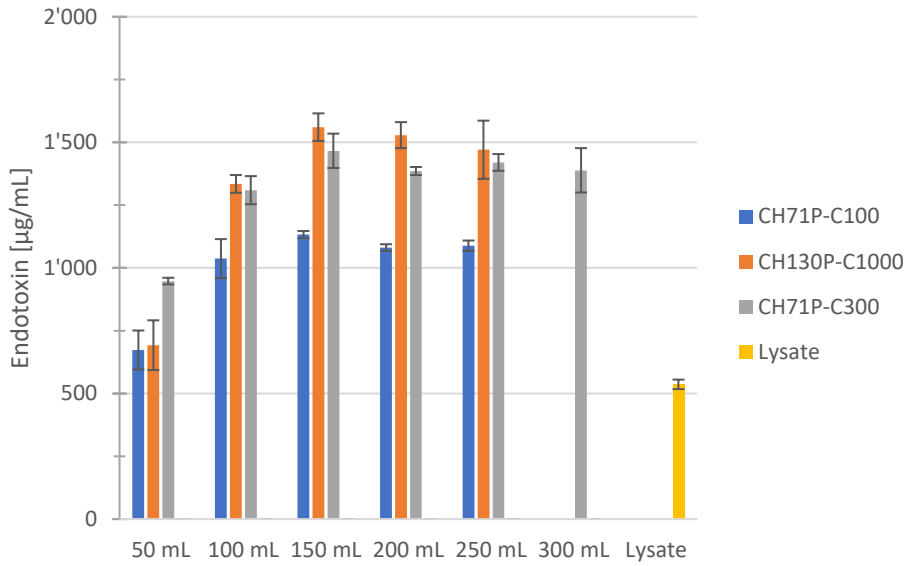

Figure 83 : Endotoxin concentration of Purafix® 50 mL filtrate fractions and the lysate before filtration. This follows the worst-case scenario where the ratio of KDO to endotoxin is 0.6 (w/w)%.

In the best-case scenario, one ET contains three KDO and has a molecular weight of 2 kDa (for a rough LPS). The ratio of KDO to endotoxin is 35.7 (w/w)%.

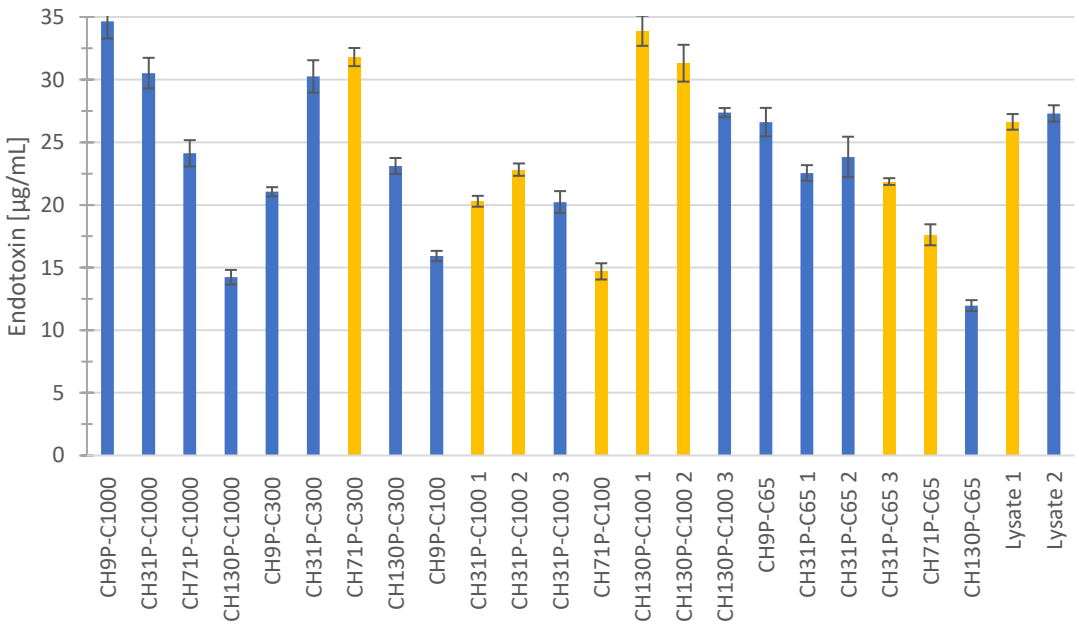

Figure 84 : Endotoxin concentration of Puraspin® filtrates and lysates before filtration. The two colors represent the two different starting materials. When the averages of triplicates couldn't be done due to the different starting materials, the concerned combination is followed either by a 1, 2 or 3. This follows the best-case scenario where the ratio of KDO to endotoxin is 35.7 (w/w)%.

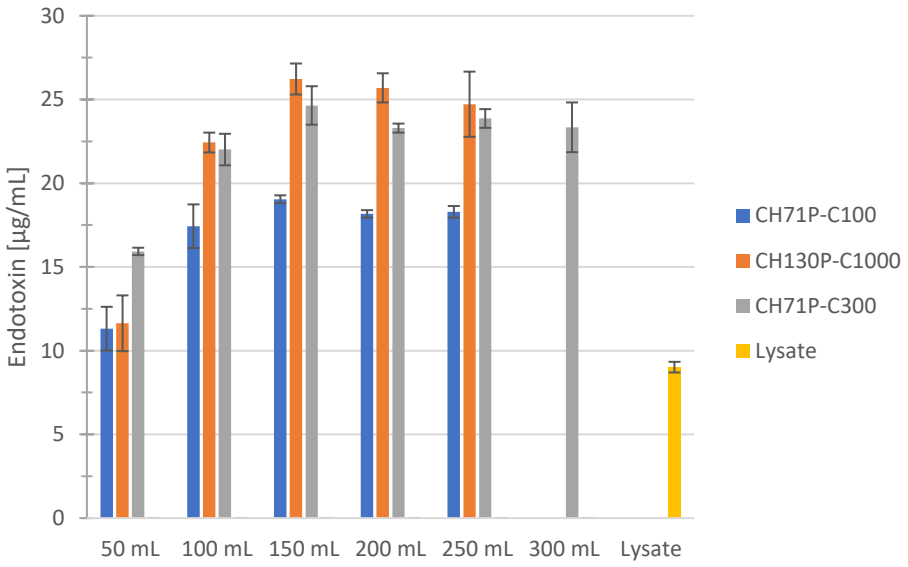

Figure 85 : Endotoxin concentration of Purafix® 50 mL filtrate fractions and the lysate before filtration. This follows the best-case scenario where the ratio of KDO to endotoxin is 35.7 (w/w)%.

Endotoxins can make up 0 to 4% of dry biomass in *E. coli*. For a 4 g/L suspension, this represents a concentration of 0 to 160 µg/mL. The worst-case scenario seems to greatly overestimate endotoxins concentration (Zinn M, 2022).

For the biological pyrogenic activity, a value also had to be assumed. The FDA reference standard endotoxin (RSE) obtained from *E. coli O113:H10:K* negative with 10 EU per ng of endotoxin was taken as a reference. The concentrations with the worst-case scenario are shown on *figures 86* and *87*.

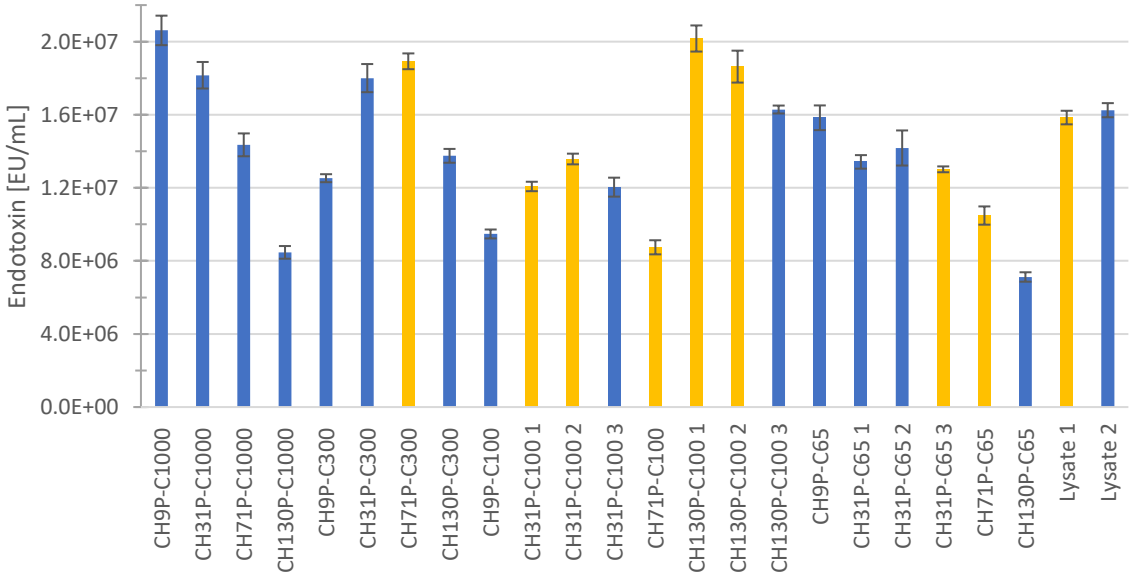

Figure 86 : Endotoxin concentration of Puraspin® filtrates and lysates before filtration. The two colors represent the two different starting materials. When the averages of triplicates couldn't be done due to the different starting materials, the concerned combination is followed either by a 1, 2 or 3. This follows the worst-case scenario where the ratio of KDO to endotoxin is 0.6 (w/w)%.

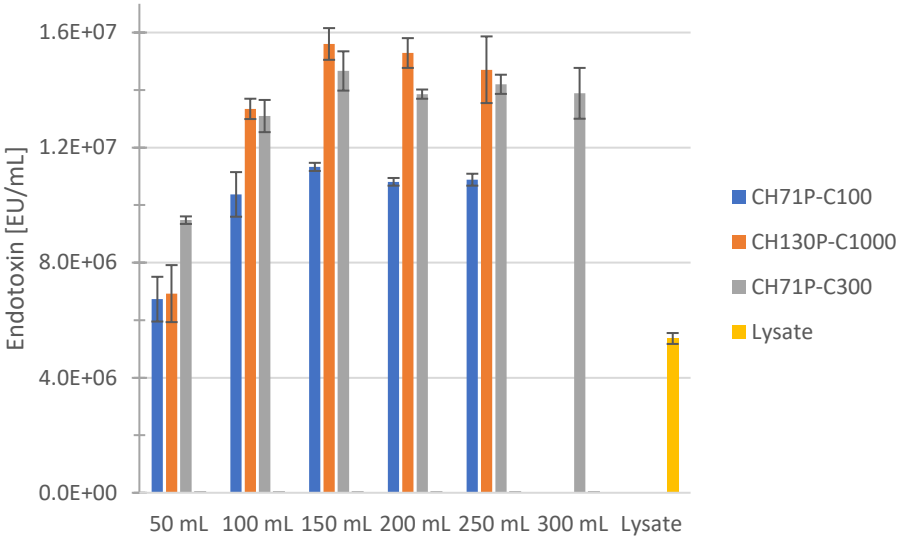

Figure 87 : Endotoxin concentration of Purafix® 50 mL filtrate fractions and the lysate before filtration. This follows the worst-case scenario where the ratio of KDO to endotoxin is 0.6 (w/w)%.

The concentrations with the best-case scenario are shown on figures *88* and *89*.

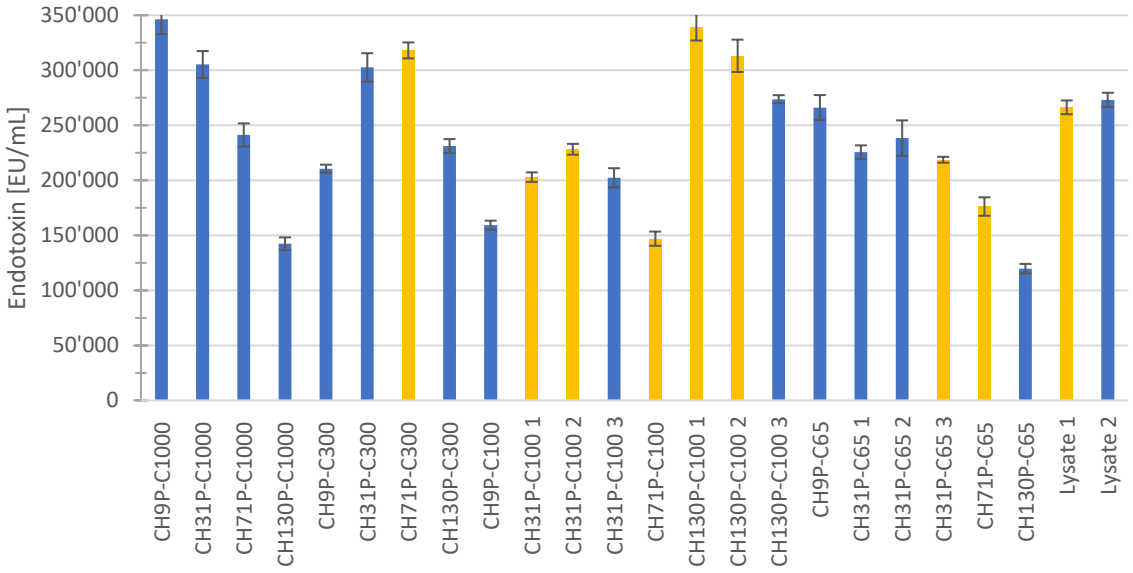

Figure 88 : Endotoxin concentration of Puraspin® filtrates and lysates before filtration. The two colors represent the two different starting materials. When the averages of triplicates couldn't be done due to the different starting materials, the concerned combination is followed either by a 1, 2 or 3. This follows the best-case scenario where the ratio of KDO to endotoxin is 35.7 (w/w)%.

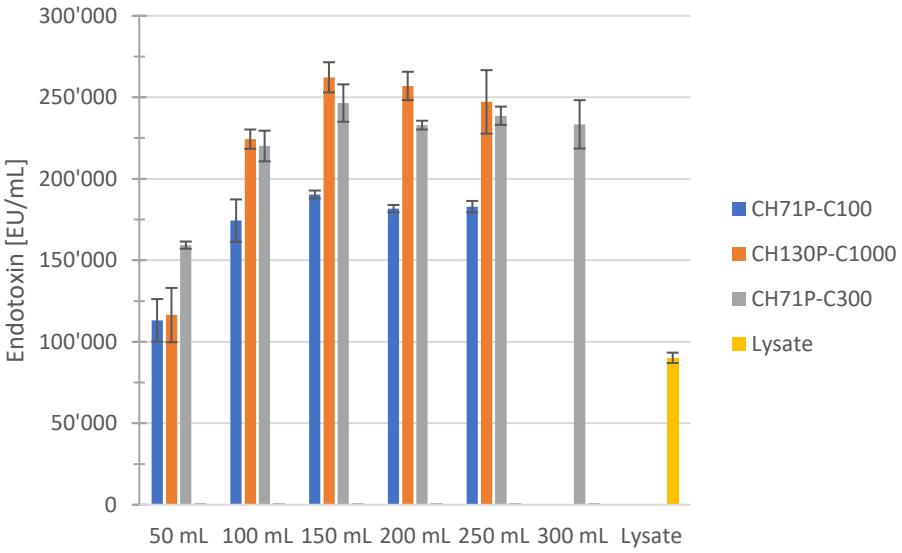

Figure 89 : Endotoxin concentration of Purafix® 50 mL filtrate fractions and the lysate before filtration. This follows the best-case scenario where the ratio of KDO to endotoxin is 35.7 (w/w)%.

The ratio of endotoxins in filtrate to lysate was then calculated to compare the results more easily.

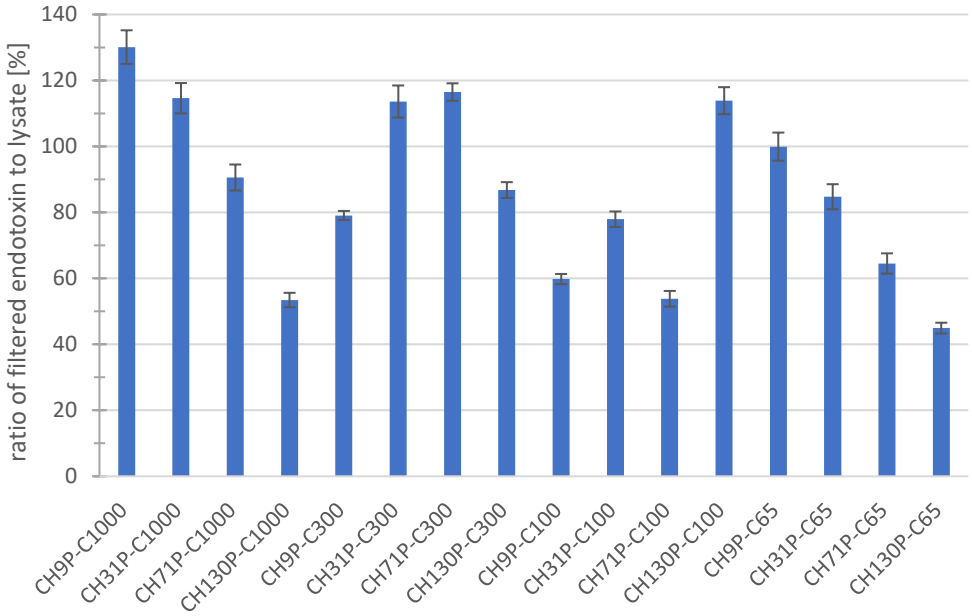

Figure 90 : Percentage of removed endotoxins of Puraspin® filtrates compared to lysates before filtration.

No trend can be perceived when looking at the whole set of combinations except for the filters used with the C1000 and C65 diatomaceous earth grades. Endotoxins removal is better with decreasing filter porosity for those filter aid grades.

The recovery of endotoxins was also superior to 100% for five combinations out of sixteen, which is an impossible value to obtain.

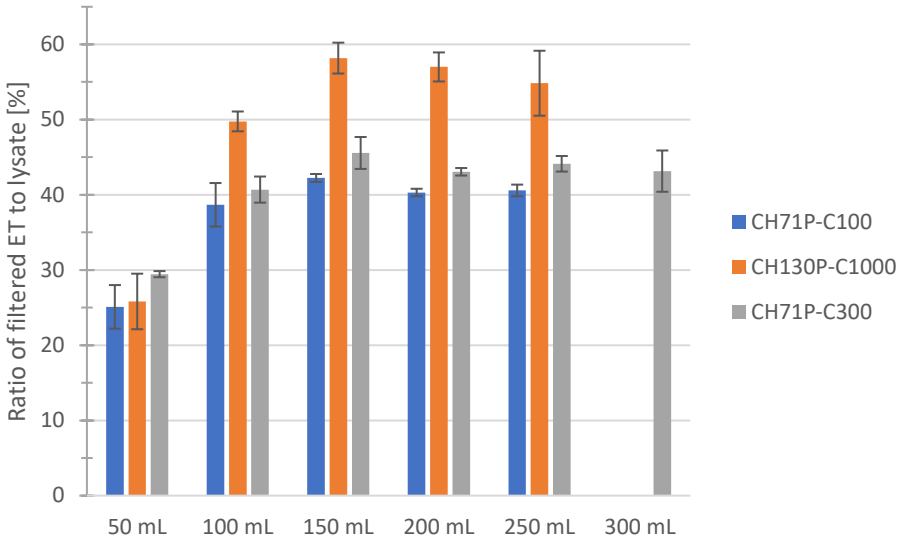

Figure 91 : Percentage of removed endotoxins of Purafix® 50 mL filtrate fractions compared to the lysate before filtration.

The overall recovery of endotoxins was also calculated for the Purafix® filtrations to better compare the three trials.

Table 29 : Overall recovery of endotoxins calculated for the Purafix® filtrations.

		CH71P-C100	CH130P-C1000	CH71P-C300
Volume of filtered lysate [mL]		250	250	300
Endotoxin quantity in unfiltered lysate [EU]	Worst case	1.3E+09	1.3E+09	1.6E+09
	Best case	2.3E+07	2.3E+07	2.7E+07
Endotoxin quantity in filtrate [EU]	Worst case	2.5E+09	3.3E+09	4.0E+09
	Best case	4.2E+07	5.5E+07	6.7E+07
Recovery [%]		187	246	246

The problem of recovering more than 100% was again encountered for the Purafix® filtrations.

Overall, endotoxin quantification presents two problems. The first one is either an underestimated endotoxin content of lysates or an overestimated endotoxin content of filtrates for both Puraspin® and Purafix®. The second one concerns the Puraspin® filtrations and the incoherent variations in the endotoxin removal capability of the combinations of filter and filter aid making it unfeasible to determine their exact influence.

All filtrates were analyzed in triplicate and showed good repeatability so manipulation errors during sample preparation are unlikely to be the cause of those variations.

The incoherent variations in the endotoxin removal capability of the Puraspin® combinations could be explained by the fact that cakes weren't uniform and a few seemed a bit too wet, resulting in inconsistent filtrations.

Another possibility is contamination. Two Puraspin® filtrations per type of filter were done with 15 mL of sterile water and no trace of endotoxins was found. The four grades of filter aids were mixed with sterile water at 57 g/L. The tubes were centrifuged 20 minutes at 10000 x g and the supernatants were analyzed. No trace of endotoxins was found. The filter aid is most likely not a source of contamination.

Contaminations in Purafix® are more likely to happen since it is more difficult to keep the system endotoxin-free. To better evaluate contaminations and elimination of endotoxins by NaOH, it would have been advantageous to take a sample of the ultrapure water used to rinse out the NaOH.

The degradation over time of the labelled KDO could be a possibility. The degradation happens by oxidation over time, which is why samples were prepared in the dark and vials were kept at 4°C during HPLC analysis to slow down the reaction. However, degradation of samples over time could probably be excluded as the C1000 samples were the first ones being injected while the C65 samples were the last ones, but both showed a similar pattern. Light exposure to some samples is also a cause that could probably be eliminated as all samples were prepared at the same time and showed good repeatability.

The sampling of unfiltered lysate may have also been incorrectly done each time, resulting in an inhomogeneous sample.

Endotoxins are very stable and resistant to heat and a range of pH. They have a complex structure and can interact with hydrophilic and hydrophobic substances under various physiological conditions (Khan MRI *et al.*, 2022). Unfiltered lysates were centrifuged after sonication to remove cell debris (like cell wall fragments, membranes and membranes bound proteins) that could clog the HPLC column (Peternel Š and Komel R, 2010). This centrifugation step wasn't done for filtrates samples. In that case, endotoxins may have bound to some components found in pellets resulting in lower concentrations of endotoxins in lysates than filtrates.

EDTA, contained in the TE buffer used for resuspension of biomass, is known to reduce the aggregation state of endotoxins at certain concentrations (Sandle T, 2021). This effect lowers the pyrogenicity and underestimates endotoxins in LAL tests. However, this shouldn't impact quantification by RP-HPLC with FLD.

It could have been interesting to use the LAL test on a few filtrates and lysates to evaluate the differences in concentration, and therefore the estimations made to calculate concentrations, with the RP-HPLC method. The effect of EDTA would also have to be taken into account.

4.5.3 DNA

Total dsDNA in filtrates was measured using the Invitrogen™ Qubit® kit from Thermo Fisher Scientific according to *method 3.2.7 "dsDNA quantification and purification - dsDNA quantification by Qubit"*. The values are shown on *figures 92* and *93*.

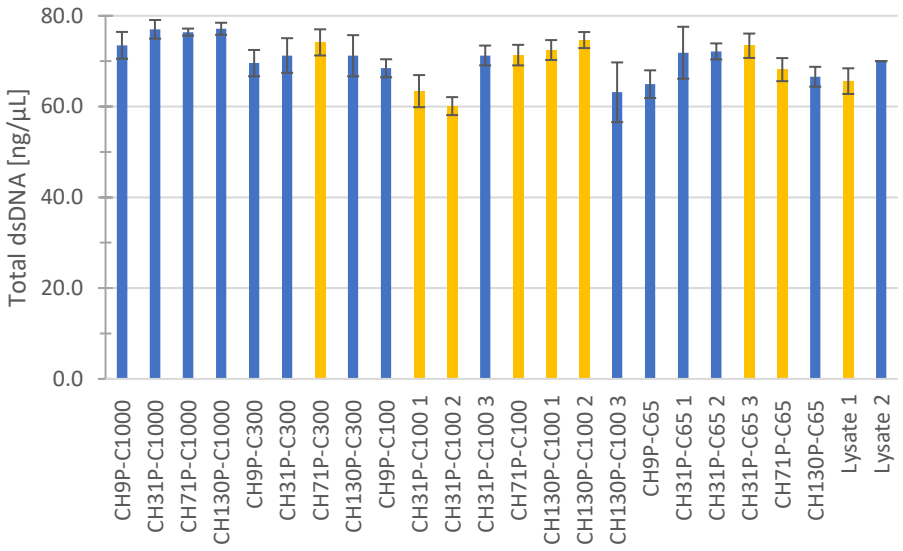

Figure 92 : Total dsDNA concentration of Puraspin® filtrates and lysates before filtration. The two colors represent the two different starting materials. When the averages of triplicates couldn't be done due to the different starting materials, the concerned combination is followed either by a 1, 2 or 3.

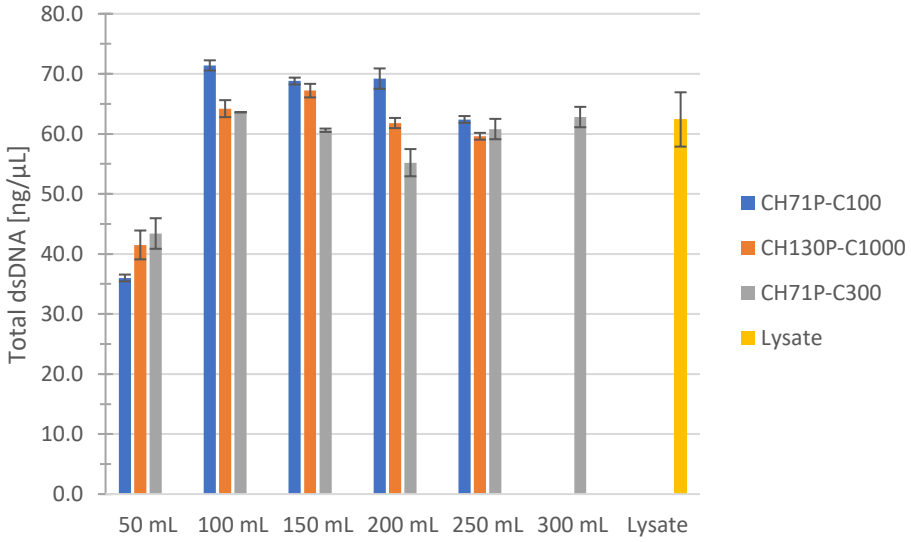

Figure 93 : Total dsDNA concentration of Purafix® 50 mL filtrate fractions and the lysate before filtration.

The overall recovery of DNA was also calculated for the Purafix® filtrations to better compare the three trials.

Table 30 : Overall recovery of total dsDNA calculated for the Purafix® filtrations.

	CH71P-C100	CH130P-C1000	CH71P-C300
Volume of filtered lysate [mL]	250	250	300
Total dsDNA quantity in unfiltered lysate [µg]	15600	15600	18720
Total dsDNA quantity in filtrate [µg]	15390	14715	17320
Recovery [%]	99	94	93

Total dsDNA does not seem to be significatively retained. Variations in dsDNA concentration are most likely a normal inconsistency in the lysate or due to the Qubit® quantification kit disparity. The Qubit® assays are quite sensitive to temperature and pipetting errors are also plausible.

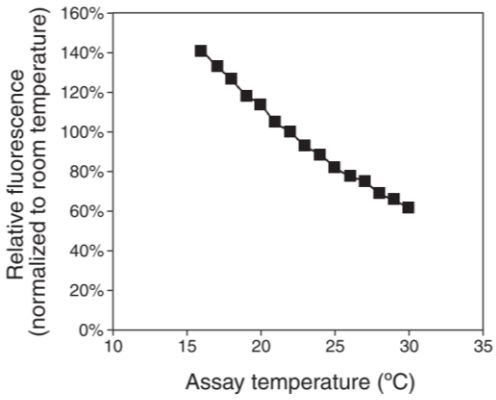

Figure 94 : Variation of relative fluorescence of the Invitrogen™ Qubit® kit from Thermo Fisher Scientific in function of temperature (Thermo Fisher Scientific, 2015).

Total dsDNA of the lysates for the Puraspin® filtrations were measured a second time after two weeks to determine if degradation occurred or not.

Table 31 : Total dsDNA concentration of two different lysates a first time and again after two weeks.

Total dsDNA [µg/mL]	Time since first quantification [weeks]		Coefficient of variation [%]
	0	2	
Lysate 1	65.6	61.0	5
Lysate 2	70.0	67.2	3

Since the coefficients of variation are low, it can be considered that preservation of samples at -20°C is adequate to avoid DNA degradation.

Two Puraspin® filtrations per filter type with 15 mL of sterile water were done and total dsDNA concentrations were all under the limit of quantification of 0.010 µg/mL. The four grades of filter aids were mixed with sterile water at 57 g/L. The tubes were centrifuged 20 minutes at 10000 x g and the supernatants were analyzed. Total dsDNA concentrations were all under the limit of quantification of 0.010 µg/mL.

The concentrations of lysates are also all within the usual range of 40 to 200 ng/µL of DNA in dry biomass.

During investigations to select the most adequate lysis method, it was found that directly analyzing filtrates made it impossible to quantify pUC18 because too much HCD was present. The Miniprep kit from Biolabs was the quick and easy solution to purify the samples and quantify pUC18. However, plasmids can't be recovered in their entirety. That is why an experience to determine the yield had to be done to know real pUC18 concentrations in filtrates.

The yield was determined by lysing in triplicate 1.5 mL of a suspension of dry biomass at 4 g/L with the Miniprep kit, measuring the total dsDNA concentration, diluting with TE buffer, purifying again by Miniprep and finally measuring the total dsDNA concentration of this second Miniprep. The way the yield was obtained is further explained in *method 3.2.7 "dsDNA quantification and purification - Yield determination of plasmid purification"*.

The TapeStation 4150 wasn't used as it was assumed that samples only contained the plasmid after the first Miniprep. This assumption is based on the electropherogram on *figure 49* showing a relatively pure sample when directly lysed by Miniprep.

Table 32 : Determination of the yield of pUC18 after a Miniprep purification.

Assay	total dsDNA in first miniprep [µg/mL]			total dsDNA in second Miniprep [µg/mL]			Yield of miniprep [%] (m/m)	
	Measurement n°1	Measurement n°2	Average	Measurement n°1	Measurement n°2	Average	Average from measurements	Average from assays
1	256	268	262	58.0	57.2	57.6	33.0	32.9 ± 0.2 (±0.1;95%;3)
2	236	237	237	52.0	52.0	52.0	33.0	
3	185	186	186	40.8	40.4	40.6	32.8	

A yield of 32.9% can be considered quite low but it must be kept in mind that the aim of this kit is to quickly obtain a very pure plasmid thus maybe sacrificing quantity recovered. Two consecutive alkaline lysis may also cause more severe DNA degradation. The only information available from the manufacturer concerning yields is that the Monarch® Plasmid Miniprep Kit allows the purification of up to 20 µg of plasmid DNA (International.neb.com 1, 2023). The assay labelled "1" had the maximum quantities of DNA loaded and recovered with 5.2 and 1.7 µg, respectively.

The samples were purified by Miniprep while total dsDNA was quantified with Qubit® and purity of pUC18 calculated with TapeStation 4150 according to *method 3.2.7 "dsDNA quantification and purification"*. The calculated concentrations of pUC18 with these methods are shown on *figures 95* and *96*.

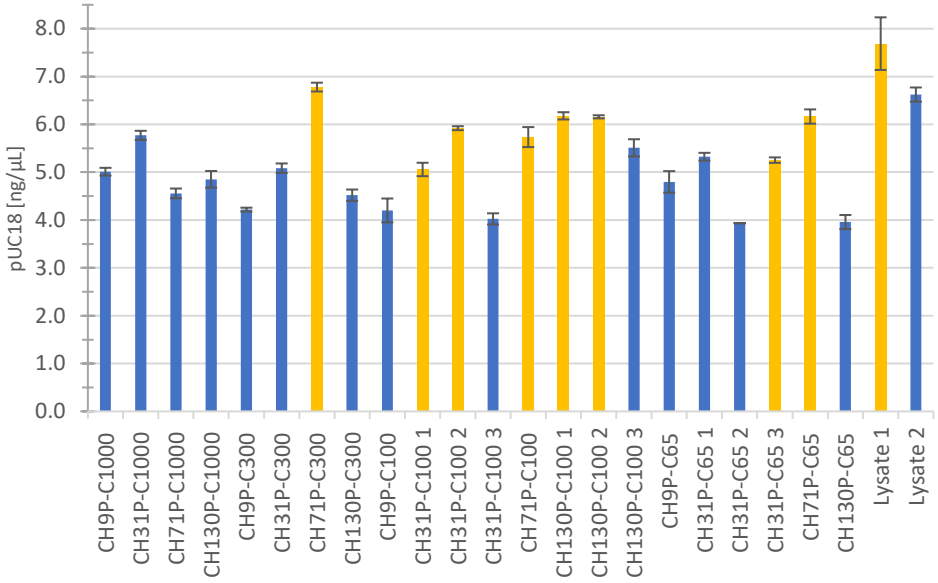

Figure 95 : pUC18 concentration of Puraspin® filtrates and lysates before filtration. The two colors represent the two different starting materials. When the averages of triplicates couldn't be done due to the different starting materials, the concerned combination is followed either by a 1, 2 or 3.

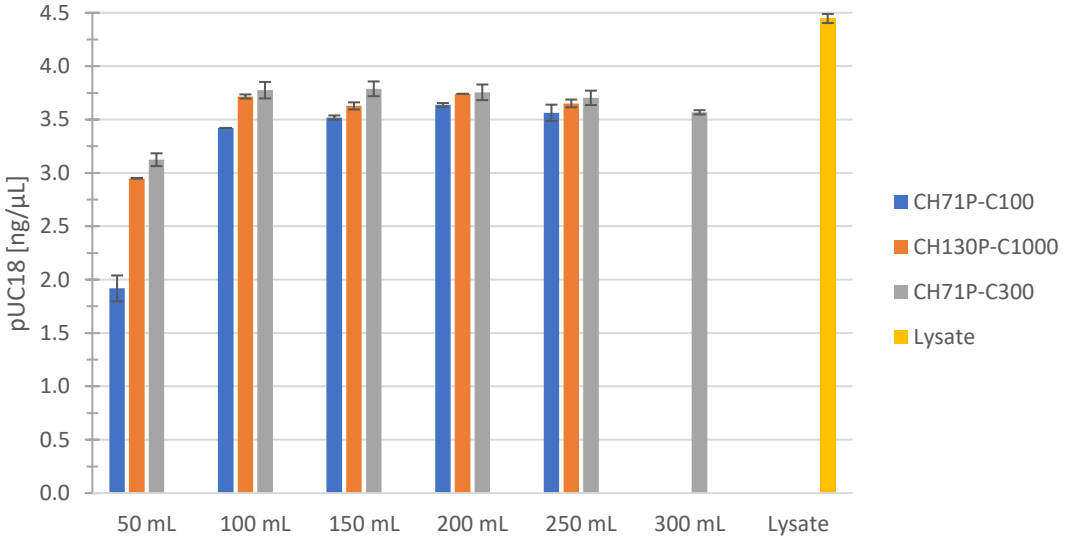

Figure 96 : pUC18 concentration of Purafix® 50 mL filtrate fractions and the lysate before filtration.

The pUC18 yields of the two lysates for Puraspin® and the one for Purafix® were 1.9, 1.7 and 1.1 mg of plasmid DNA per gram of dry biomass, respectively.

Yields of plasmid DNA depend on a variety of parameters like the plasmid itself and its size, the strain or growth conditions.

A study has previously done cultures with thirteen strains of *E. coli* containing the pLL14 plasmid in shake flasks with a chemically defined medium and obtained a maximal yield of 8.7 mg/g with the SCS1-S strain (Singer A *et al.*, 2009).

Another study chose fed batch conditions to grow *E. coli* DH10B bearing the plasmid pIDKE2 in a complex medium. The yield obtained was 0.44 mg/g (Cosme KM *et al.*, 2009).

The recovery of the plasmid after filtration was then calculated to compare the results more easily.

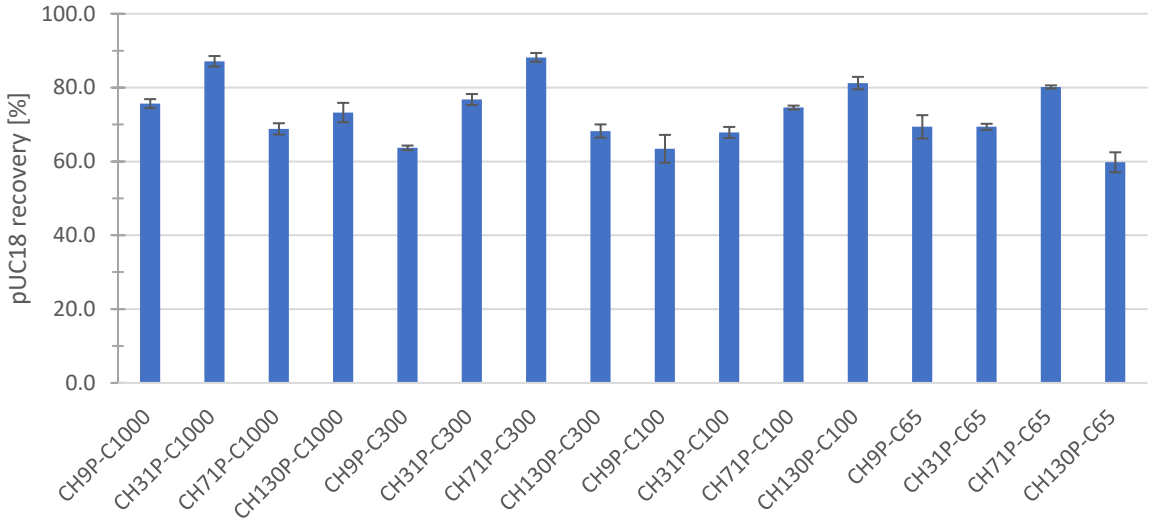

Figure 97 : pUC18 recovery of Puraspin® filtrates compared to lysates before filtration.

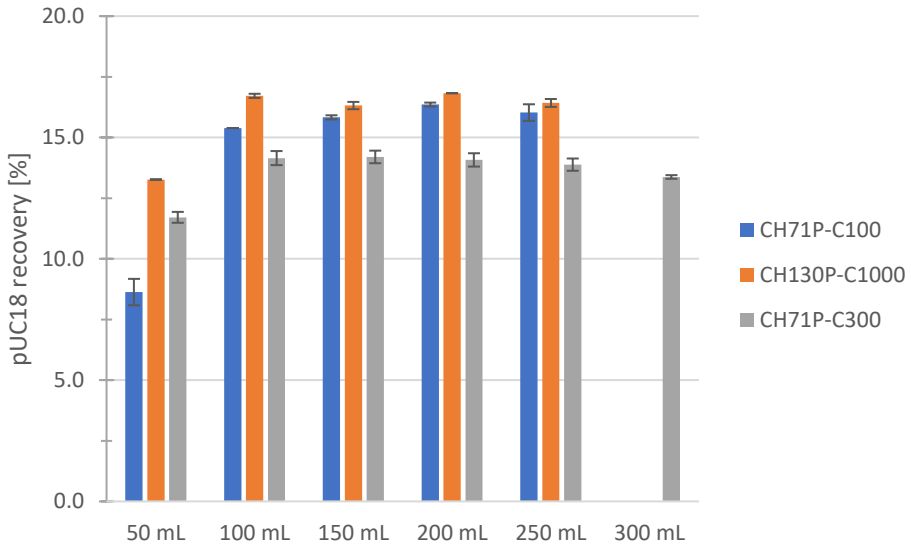

Figure 98 : pUC18 recovery of Purafix® 50 mL filtrate fractions compared to the lysate before filtration.

The overall recovery of pUC18 was also calculated for the Purafix® filtrations to better compare the three trials.

Table 33 : Overall recovery of pUC18 calculated for the Purafix® filtrations.

	CH71P-C100	CH130P-C1000	CH71P-C300
Volume of filtered lysate [mL]	250	250	300
pUC18 quantity in unfiltered lysate [µg]	1112	1112	1334
pUC18 quantity in filtrate [µg]	803	884	1086
Recovery [%]	72	80	81

The CH71P-C100 combination achieved a similar recovery for the Puraspin® and Purafix® filtrations, 75% and 72%, respectively.

The CH130P-C1000 combination achieved a slightly better recovery for the Purafix® filtration with 80%. The Puraspin® one achieved a recovery of 73%.

The CH71P-C300 combination achieved a slightly better recovery for the Puraspin® filtration with 88%. The Purafix® one achieved a recovery of 81%.

The fact that total dsDNA isn't really retained while recoveries of pUC18 aren't closer to 100% is quite contradictory.

Purification of samples using the Miniprep kit may not be reproducible. The manufacturer recommends to not wait longer than 1 minute before the neutralization step to prevent irreversible plasmid degradation. Since big amounts of Minipreps were done at once, incubation times may have varied consequently degrading DNA. The Miniprep kit is not really meant to process large amounts of samples at the same time.

Additionally, the experience to determine a Miniprep yield was based on samples already lysed once by Miniprep while samples from filtrates were lysed by French Press. The impact of the second Miniprep on those samples may vary as their DNA quality may differ, thus performing calculations with an inaccurate yield.

Also, measurements on TapeStation 4150 were only done once due to money constraints and manipulation errors are plausible since only 1 µL of sample is added to 10 µL of Genomic DNA Sample Buffer before analysis. Besides that, the TapeStation 4150 is more generally used for qualitative aspects rather than quantitative ones as stated by the Genomics Research Center of the University of Rochester (Genomics Research Center of the University of Rochester, 2023). The analysis costs 624 Swiss francs in Tapes and reagents to analyze 105 samples.

Finally, variations in quantification of pUC18 may be normal like in quantification of total dsDNA. Since concentrations are very low, minimal differences have a bigger impact on recoveries.

Two Puraspin® filtrations per filter type were also done but without any filter aid to further assess the influence of filter aid. The dsDNA concentrations are shown on *figure 99*.

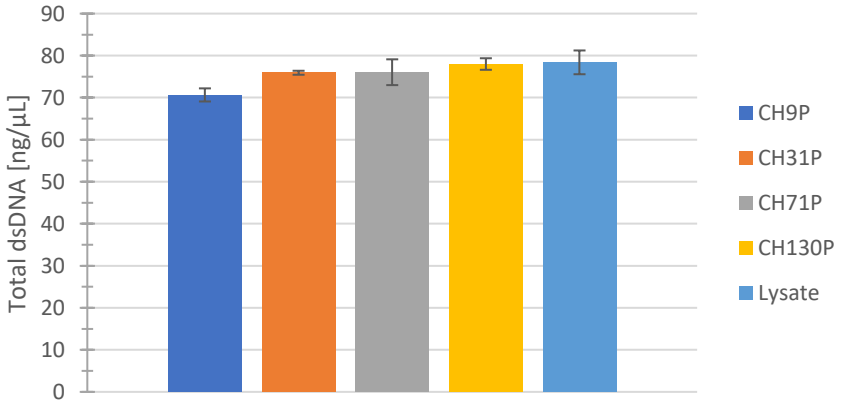

Figure 99 : Total dsDNA concentration of Puraspin® filtrates and lysate before filtration. The filtrations were performed without filter aids.

Total dsDNA does not seem to be retained. This observation is the same as made before with the Puraspin® and Purafix® filtrations.

The quantification of plasmids can be quite tricky as they have a similar nature to contaminant dsDNA. Additionally, the amounts recovered seemed very low thus confirming the needs of strong analytical methods.

The protocol established here was easy to perform with kits readily available but other approaches could have been more accurate.

Performing the lysis with the alkaline method would have already eliminated most contaminants removing the purification by Miniprep step and the variations associated. In that case, the effect of sodium hydroxide on the endotoxins would have been investigated to ensure no degradation occurred and quantification was still possible.

Other methods specifically quantifying plasmids include hydrophobic interaction chromatography (Diogo MM *et al.*, 2003), or quantitative PCR (Liang L *et al.*, 2013). However, finding the right conditions and preparing standards would take a lot of time.

4.5.4 Proteins

HCPs released upon lysis were also quantified using the Bradford method according to *method 3.2.8 "Proteins quantification"*. The total proteins concentrations for the sixteen combinations of Puraspin® filtrations are shown in *figure 100*.

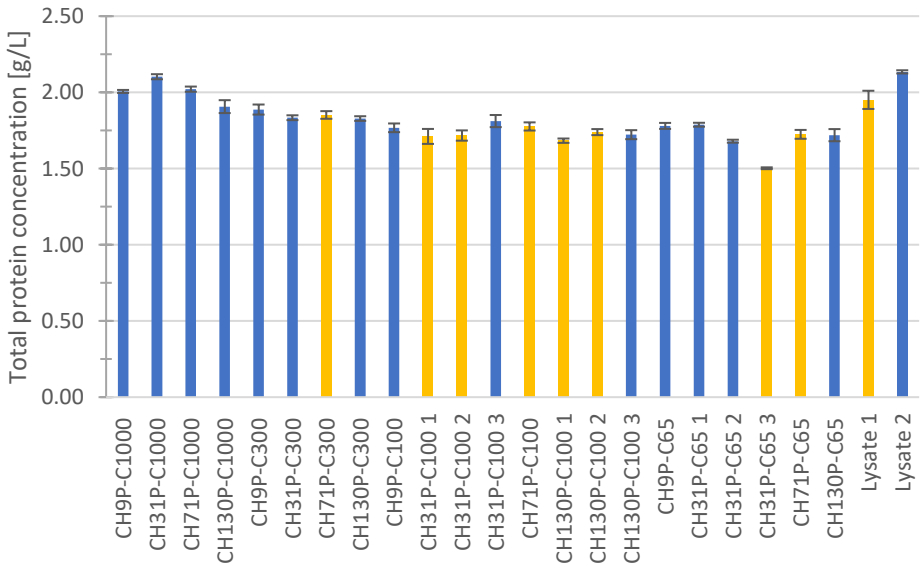

Figure 100 : Proteina concentration of Puraspin® filtrates and lysates before filtration. The two colors represent the two different starting materials. When the averages of triplicates couldn't be done due to the different starting materials, the concerned combination is followed either by a 1, 2 or 3.

They also were measured for all the fractions of the three Purafix® filtrations completed.

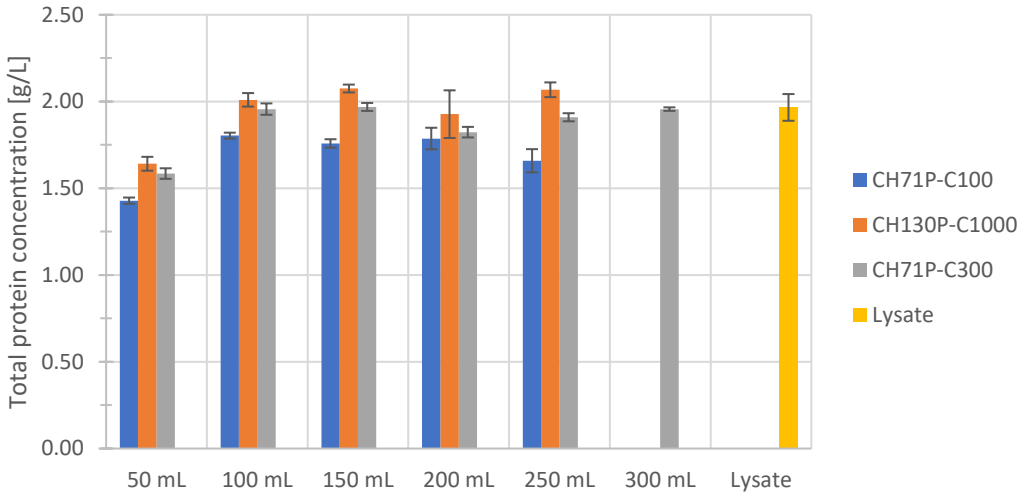

Figure 101 : Proteins concentration of Purafix® 50 mL filtrate fractions and the lysate before filtration.

The ratio of the concentration in filtrate to lysate was also calculated to better compare the sixteen combinations of Puraspin®.

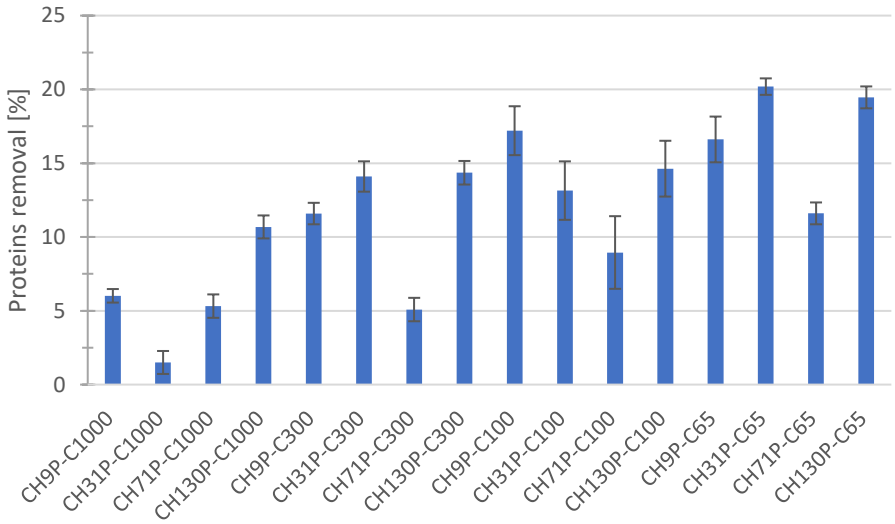

Figure 102 : Percentage of removed proteins of Puraspin® filtrates compared to lysates before filtration.

The removal of HCPs is varying but a trend can be roughly seen. Decreasing granulometry of filter aid and porosity of filter could have the effect of reducing the proteins concentration. This is only an assumption since there are multiple exceptions.

Table 34 : Overall recovery of proteins calculated for the Purafix® filtrations.

	CH71P-C100	CH130P-C1000	CH71P-C300
Volume of filtered lysate [mL]	250	250	300
Proteins quantity in unfiltered lysate [mg]	492	492	590
Protein quantity in filtrate [mg]	422	486	560
Recovery [%]	86	99	95

An overall recovery calculated for the Purafix® filtrations also further proves the assumption made before. The CH71P-C300 and CH71P-C100 combinations show a similar removal percentage when comparing Puraspin® and Purafix® filtrations. The CH130P-C1000 combination reduced proteins concentration of 11% with the Puraspin® but 1% with the Purafix®.

All filtrates were analyzed in triplicate and showed good repeatability, so manipulation errors are unlikely to be the cause of those variations.

The concentrations are also all within the usual range of 0.6 to 3 g/L of proteins in dry biomass.

4.5.5 Overall content of dsDNA, proteins and endotoxins

To evaluate contaminants quantified as a whole, the addition of concentrations of total dsDNA, proteins and endotoxins was calculated for each filtrate in Puraspin® and Purafix®. The concentration of total contaminants was also calculated in the form of a percentage to dry biomass concentration.

The statement made before that the worst-case scenario greatly overestimates endotoxins is confirmed here as DNA, proteins and endotoxins quantities altogether made up more than 100% of dry biomass for some filtrates.

The rest of dry biomass is made up of RNA, lipids, peptidoglycan, glycogen and polyamines. Those components take on average 35% of the dry biomass (Zinn M, 2022).

Table 35 : Total contaminants concentration and percentage of total contaminants to dry biomass of Purafix® filtrates and lysate. Contaminants measured include total dsDNA, proteins and endotoxins. The dry biomass concentration was 4 g/L.

	dsDNA, proteins and endotoxins [g/L]		dsDNA, proteins and endotoxins [%]	
	Best-case	Worst case	Best-case	Worst case
CH71P-C100	1.5	2.7	37	67
CH130P-C1000	2.0	3.3	51	83
CH71P-C300	1.9	3.2	49	81
Lysate	2.0	2.6	51	64

Table 36 : Total contaminants concentration and percentage of total contaminants to dry biomass of Puraspin® filtrates and lysates. Contaminants measured include total dsDNA, proteins and endotoxins. The dry biomass concentration was 4 g/L.

	dsDNA, proteins and endotoxins [g/L]		dsDNA, proteins and endotoxins [%]	
	Best-case	Worst case	Best-case	Worst case
CH9P-C1000 1	2.1	4.1	53	104
CH9P-C1000 2	2.1	4.2	53	106
CH9P-C1000 3	2.1	4.0	53	101
CH31P-C1000 1	2.2	4.0	55	100
CH31P-C1000 2	2.2	4.0	55	101
CH31P-C1000 3	2.2	3.9	55	99
CH71P-C1000 1	2.1	3.4	53	84
CH71P-C1000 2	2.3	3.8	57	94
CH71P-C1000 3	2.0	3.5	50	86
CH130P-C1000 1	2.0	2.8	49	71
CH130P-C1000 2	2.0	2.9	49	72
CH130P-C1000 3	2.1	2.8	51	69
CH9P-C300 1	2.0	3.3	49	82
CH9P-C300 2	2.0	3.2	50	80
CH9P-C300 3	2.0	3.2	49	79
CH31P-C300 1	2.0	3.5	50	87
CH31P-C300 2	1.9	3.7	46	93
CH31P-C300 3	1.9	3.9	49	97
CH71P-C300 1	1.9	4.0	48	99
CH71P-C300 2	2.0	3.7	49	93
CH71P-C300 3	2.0	3.8	50	94
CH130P-C300 1	1.9	3.4	49	86
CH130P-C300 2	1.9	3.1	48	79
CH130P-C300 3	1.9	3.2	48	81
CH9P-C100 1	1.8	2.7	46	68
CH9P-C100 2	1.9	2.8	47	70
CH9P-C100 3	1.8	2.8	46	71
CH31P-C100 1	1.8	3.0	45	75
CH31P-C100 2	1.8	3.1	45	78
CH31P-C100 3	1.9	3.1	48	77
CH71P-C100 1	1.9	2.5	47	64
CH71P-C100 2	1.9	2.9	48	73
CH71P-C100 3	1.8	2.7	45	68
CH130P-C100 1	1.8	3.8	45	94
CH130P-C100 2	1.8	3.7	46	92
CH130P-C100 3	1.8	3.4	45	85
CH9P-C65 1	1.9	3.6	47	90
CH9P-C65 2	1.9	3.6	46	89
CH9P-C65 3	1.9	3.1	47	78
CH31P-C65 1	1.9	3.2	47	80
CH31P-C65 2	1.8	3.2	44	79
CH31P-C65 3	1.6	2.9	40	72
CH71P-C65 1	1.8	2.7	44	69
CH71P-C65 2	1.8	2.8	45	71
CH71P-C65 3	1.8	2.9	46	74
CH130P-C65 1	1.8	2.6	44	64
CH130P-C65 2	1.8	2.4	45	61
CH130P-C65 3	1.8	2.5	46	62
Lysate 1	2.0	3.6	51	90
Lysate 2	2.2	3.8	56	96

5. Conclusion and outlooks

Alluvial filtration is a very efficient method for the clarification of lysates. The sheets developed by Filtrox AG in combination with diatomaceous earth can improve the removal of turbid matter and endotoxins.

Reduction of turbidity was very efficient, up to 73% with the CH31P filter and C65 filter aid, for Puraspin®. A clear trend could be determined : Finer Celpure® grades and less porous filter types improved clarification. In Purafix® trials, the combination of the CH71P filter and C100 filter aid had the highest reduction with 80% probably thanks to a lower filtrate flux compared to other trials. The importance of filter aid was also assessed by performing Puraspin® filtrations without it. The highest reduction of turbidity was only 45% with the CH130P filter.

Removal of endotoxins was observed in Puraspin® filtrations but several ones had recoveries higher than 100%, up to 130%. This problem was exacerbated in Purafix® filtrations as recoveries went up to 246%. No influence from filter type or Celpure® grade in removal could be determined due to too many variations in filter and filter aid combinations. Repeatability was acceptable but a few explanations, in a non-exhaustive order, are : degradation of labelled KDO, non-uniformities in cakes or an inhomogeneous sampling of unfiltered lysates. Doing LAL tests would confirm if RP-HPLC is a good alternative and how far the assumed pyrogenicity and endotoxin content are from the reality.

Overall, total dsDNA wasn't really retained except for the first 50 mL fractions of all Purafix® filtrations. Their recovery of DNA were on average 7.3% lower compared to all other 50 mL fractions. In general, no influence from filter type or Celpure® grade in removal was observed.

Recoveries of pUC18 were between 60 and 88% for Puraspin® filtrations but no influence from filter type or Celpure® grade could be observed. Overall recoveries for Purafix® filtrations were between 72 and 81%. Quantification on TapeStation 4150 would have given more reliable data if performed in triplicate and not only once because of the price of the analysis.

Removal of proteins was minimal. The highest reduction in proteins observed in Puraspin® trials was 20% with the CH31P filter and C65 filter aid. Finer Celpure® grades and less porous filter types seemed to improve removal but variations persisted. In Purafix® trials, the combination of the CH71P filter and C100 filter aid had the highest reduction with 14% probably thanks to a lower filtrate flux compared to other trials.

In Puraspins®, the CH71P filter with C300 Celpure® had the highest pUC18 recovery while the CH130P filter with C1000 Celpure® and the CH71P filter with C100 Celpure® had the highest removal of endotoxins. Those three were chosen for the scaled-up filtration using the capsule.

The main parameter that seemed to influence cake and filter resistance was the maximal differential pressure reached. Due to varying filtrate flux, assessing the influence of the type of filter and filter aid wasn't conclusive.

It would be necessary to redo the three trials with Purafix® BIO SD 2" capsule in the same conditions for better comparisons and to further investigate the sudden drop of differential pressure observed for all of them.

To save time, a one-time batch culture in a bioreactor and concentrating biomass for lysis could be useful approaches.

6. References

Aatbio.com, 2023. https://www.aatbio.com/resources/buffer-preparations-and-recipes/te-buffer-10x (consulted the 08.08.2023)

Agilent.com 1, 2023. https://www.agilent.com/cs/library/usermanuals/public/4200-TapeStation_SystemManual.pdf (consulted the 06.08.2023)

Agilent.com, 2023. https://www.agilent.com/en/product/mutagenesis-cloning/competent-cells-competent-cell-supplies/competent-cells-for-routine-cloning/xl1-blue-competent-cells-233099#howitworks (consulted the 06.08.2023)

Bächle V et *al.*, 2021. Bächle V, Morsch P, Gleiss M and Nirschl H : Influence of the Precoat Layer on the Filtration Properties and Regeneration Quality of Backwashing Filters, Eng 2, 181-196 (2021)

Baeshen NA *et al.*, 2014. Baeshen NA, Baeshen MN, Sheikh A, Bora RS, Ahmed MM, Ramadan HA, Saini KS and Redwan EM : Cell factories for insulin production. Microb Cell Fact, 13, 141 (2014)

Beei.com, 2023. https://www.beei.com/blog/french-press-cell-lysis-how-does-it-compare-to-homogenization#:~:text=The%20French%20press%20consists%20of,stress%2C%20resulting%20in%20cellular%20disruption. (consulted the 06.08.2023)

Bocascientific.com, 2023. https://bocascientific.com/v33002-15-detail (consulted the 05.08.2023)

Bradford MM, 1976. Bradford MM : A rapid and sensitive method for the quantitation of microgram quantities of protein utilizing the principle of protein-dye binding, Analytical Biochemistry, 72, 248-254 (1976)

Bucsella B *et al.*, 2020. Bucsella B, Hoffmann A, Zollinger M, Stephan F, Pattky M, Daumke R, Heiligtag FJ, Frank B, Bassas-Galia M, Zinn M and Kalman F : Novel RP-HPLC based assay for selective and sensitive endotoxin quantification, Anal Methods, 12(38), 4621-4634 (2020)

Chemicalprocessing.com, 2023. https://www.chemicalprocessing.com/processing-equipment/powder-solids/article/11306909/make-the-most-of-filter-aids (consulted the 05.08.2023)

Chih-Hui L *et al.*, 2011. Lin CH, Chen YC and Pan TM : Quantification Bias Caused by Plasmid DNA Conformation in Quantitative Real-Time PCR Assay, PLOS ONE, 6(12) (2011)

Cosme KM *et al.*, 2009. Cosme KM, Martínez E, Jimenez YP, de la Iglesia MP, Hernández JV, Idahody DT, Gómez SM, Hernández OR, Pupo M and Fernández ML : High-Cell-Density Culture to Produce Plasmid DNA for Gene Therapy in *E. coli*, BioPharm International, 22(7) (2009)

Crelier S and Rüdt M 1, 2022. Crelier S and Rüdt M, Course « Industrial purification of biomolecules », chapter 3 – part 1 : Membranes Techniques, HES-SO Valais Wallis, Sion (2022)

Crelier S and Rüdt M 2, 2022. Crelier S and Rüdt M, Course « Industrial purification of biomolecules », chapter 4 – part 1 : cell lysis, HES-SO Valais Wallis, Sion (2022)

Crelier S and Rüdt M 3, 2022. Crelier S and Rüdt M, Course « Bioprocesses », chapter 2 - part 3 : Bioreactors, HES-SO Valais Wallis, Sion (2022)

Crelier S and Rüdt M, 2022. Crelier S and Rüdt M, Course « Industrial purification of biomolecules », chapter 2 – part 3 : Filtration, HES-SO Valais Wallis, Sion (2022)

Crelier S and Rüdt M, 2023. Crelier S and Rüdt M, Course « Industrial purification of biomolecules », chapter 9 : mAb platform process, HES-SO Valais Wallis, Sion (2023)

Crelier S, 2017. Crelier S, Course « Downstream Processing », chapter 2 – part c, HES-SO Valais Wallis, Sion (2017)

Cshprotocols.cshlp.org, 2023. https://cshprotocols.cshlp.org/content/2015/7/pdb.rec087874.full?text_only=true (consulted the 08.08.2023)

Cytivalifesciences.com, 2023. https://www.cytivalifesciences.com/en/us/shop/bioprocessing-filtration/normal-flow-filtration/depth-filtration/stax-disposable-depth-filter-systems-p-36559 (consulted the 07.08.2023)

Cytivalifesciences.com, 2023. https://www.cytivalifesciences.com/en/us/news-center/the-why-and-how-of-hcp-elisas-10001 (consulted the 06.08.2023)

De Mattos JCP *et al.*, 2004. De Mattos JCP, Dantas FJS, Caldeira-de-Araújo A and Moraes MO : Agarose gel electrophoresis system in the classroom: Detection of DNA strand breaks through the alteration of plasmid topology, Biochemistry and Molecular Biology Education, 32(4), 254-257 (2004)

Diogo MM *et al.*, 2003. MM Diogo, JA Queiroz and DMF Prazeres : Assessment of purity and quantification of plasmid DNA in process solutions using high-performance hydrophobic interaction chromatography, Journal of Chromatography A, 998(1–2), 109-117 (2003)

Falcotet F, 2022. Falcotet F, Course «Process Engineering», Introduction to process engineering, HES-SO Valais Wallis, Sion (2022)

FDA, 2018. https://www.fda.gov/vaccines-blood-biologics/cellular-gene-therapy-products/what-gene-therapy (consulted the 04.08.2023)

Ferreira GNM *et al.*, 2000. Ferreira GNM, Monteiro GA, Prazeres DMF and Cabral JMS : Downstream processing of plasmid DNA for gene therapy and DNA vaccine applications, Trends in Biotechnology, 18(9), 380-388 (2000)

Filtrox AG 1, 2023. Filtrox AG : Product specification – Depth filter sheets with zeta-potential - Purafix® ZP, version 2.0, St. Gallen (2023)

Filtrox AG 2, 2020. Filtrox AG : Product specification – Filter aid - CELPURE® C1000, version 03-2020_R01, St. Gallen (2020)

Filtrox AG 2, 2023. Filtrox AG : Scale-up Test Kit - Quick Reference Guide, St. Gallen (2023)

Filtrox AG 3, 2020. Filtrox AG : Product specification – Filter aid - CELPURE® C300, version 03-2020_R01, St. Gallen (2020)

Filtrox AG 4, 2020. Filtrox AG : Product specification – Filter aid - CELPURE® C100, version 03-2020_R01, St. Gallen (2020)

Filtrox AG 5, 2020. Filtrox AG : Product specification – Filter aid - CELPURE® C65, version 03-2020_R01, St. Gallen (2020)

Filtrox AG 6, 2020. Filtrox AG : Product specification – Filter modules - FILTRODISC™ CH 09P, version 01-2020_R01, St. Gallen (2020)

Filtrox AG 7, 2020. Filtrox AG : Product specification – Filter modules - FILTRODISC™ CH 31P, version 01-2020_R01, St. Gallen (2020)

Filtrox AG 8, 2020. Filtrox AG : Product specification – Filter modules - FILTRODISC™ CH 71P, version 01-2020_R01, St. Gallen (2020)

Filtrox AG 9, 2020. Filtrox AG : Product specification – Filter modules - FILTRODISC™ CH 130P, version 01-2020_R01, St. Gallen (2020)

Filtrox AG, 2023. Filtrox AG, St. Gallen (2023)

Filtrox.com 1, 2023. https://www.filtrox.com/wp-content/uploads/2017/12/FILTRODISC-BIO-SD_07_2019_E.pdf (consulted the 05.08.2023)
Filtrox.com 2, 2023. https://www.filtrox.com/wp-content/uploads/2018/05/Filter-Sheets-NOVOX_04_2018_E.pdf (consulted the 05.08.2023)

Filtrox.com 3, 2023. https://www.filtrox.com/applications/filtration-for-life-science/bio-sd/ (consulted the 06.08.2023)

Filtrox.com, 2023. https://www.filtrox.com/filtration-services/depth-filtration/ (consulted the 04.08.2023)

Fisher Scientific, 2023. https://beta-static.fishersci.com/content/dam/fishersci/en_US/documents/programs/scientific/brochures-and-catalogs/guides/millipore-sigma-membrane-filtration-guide.pdf (consulted the 04.08.2023)

Frewitt.com, 2023. https://frewitt.com/en-us/Products/Lab-Mills/D50-50nm/milling-machine-nano-milling (consulted the 30.07.2023)

Fux AC *et al.*, 2023. Fux AC, Casonato Melo C, Michelini S, Swartzwelter BJ, Neusch A, Italiani P and Himly M : Heterogeneity of Lipopolysaccharide as Source of Variability in Bioassays and LPS-Binding Proteins as Remedy, Int. J. Mol. Sci, 24(9), 8395 (2023)

Galindo J *et al.*, 2016. Galindo J, Barrón BL and Lara AR : Improved production of large plasmid DNA by enzyme-controlled glucose release, Ann Microbiol 66, 1337–1342 (2016)

Gassmann M and McHoull B, 2015. : DNA Integrity Number (DIN) with the Agilent 2200 TapeStation System and the Agilent Genomic DNA ScreenTape Assay, Agilent Technologies, Inc., technical overview (2015)

Genomics Research Center of the University of Rochester, 2023. https://www.urmc.rochester.edu/MediaLibraries/URMCMedia/research/for-researchers/shared-resource-labs-facilities/rochester-genomics-center/images/Interpretation-of-Tapestation-PPT_071921_EMP.pdf (consulted the 01.08.2023)

Geologyforinvestors.com, 2023. https://www.geologyforinvestors.com/silica-diatomite-commodity-overview/ (consulted the 10.08.2023)

HES-SO Valais Wallis 1, 2023. Downstream processing laboratory : protocol 7.1 « Bradford total protein assay », HES-SO Valais Wallis, Sion (2023)

HES-SO Valais Wallis, 2023. Molecular biology laboratory : protocol 6.1 « Preparation of the electrophoresis solution », HES-SO Valais Wallis, Sion (2023)

Homogenisingsystems.com, 2023. https://www.homogenisingsystems.com/french-press-cell-lysis-disruption.html (consulted the 06.08.2023)

Icermax.com, 2023. https://icermax.com/literature-2/ (consulted the 04.08.2023)

International.neb.com 1, 2023. https://international.neb.com/products/t1010-monarch-plasmid-miniprep-kit#Product%20Information (consulted the 01.08.2023)

International.neb.com, 2023. https://international.neb.com/products/t1010-monarch-plasmid-miniprep-kit#Product%20Information (consulted the 06.08.2023)

Kawahara K, 2021. Kawahara K : Variation, Modification and Engineering of Lipid A in Endotoxin of Gram-Negative Bacteria, International Journal of Molecular Sciences, 22(5), 2281 (2021)

Khan MRI *et al.*, 2022. Khan MRI, Thangarasu M, Kang H and Hwang I : Plant produced endotoxin binding recombinant proteins effectively remove endotoxins from protein samples, Sci Rep 12, 16377 (2022)

Liang L *et al.*, 2013. Liang L, Xiujie Z, Yusong W and Wujun Jin : Development of a Novel Reference Plasmid for Accurate Quantification of Genetically Modified Kefeng6 Rice DNA in Food and Feed Samples, BioMed Research International, 2013, 134675 (2013**)**

Liu Z and Smith S, 2021. Liu Z and Smith S : Enzyme Recovery from Biological Wastewater Treatment, Waste and Biomass Valorization, 12 (2021)

Mahdi FM and Holdich RG, 2013. Mahdi FM and Holdich RG : Laboratory cake filtration testing using constant rate, Chemical Engineering Research and Design, 91(6), 1145-1154 (2013)

Mahdi FM *et al.*, 2019. Mahdi FM, Hunter TN and Holdich RG : A Study of Cake Filtration Parameters Using the Constant Rate Process, Processes, 7(10), 746 (2019)

Mali S, 2013. Mali S : Delivery systems for gene therapy, Indian J Hum Genet, 19(1), 3-8 (2013)

Martínez-Puente DH *et al.*, 2022. Martínez-Puente DH, Pérez-Trujillo JJ, Zavala-Flores LM, García-García A, Villanueva-Olivo A, Rodríguez-Rocha H, Valdés J, Saucedo-Cárdenas O, Montes de Oca-Luna R and Loera-Arias MdJ : Plasmid DNA for Therapeutic Applications in Cancer, Pharmaceutics, 14(9), 1861(2022)

Mazgaeen L and Gurung P, 2020. Mazgaeen L and Gurung P : Recent Advances in Lipopolysaccharide Recognition Systems, Int. J. Mol. Sci., 21, 379 (2020)

Medium.com, 2023. https://medium.com/@seemaminerals11/diatomite-manufacturer-72be5a8bb4a6 (consulted the 10.08.2023)

Microlabgallery.com, 2023. http://wwww.microlabgallery.com/gallery/72-10%20535-44.aspx (consulted the 28.07.2023)

Multimedia.3m.com, 2023. https://multimedia.3m.com/mws/media/591423O/zeta-plus-single-use-depth-filtration-product-portfolio-pdf.pdf (consulted the 07.08.2023)

Nejatishahidein N and Zydney AL, 2021. Nejatishahidein N and Zydney AL : Depth filtration in bioprocessing — new opportunities for an old technology, Current Opinion in Chemical Engineering, 34 (2021)

Nejatishahidein N and Zydney AL, 2021. Nejatishahidein N and Zydney A L : Depth filtration in bioprocessing — new opportunities for an old technology, Current Opinion in Chemical Engineering, 34, 100746 (2021)

Ohlson J, 2020. Ohlson J : Plasmid manufacture is the bottleneck of the genetic medicine revolution, Drug Discov Today, 25(11), 1891–3 (2020)

Orzikowski H, 2023. https://blog.wika.us/knowhow/8-common-reasons-for-pressure-gauge-failure/ (consulted the 31.07.2023)

Ottinger M *et al.*, 2022. Ottinger M, Wenk I, Carvalho Pereira J, John G and Junne S : Single-Use Technology in the Biopharmaceutical Industry and Sustainability: A Contradiction?, Chemie Ingenieur Technik, 94, 1883-1891 (2022)

Peternel Š and Komel R, 2010. Peternel Š and Komel R : Isolation of biologically active nanomaterial (inclusion bodies) from bacterial cells, Microb Cell Fact 9, 66 (2010)

Pharmaceutical-technology.com, 2023. https://www.pharmaceutical-technology.com/products/single-use-filter/ (consulted the 07.08.2023)

Prazeres DMF and Monteiro GA, 2014. Prazeres DMF and Monteiro GA : Plasmid Biopharmaceuticals, Microbiol Spectr, 2(6) (2014)

Prazeres DMF and Monteiro GA, 2014. Prazeres DMF and Monteiro GA : Plasmid Biopharmaceuticals, Microbiology Spectrum, 2(6) (2014)

Progressiveplanet.com, 2023. https://progressiveplanet.com/myth-6-de-mines-are-destructive/ (consulted the 10.08.2023)

Qiagen.com, 2023. https://www.qiagen.com/ja-us/knowledge-and-support/knowledge-hub/bench-guide/plasmid/working-with-plasmids/lysis-of-bacterial-cells-for-plasmid-purification (consulted the 04.08.2023)

Rajnovic D *et al.*, 2019. Rajnovic D, Muñoz-Berbel X and Mas J : Fast phage detection and quantification: An optical density-based approach, PLOS ONE, 14(5) (2019)

Ripperger S *et al.*, 2013. Ripperger S, Gösele W, Alt C and Loewe T : Filtration, 1. Fundamentals. Ullmann's Encyclopedia of Industrial Chemistry (Ed.), 1-38 (2013)

Saleem M *et al.*, 2012. Saleem M, Krammer G and Tahir MS : The effect of operating conditions on resistance parameters of filter media and limestone dust cake for uniformly loaded needle felts in a pilot scale test facility at ambient conditions, Powder Technol, 228(44-2), 100-107 (2012)

Sandle T, 2016. Sandle T : 11 - Endotoxin and pyrogen testing, Pharmaceutical Microbiology, Woodhead Publishing, 131-145 (2016)

Sandle T, 2021. Sandle T : Bacterial Endotoxin Test using LAL methodology: overcoming interfering factors, European Pharmaceutical Review, 4 (2021)

Sartorius.com, 2023. https://www.sartorius.com/download/1102304/vivapure-endotoxin-removal-application-note-en-l-sartorius-p-1--data.pdf (consulted the 06.08.2023)

Schreiber S *et al.*, 2017. Schreiber S, Thiefes A, Schuldt U, Dähne L, Scheper Thomas and Beutel S : New application of depth filters for the immobilization of Candida antarctica lipase B, Applied Microbiology and Biotechnology, 101 (2017)

Shahid M *et al.*, 2022. Shahid M, Faure C, Ottoboni S, Lue L and Price C : Employing Constant Rate Filtration To Assess Active Pharmaceutical Ingredient Washing Efficiency, Org Process Res Dev, 26(1), 97-110 (2022)

Simplepharmanotes.com, 2023. https://www.simplepharmanotes.com/2022/01/filtration-filter-aids.html (consulted the 05.08.2023)

Singer A *et al.*, 2009. Singer A, Eiteman MA and Altman E : DNA plasmid production in different host strains of Escherichia coli, Journal of Industrial Microbiology and Biotechnology, 36(4), 521–530 (2009)

Slideshare.net, 2023. https://www.slideshare.net/sjykmuch/filtration-17008170 (consulted the 05.08.2023)

Stjohnslabs.com, 2023. https://stjohnslabs.com/how-to-prepare-phosphate-buffered-saline-pbs/ (consulted the 08.08.2023)

Storhas W, 2003. Storhas W : Bioverfahrensentwicklung. WILEY-VCH, Weinheim (2003), 283-287

Surfanet.org, 2023. http://www.surfanet.org/echelle-des-duretes-mohs/ (consulted the 30.07.2023)

Susupport.com, 2023. https://www.susupport.com/knowledge/single-use-technology/single-use-filtration-systems-their-impact-process-integrity-biopharma (consulted the 07.08.2023)

Technologynetworks.com, 2023. https://www.technologynetworks.com/analysis/articles/agarose-gel-electrophoresis-how-it-works-and-its-uses-358161 (consulted the 06.08.2023)

Thakur G *et al.*, 2020. Thakur G, Hebbi V, Parida S and Rathore AS : Automation of dead-end filtration: an enabler for continuous processing of biotherapeutics, Front Bioeng Biotechnol, 8, 758 (2020)

Thegenehome.com, 2023. https://www.thegenehome.com/how-does-gene-therapy-work/vectors (consulted the 04.08.2023)

Thermo Fisher Scientific, 2015. https://tools.thermofisher.com/content/sfs/manuals/Qubit_dsDNA_BR_Assay_UG.pdf (2015) (consulted the 01.08.2023)

ThermoFisher.com, 2023. https://www.thermofisher.com/ch/en/home/industrial/spectroscopy-elemental-isotope-analysis/molecular-spectroscopy/fluorometers/qubit/features.html#uv-absorbance (consulted the 06.08.2023)

Thomas GB and Finney RL, 1979. Thomas GB and Finnney RL : Calculus and Analytic Geometry (fifth ed.), Addison-Wesley (1979), 434.

Thomaspumps.com, 2023. https://www.thomaspumps.com/en-hk/industries-and-applications/bio-pharmaceutical (consulted the 04.08.2023)

Tools.thermofisher.com, 2023. https://tools.thermofisher.com/content/sfs/manuals/Qubit_dsDNA_BR_Assay_UG.pdf (consulted the 08.08.2023)

Un.org, 2023. https://www.un.org/sustainabledevelopment/blog/2015/12/sustainable-development-goals-kick-off-with-start-of-new-year/ (consulted the 10.08.2023)

Voronin D *et al.*, 2020. Voronin D, Kozlova A, Verkhovskii R, Ermakov A, Makarkin M, Inozemtseva O and Bratashov Daniil : Detection of Rare Objects by Flow Cytometry: Imaging, Cell Sorting, and Deep Learning Approaches, International Journal of Molecular Sciences, 21, 2323 (2020)

Wikimedia.org, 2023. https://commons.wikimedia.org/wiki/File:OrbitalEccentricityDemo.svg (consulted the 30.07.2023)

Williams PD and Kingston PA, 2011. Williams PD and Kingston PA : Plasmid-mediated gene therapy for cardiovascular disease, Cardiovascular Research, 91 (4), 565–576 (2011)

Wood WN *et al.*, 2016. Wood WN, Smith KD, Ream JA and Lewis LK :Enhancing yields of low and single copy number plasmid DNAs from *Escherichia coli* cells, J Microbiol Methods 133, 46-51 (2016)

Yagi N *et al.*, 1996. Yagi N, Satonaka K, Horio M, Shimogaki H, Tokuda Y and Maeda S : The role of DNase and EDTA on DNA degradation in formaldehyde fixed tissues, Biotechnic & Histochemistry, 71(3), 123–129 (1996)

Zinn M, 2022. Zinn M, Course « Bioprocess engineering », chapter 5 : Medium design, HES-SO Valais Wallis, Sion (2022)

Zor T and Selinger Z, 1996. Zor T and Selinger Z : Linearization of the Bradford protein assay increases its sensitivity: theoretical and experimental studies, Analytical Biochemistry, 236, 302-308 (1996)

7. Abbreviations

BSA : Bovine serum albumin

CDW : Cell dry weight

DIN : DNA Integrity number

DMB : 1,2-diamino-4,5-methylenedioxybenzene dihydrochloride

DNA : Desoxyribonucleic acid

dsDNA : double stranded DNA

EDTA : Ethylenediaminetetraacetic acid

ELISA : Enzyme-linked immunosorbent assay

EU : Endotoxin unit

FDA : Food and Drug Administration

FLD : Fluorescence detection

HCD : Host cell DNA

HCP : Host cell protein

HPLC : High-performance liquid chromatography

KDO : 3-deoxy-D-manno-oct-2-ulosonic acid

LAL : Limulus amoebocyte lysate

LB : Luria-Bertani

LPS : Lipopolysaccharides

NA : Nutrient agar

OD_{600} : Optical density at 600 nm

PBS : Phosphate buffered saline

RNA : Ribonucleic acid

RP-HPLC : Reversed-phase high-performance liquid chromatography

SDS : Sodium dodecyl sulfate

TB : Terrific broth

TBE : Tris-borate-EDTA

TE : Tris-EDTA

Δp : Differential pressure [Pa]

Δp_{max} : Maximal differential pressure [Pa]

μ_{max} : Maximal specific growth rate [h^{-1}]

A : filter area [m^2]

a : slope of regression line [L/g] or slope of regression line, corresponding to the maximal specific growth rate μ_{max}

A_1 : Filter area with Purafix® BIO SD 2" capsule [m^2]

$A_{450\,nm}$: absorbance at 450 nm [-]

$A_{595\,nm}$: absorbance at 595 nm [-]

b : intercept of regression line [-]

b_d : dry mass [g]

b_w : wet biomass mass in suspension [g]

c_1 : Cake volume obtained with Purafix® BIO SD 2" capsule [m^3]

c_1 : total dsDNA concentration of sample after Miniprep purification by Qubit [ng/µL]

C_2 : Cake volume obtained with Puradisc® BIO SD 12" 12M module [m^3]

c_2 : pUC18 concentration of sample after Miniprep purification by TapeStation 4150 [ng/µL]

c_3 : total dsDNA concentration of sample after Miniprep purification by TapeStation 4150[ng/µL]

c_{ms} : dry matter concentration in filtrate [kg/m^3]

d : dilution factor [-]

$ET_{activity}$: endotoxin biological pyrogenic activity [EU/ng]

$ET_{conc.}$: endotoxin concentration [ng/mL]

f : fraction of KDO in endotoxin [-] (w/w)

h_1 : Cake height with Purafix® BIO SD 2" capsule [m]

$KDO_{conc.}$: KDO concentration [ng/mL]

m_1 : filter mass tare [mg]

M_1 : total dsDNA concentration of sample after first Miniprep purification [ng/µL]

m_2 : filter mass after filtration of culture [mg]

M_2 : total dsDNA concentration of sample after second Miniprep purification [ng/µL]

$OD_{600, m}$: OD_{600} of medium [-]

$OD_{600, p}$: OD_{600} of preculture [-]

Q_f : suspension flow rate [m^3/s]

s_1 : suspension mass [g]

s_2 : initial suspension mass loaded on moisture analyzer [g]

std : KDO standard peak area [LU·s] or height [LU]

$std_{conc.}$: KDO standard concentration [ng/mL]

t : time [s]

V : volume of culture [mL]

V_1 : volume of sample after first Miniprep purification for second purification [µL]

V_1 : volume of sample before Miniprep purification [µL]

V_1 : Volume to filter with Purafix® BIO SD 2" capsule [m^3]

V_2 : volume of sample after Miniprep purification [µL]

V_2 : volume of sample after second Miniprep purification [µL]

V_2 : Volume to filter with Puradisc® BIO SD 12" 12M module [m^3]

x : sample peak area [LU·s] or height [LU]

x [h] : time

Y : yield of purification by Miniprep [%]

y [-] : natural logarithm of OD_{600}

α : cake specific resistance [m/kg]

β : filter resistance [m^{-1}]

Δp : differential pressure [Pa]

η : dynamic viscosity [kg/m·s)]

8. Appendixes

8.1 Measurement of the viscosity of the lysate

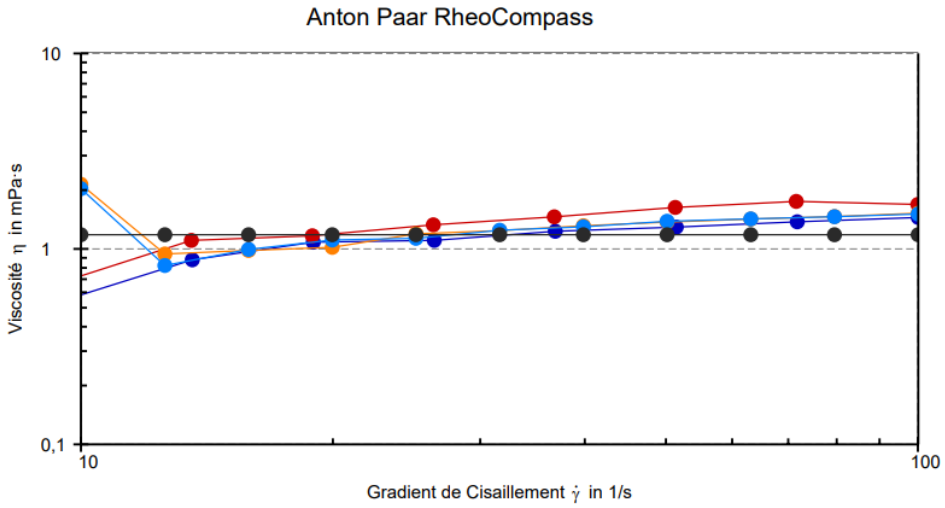

Figure 1 : Graph generated by the Rheocompass of Anton Paar for the measurement of viscosity of the lysate at 4 g/L of dry biomass. It measures the viscosity in function of shear rate on a logarithmic scale.

8.2 Calibration curves for the quantification of proteins

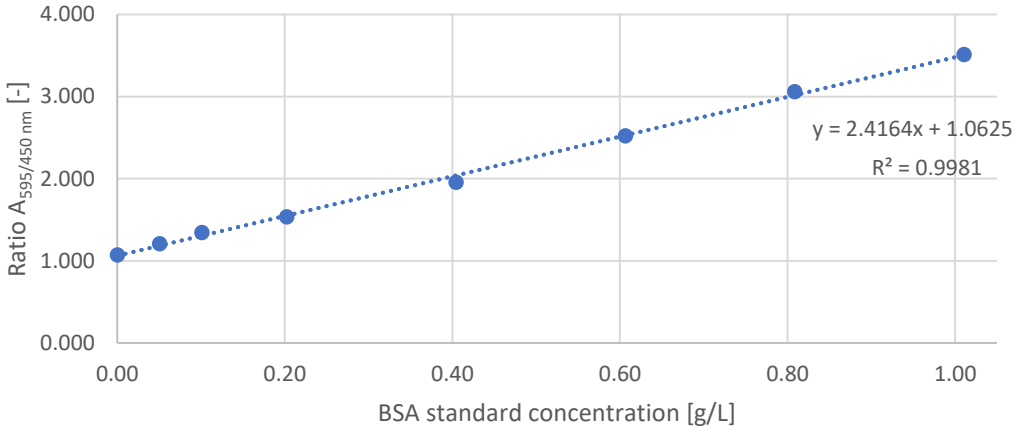

Figure 2 : Ratio of absorbance at 595 nm to 450 nm in function of the concentration in BSA of the standards. This calibration was used to assess bead mill and French Press lysis methods.

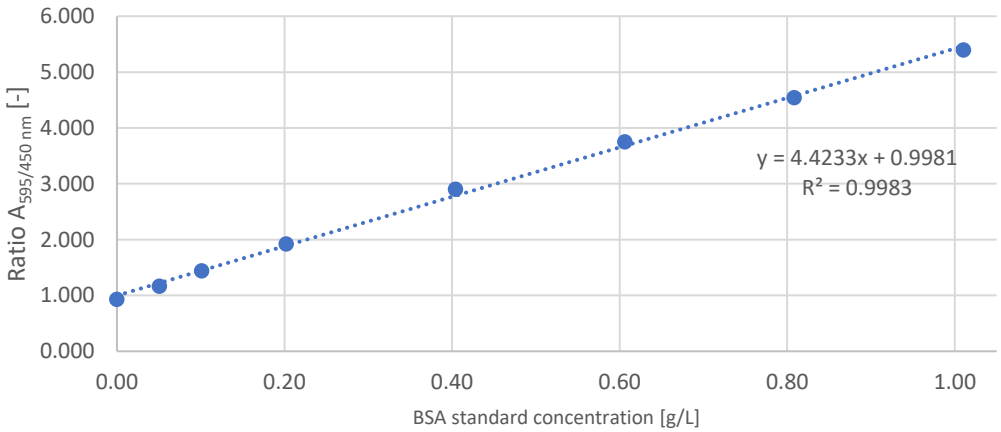

Figure 3 : Ratio of absorbance at 595 nm to 450 nm in function of the concentration in BSA of the standards. This calibration was used to assess Puraspin® filtrations.

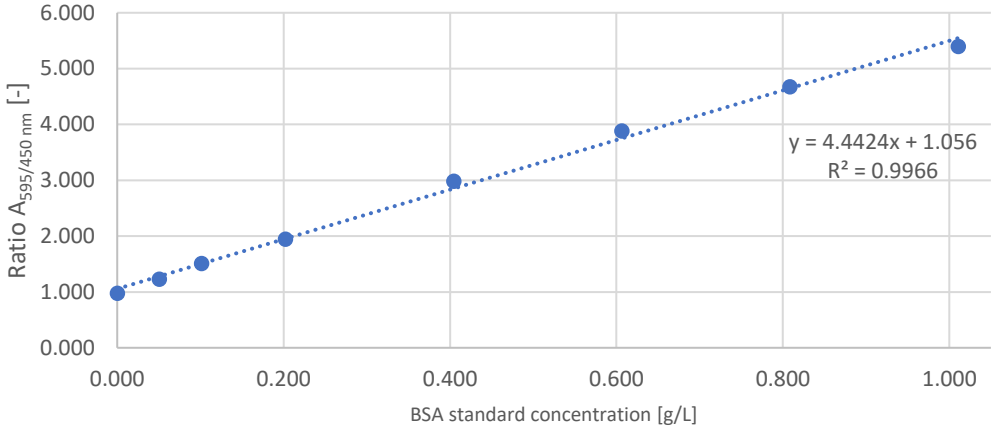

Figure 4: Ratio of absorbance at 595 nm to 450 nm in function of the concentration in BSA of the standards. This calibration was used to assess Purafix® filtrations.

8.3 Raw data

Table 1 : Raw data of all analytics performed on Puraspin® trials and corresponding lysates.

Sample	Turbidity		Endotoxins			Proteins				Total dsDNA			pUC18			
	Turbidity [NTU]		Area of peak [LU*s]			Height of peak [LU]			Absorbance at 595 nm [-]			Absorbance at 450 nm [-]			Total dsDNA in supernatant (Qubit) [µg/mL]			Total dsDNA in Miniprep		Total dsDNA in Miniprep (TapeStation) [µg/mL]		pUC18 in Miniprep (TapeStation) [µg/mL]
	1		1	2	3	1	2	3	1	2	3	1	2	3	1	2	3	1	2	1	2	1
CH9P-C1000 1	172		48805.267	51897.585	50856.61	2161.589	2315.778	2236.054	0.842	0.843	0.839	0.262	0.262	0.262	75.9	76.5		68.4	67.6		84		13.7
CH9P-C1000 2	170		52109.016	52281.294	53009.493	2326.327	2313.697	2333.993	0.846	0.839	0.838	0.263	0.262	0.259	74.6	70.9		68.8	66.8		71.5		12
CH9P-C1000 3	177		49391.476	49647.525	88697.01	2186.117	2192.234	4074.891	0.84	0.848	0.84	0.261	0.263	0.261	68.4	74.6		67.6	69.2		83.4		12.8
CH31P-C1000 1	152		90606.734	86690.258	89457.133	4127.448	4082.719	3998.95	0.836	0.833	0.83	0.25	0.251	0.25	80.9	77.7		74.8	72.8		78.4		14.6
CH31P-C1000 2	153		87772.327	88912.563	93243.502	4007.997	4170.547	4268.012	0.836	0.832	0.835	0.25	0.25	0.251	77.1	73.4		64.8	64.4		83.2		13.7
CH31P-C1000 3	152		90155.571	81007.976	89185.774	4171.845	3750.481	4088.36	0.83	0.83	0.835	0.252	0.252	0.25	75.9	77.1		80.0	82.0		88.8		14.9
CH71P-C1000 1	135		63457.808	63083.637	60159.9	2928.32	2903.221	2756.327	0.825	0.824	0.824	0.255	0.256	0.255	75.9	74.6		64.4	61.6		70		11.5
CH71P-C1000 2	147		76348.457	75415.259	73707.466	3536.813	3460.494	3356.762	0.823	0.821	0.826	0.243	0.245	0.242	77.1	77.8		65.2	66.0		69		11.4
CH71P-C1000 3	144		76280.193	74215.824	67164.38	3480.564	3396.578	3081.389	0.836	0.846	0.837	0.271	0.274	0.271	75.9	77.1		53.6	55.2		40		6.47
CH130P-C1000 1	114		40424.522	44432.354	44723.558	1943.37	2102.835	2142.923	0.822	0.822	0.833	0.266	0.266	0.271	74.6	77.8		64.0	58.4		63.6		9.7
CH130P-C1000 2	120		46611.153	46232.244	46077.028	2177.72	2212.677	2190.064	0.832	0.836	0.834	0.269	0.27	0.28	79.0	79.6		69.6	70.4		77.9		12.3
CH130P-C1000 3	126		35963.04	34448.435	32663.242	1761.677	1737.404	1660.745	0.825	0.83	0.824	0.262	0.257	0.261	75.9	75.9		78.8	76.4		79.4		11.8
CH9P-C300 1	131		64866.8	64999.521	62569.547	3153.504	3144.938	2972.923	0.809	0.819	0.818	0.269	0.263	0.263	76.5	72.2		54.8	55.2		68.5		11.8
CH9P-C300 2	110		59536.095	59284.331	61438.571	2916.603	2893.184	2930.524	0.811	0.827	0.82	0.26	0.267	0.266	66.6	65.9		60.4	60.0		69.7		11.1
CH9P-C300 3	124		58587.721	59114.285	59331.009	2846.962	2966.103	2954.292	0.827	0.835	0.822	0.269	0.271	0.267	70.9	65.3		52.4	53.6		62.8		10.3
CH31P-C300 1	108		74507.246	73173.43	72991.083	3611.916	3486.526	3524.136	0.8	0.795	0.791	0.258	0.255	0.253	69.7	75.3		68.0	70.4		78		13.3
CH31P-C300 2	110		87068.63	99891.54	92653.23	3976.386	4451.373	4146.456	0.835	0.829	0.817	0.286	0.285	0.276	76.5	69.7		59.2	61.2		72.5		12.1
CH31P-C300 3	113		97084.576	96046.339	96649.466	4360.12	4277.594	4339.683	0.863	0.859	0.862	0.285	0.283	0.284	69.7	66.6		66.0	66.4		83.3		14.6
CH71P-C300 1	86.8		103386.297	97585.46	102409.227	4546.074	4293.347	4558.448	0.851	0.861	0.857	0.283	0.286	0.285	74.6	70.3		99.6	99.6		102		14.7
CH71P-C300 2	86.6		87534.818	85574.917	89053.207	3822.102	3791.806	3940.238	0.845	0.847	0.82	0.279	0.278	0.269	77.8	75.3		88.8	91.6		67.3		11.6
CH71P-C300 3	86.4		88341.67	89098.455	87519.141	3990.217	3949.57	3862.194	0.835	0.829	0.815	0.275	0.265	0.263	75.9	70.9		94.7	95.4		117		18.1
CH130P-C300 1	84		76150.739	71523.393	76551.061	3379.965	3176.777	3361.231	0.836	0.832	0.811	0.275	0.275	0.266	74.6	68.4		56.4	58.2		78.7		13.6
CH130P-C300 2	89.4		61003.865	61312.099	61691.533	2680.175	2668.322	2711.875	0.809	0.819	0.796	0.269	0.274	0.263	68.4	74.6		64.8	68.0		74.8		12.2
CH130P-C300 3	84.8		65805.185	63315.95	66069.185	2884.48	2772.135	2936.262	0.823	0.821	0.821	0.275	0.272	0.271	67.2	74.0		54.8	53.6		62.6		10.4
CH9P-C100 1	84.7		45127.301	43182.02	44013.132	1999.561	1898.453	1967.017	0.813	0.825	0.817	0.276	0.284	0.278	67.2	66.6		56.4	58.0		66.4		11.2
CH9P-C100 2	83.8		43407.504	44142.571	46658.234	1912.931	1938.958	2044.954	0.8	0.807	0.82	0.27	0.272	0.27	71.5	67.8		57.6	55.2		64.6		9.85
CH9P-C100 3	87.9		50146.205	49006.52	50075.189	2129.822	2097.941	2111.821	0.812	0.814	0.819	0.275	0.28	0.277	67.2	70.3		60.4	52.8		66.9		11.1
CH31P-C100 1	79.7		57494.883	59158.232	59965.115	2727.81	2686.794	2734.765	0.77	0.798	0.799	0.272	0.275	0.272	65.9	60.9		70.0	72.8		97.2		15.1
CH31P-C100 2	78.5		65696.735	65097.977	67813.368	2753.079	2742.68	2837.801	0.794	0.789	0.789	0.274	0.276	0.269	61.5	58.7		82.0	81.2		90.5		14.4
CH31P-C100 3	77.8		60474.097	55796.611	59800.685	2578.012	2404.047	2602.16	0.817	0.825	0.816	0.272	0.271	0.276	69.7	72.8		59.6	57.2		67.5		10.2
CH71P-C100 1	71.6		33289.083	32485.234	33299.68	1471.816	1442.546	1487.842	0.817	0.811	0.808	0.276	0.273	0.269	74.6	72.2		76.9	82.0		89		15.6
CH71P-C100 2	64		49323.761	49703.267	49959.196	2156.72	2164.597	2206.583	0.79	0.794	0.804	0.261	0.266	0.262	73.4	68.4		67.6	71.4		86.1		15.2
CH71P-C100 3	71.7		48882.264	42888.265	43890.383	1903.519	1951.338	3712.676	0.798	0.81	0.813	0.279	0.28	0.281	69.7	69.7		66.7	67.3		79		13.6
CH130P-C100 1	54.4		102383.544	96293.989	96396.73	4446.283	4135.648	4135.648	0.805	0.799	0.812	0.28	0.281	0.284	74.0	70.9		85.7	87.2		111		17.4
CH130P-C100 2	58.7		95772.88	88202.959	88592.324	4055.683	3749.531	3810.191	0.808	0.826	0.817	0.276	0.281	0.282	75.9	73.4		94.1	94.8		107		15.3
CH130P-C100 3	57.2		78741.891	80625.842	78860.124	3369.823	3431.713	3337.294	0.796	0.808	0.814	0.277	0.275	0.281	58.5	67.8		67.6	70.8		81.9		14.3
CH9P-C65 1	66.2		85263.978	83848.099	85872.038	3615.088	3516.766	3560.466	0.808	0.809	0.809	0.271	0.271	0.271	58.7	64.7		73.6	67.6		106		16.6
CH9P-C65 2	65.6		83515.34	89647.301	83656.438	3477.886	3720.436	3535.318	0.799	0.817	0.811	0.272	0.276	0.277	67.2	62.8		59.6	56.8		61.2		10.1
CH9P-C65 3	62.7		64260.393	56011.005	62769.623	2700.227	2362.988	2632.228	0.806	0.81	0.825	0.27	0.27	0.281	68.4	67.8		74.0	70.0		79.9		12.1
CH31P-C65 1	67.2		65521.31	67194.567	63582.252	2964.237	2987.019	2855.533	0.787	0.793	0.803	0.264	0.268	0.269	75.9	67.8		75.2	73.6		72		11.3
CH31P-C65 2	61.8		73712.476	64357.519	69360.825	3063.454	2636.049	2838.115	0.825	0.819	0.826	0.288	0.288	0.289	73.4	70.9		59.6	59.6		67.2		9.73
CH31P-C65 3	71.3		62584.929	64110.447	63635.904	2591.951	2643.504	2621.314	0.768	0.773	0.799	0.288	0.291	0.301	71.5	75.3		77.6	78.8		61.7		9.09
CH71P-C65 1	58.9		50171.25	49234.336	45615.583	2066.698	2057.779	1919.331	0.822	0.823	0.825	0.286	0.288	0.289	67.2	66.6		79.6	78.9		77.1		11.9
CH71P-C65 2	52.9		47457.038	52078.186	51718.9	1979.133	2142.218	2134.165	0.806	0.811	0.828	0.281	0.278	0.281	72.2	72.2		73.5	75.5		82.1		14.1
CH71P-C65 3	56.6		53139.935	57243.196	53345.669	2179.61	2341.658	2181.121	0.811	0.82	0.829	0.279	0.279	0.278	68.4	62.2		88.4	84.4		96.8		17.4
CH130P-C65 1	53		39231.583	40163.502	39914.858	1640.643	1658.261	1664.379	0.801	0.803	0.814	0.279	0.283	0.28	59.7	64.7		56.0	51.6		58.5		9.37
CH130P-C65 2	56.9		30817.361	34024.956	31401.1	1310.842	1439.574	1343.467	0.815	0.802	0.816	0.281	0.281	0.281	69.7	71.5		63.6	61.6		66.7		10
CH130P-C65 3	54.4		33195.859	32858.047	30848.65	1442.887	1420.187	1333.48	0.789	0.793	0.808	0.27	0.272	0.271	66.6	67.2		62.4	60.8		68		8.87
Lysate 1	153		38589.051	39559.548	37746.955	1660.578	1685.171	1675.573	0.534	0.52	0.52	0.37	0.364	0.367	67.6	63.6		97.6	108		81.7		13.4
Lysate 2	201		40065.397	40243.312	38529.502	1686.204	1729.438	1662.599	0.527	0.521	0.531	0.358	0.355	0.361	70.0	70.0		87.2	90.0		73.8		12.1

Table 2 : Raw data of all analytics performed on Purafix® trials and corresponding lysate.

Filtration trial	Fraction	Turbidity	Endotoxins			Proteins						Total dsDNA		pUC18			
		Turbidity [NTU]	Area of peak [LU*s]			Height of peak [LU]			Absorbance at 595 nm [-]			Absorbance at 450 nm [-]			Total dsDNA in supernatant (Qubit) [µg/mL]		Total dsDNA in Miniprep (Qubit) [µg/mL]		Total dsDNA in Miniprep (TapeStation) [µg/mL]	pUC18 in Miniprep (TapeStation) [µg/mL]
		1	1	2	3	1	2	3	1	2	3	1	2	3	1	2	1	2	1	1
CH71P-C100	50 mL	39.2	36576.997	35942.909	14738.209	1527.874	1452.432	684.139	0.791	0.783	0.775	0.302	0.295	0.292	36.4	35.6	29.3	26.8	32.2	4.8
	100 mL	40.8	53431.622	55682.536	24029.5	2236.643	2213.801	1068.661	0.806	0.816	0.819	0.265	0.265	0.268	72	70.8	53.6	53.6	61.7	8.6
	150 mL	43.9	57187.472	56527.486	115907.181	2396.32	2221.6	4335.24	0.79	0.796	0.788	0.263	0.262	0.264	68.4	69.2	51.6	52	55.4	8.3
	200 mL	42.9	54503.409	55319.532	53981.83	2285.559	2212.714	2145.111	0.806	0.799	0.808	0.272	0.258	0.264	68	70.4	58	57.6	66.2	9.1
	250 mL	33.2	54050.108	56110.847	54768.446	2266.819	2269.888	2272.037	0.808	0.8	0.799	0.287	0.274	0.27	62	62.8	52	53.6	58.4	8.6
CH130P-C1000	50 mL	32.9	29220.319	37375.703	38325.199	1242.016	1520.475	1547.02	0.809	0.804	0.796	0.285	0.28	0.272	43.2	39.8	41.2	41.2	45.2	7.1
	100 mL	70.2	67468.821	65596.32	69166.584	2705.53	2568.158	2700.268	0.816	0.815	0.815	0.252	0.246	0.246	65.2	63.2	54.5	54.9	54.9	8.2
	150 mL	90.6	75789.332	79369.102	81272.479	3086.945	3085.317	3153.509	0.837	0.827	0.836	0.25	0.244	0.25	66.4	68	61.6	60.8	70.5	9.2
	200 mL	95.6	79116.734	78309.665	74239.486	3229.302	3017.235	3025.096	0.828	0.817	0.834	0.257	0.245	0.275	61.2	62.4	58.6	58.6	65.3	9.1
	250 mL	98.8	76253.728	67700.501	78900.166	3139.693	2668.192	2754.363	0.84	0.838	0.836	0.253	0.246	0.251	59.2	60	56.8	57.6	65.6	9.2
CH71P-C300	50 mL	57.8	47411.418	47569.07	48630.865	1942.463	1823.646	1728.853	0.781	0.804	0.8	0.276	0.283	0.288	45.2	41.6	43.6	44.8	50.3	7.8
	100 mL	72.3	64698.02	69409.545	64347.494	2573.61	2716.538	2311.341	0.823	0.811	0.823	0.252	0.254	0.255	63.6	63.6	54.4	56	64.2	9.6
	150 mL	76.5	75329.652	70165.072	76713.868	2995.985	2732.746	2725.556	0.821	0.831	0.835	0.254	0.254	0.259	60.4	60.8	62.8	61.2	65.8	8.8
	200 mL	73.8	70573.805	69073.158	70358.951	2807.82	2708.436	2470.972	0.794	0.816	0.818	0.261	0.263	0.264	56.8	53.6	57.2	58.8	66.6	9.5
	250 mL	79	69934.6	73272.405	71980.044	2542.617	2928.186	2544.188	0.835	0.836	0.832	0.263	0.261	0.264	59.6	62	61.2	62.8	60	7.86
	300 mL	78.9	69621.928	74843.804	65968.049	2795.375	2837.526	2470.591	0.836	0.836	0.827	0.258	0.259	0.257	61.6	64	50.8	50.4	58.2	9
Lysat		179	27735.485	25994.011	27553.868	1179.726	1081.389	1097.034	0.536	0.552	0.545	0.361	0.365	0.368	59.2	65.6	59.2	58.4	62.1	10.3